Requirements of *Escherichia coli* to survive stress induced by the secretin, pIV

A thesis presented in partial fulfilment of the requirements for the degree of

Master of Science

in

Microbiology

at Massey University, Manawatū,

New Zealand.

Stefanie Jayne Bagley

2018

Abstract

Pathogenic Gram-negative bacteria utilise complex multiprotein and functionally unrelated *trans*-envelope machineries to secrete toxins and other virulence factors. Such machineries are referred to as secretion systems. These contain large, membrane-inserted homologous channels called a secretin. These secretion systems include the type II and III secretion systems (T2SS and T3SS), type IV pili assembly system (T4PS), and the filamentous phage assembly-secretion system (FFSS). Secretins are homomultimers with radial symmetry blocked by an inner gate or septum and have a pore size of up to 10 nm.

As determined by previous studies on the FFSS secretin, pIV, and the T3SS secretin, InvG, there is a cost associated with the insertion of large membrane channels. Membrane integrity is disrupted, leaving the bacterial cell highly susceptible to antibiotics and environmental stressors. As a result, Gram-negative bacteria have developed stress response pathways which upregulate genes to mitigate this secretin-induced stress. These are the Phage Shock Protein response (Psp), Conjugative plasmid expression (Cpx), Regulation of capsular synthesis (Rcs), and SoxRS Superoxide response (Sox). Not all individual genes within these stress response pathways are necessarily required for the survival of *Escherichia coli* expressing secretin.

Stress can be induced in *E. coli* by expression of leaky pIV mutants as they are open, not gated, under physiological conditions and imitate the actively secreting channel. A synthetic lethality assay was performed to determine the importance of the key regulators from four stress response pathways (PspF, CpxR, RcsA, RcsB, SoxR, and SoxS) on cell viability in the presence of the leaky secretin mutant, pIV-E292K. Here it was determined that the Psp, Rcs and, (to a lesser extent), Cpx regulons, confer a protective effect on *E. coli* K-12 experiencing stress induced by pIV-E292K. Expression of pIV-E292K mutant also induced an Rcs-dependent capsular polysaccharide phenotype indicating upregulation of Rcs in response to leaky pIV production. These three responses are potential drug targets in the fight against antibiotic-resistant infections. Inhibition of the stress response may prevent mitigation of membrane stress, thereby killing the channel-expressing bacteria.

Acknowledgements

My research would not have been possible without the expertise, support, and encouragement of my supervisor Dr. Jasna Rakonjac. Thank you also to Dr. Helen Fitzsimons who provided valuable feedback on this thesis.

I am profoundly grateful to Dr. Sofia Khanum and Dr. Julian Spagnuolo for sharing their expertise with experiments and statistical analysis, respectively.

My sincere thanks to the members of the Helipad lab – you made my time completing this research very enjoyable.

I would also like to acknowledge Massey University for supporting me with the Massey University Masterate Scholarship.

Thank you also to Jordan Taylor and Niki Minards of the Manawatu Microscopy and Imaging Centre for their work in carrying out the transmission electron microscopy.

Finally, I would like to thank the Massey Genome service for sequencing my plasmid.

Abbreviations

ATP	Adenosine triphosphate
Amp	Ampicillin
cAMP	3’,5’-cyclic adenosine monophosphate
CFU	Colony forming units
Cm	Chloramphenicol
Cm^R	Chloramphenicol resistance
Cpx	Conjugative pilus expression response
Cryo-EM	Cryo-Electron microscopy
dsDNA	Double-stranded DNA
DNA	Deoxyribonucleic acid
EM	Electron microscopy
EPEC	Enteropathogenic *Escherichia coli*
ETEC	Enterotoxigenic *Escherichia coli*
FFSS	Filamentous phage assembly-secretion system
IM	Inner membrane
IPTG	Isopropyl β-*D*-1-thiogalactopyranoside
Km	Kanamycin
Km^R	Kanamycin resistance
LPS	Lipopolysaccharide
MIC	Minimum inhibitory concentration
nt	Nucleotide
OD	Optical density
OM	Outer membrane
PMF	Proton motive force
ppGpp	Guanosine 5’,3’ bispyrophosphate
Psp	Phage-shock-protein
R	Resistant
ROS	Reactive oxygen species

Rcs	Regulation of capsular synthesis
RNA	Ribonucleic acid
RNA-Seq	RNA sequencing
SecYEG	General secretory translocon
Sox	Superoxide stress response
SPA	Single particle analysis
ssDNA	Single-stranded DNA
T2SS	Type II secretion system
T3SS	Type III secretion system
T4PS	Type IV pilus assembly system
T4SS	Type IV secretion system
T5SS	Type V secretion system
Tat	Twin-arginine translocon
TEM	Transmission electron microscopy
Tet	Tetracycline
Tet^R	Tetracycline resistance
Vn	Vancomycin
WT	Wild-type

Table of Contents

List of Figures

List of Tables

Chapter One: Literature Review

1.1 Secretion systems of Gram-negative bacteria

The bacterial cell membrane maintains a stable internal environment for cellular functions, protecting against external changes in pH, nutrient availability, and osmolarity (Silhavy, Kahne, & Walker, 2010). This protective function relies on an undisrupted membrane. Yet, the ability to transfer proteins across the cellular membrane is also an essential component of the living bacterial cell. Protein secretion in bacteria has many roles, such as inter- and intra-species communication, nutrient sequestration, the promotion of survival in certain environments, and virulence (Koraimann, 2003; Kulp & Kuehn, 2010; Schauder & Bassler, 2001; Skaar, 2010; Tseng, Tyler, & Setubal, 2009). Secreted substances include proteins, macromolecular complexes, enzymes, and toxins, which can be released into the extracellular environment, associated to the outer membrane, or released directly into target cells (Thanassi & Hultgren, 2000).

The cell wall of Gram-negative bacteria (such as *Escherichia coli* and *Salmonella* spp.) contains both an inner and outer membrane (Figure 1), which contrasts with that of Gram-positive bacteria, (including, *Streptococcus* spp. and *Staphylococcus* spp.), which have a single membrane. Possessing two membranes allows the Gram-negative bacteria to be particularly resilient to environmental change and impermeable to many toxic compounds that they may encounter (Zgurskaya, López, & Gnanakaran, 2015). However, protein secretion becomes complex as fatal disruption of membrane integrity must be avoided. In consequence, secretion systems with rather complex secretion machinery have evolved.

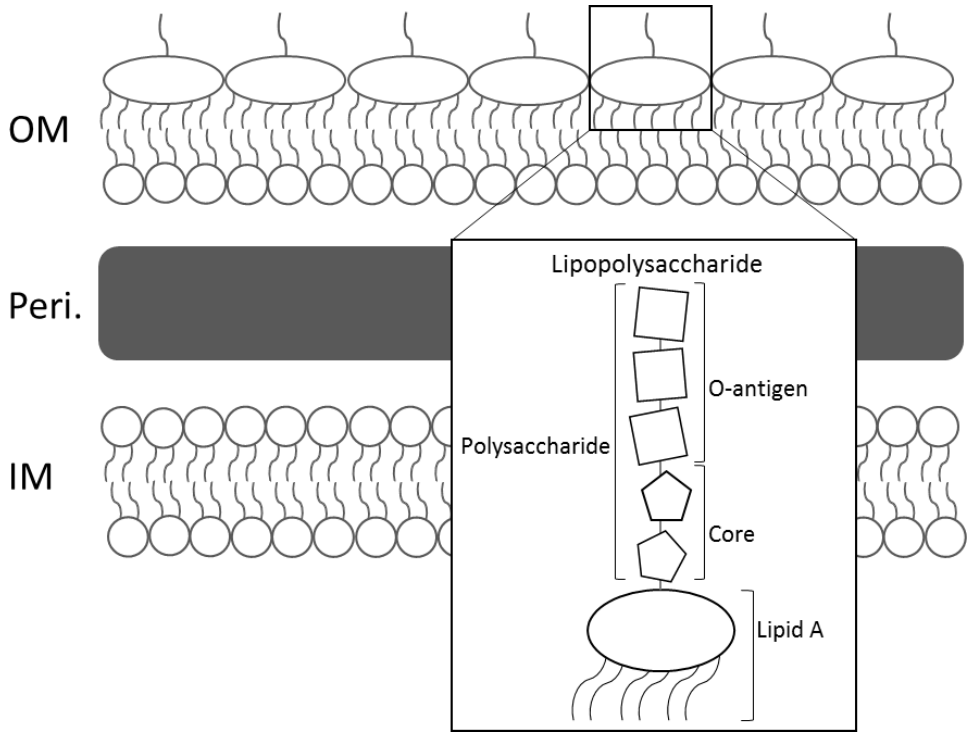

Figure 1: Structure of the Gram-negative cell wall.

The cell wall comprises of an inner membrane (IM) consisting of the phospholipid bilayer for rigidity, a periplasm (Peri.), and an outer membrane (OM). The outer membrane is made up of a single phospholipid layer and lipopolysaccharide (LPS) (inset) with hydrophobic lipid A, core polysaccharide, and variable O-antigen polysaccharides. Reproduced with modification and permission from Spagnuolo (2015).

The secretion systems of Gram-negative bacteria can be separated into two categories; those that span the outer membrane only, and those that span both the inner and outer membrane. The former includes the type V secretion system (T5SS) in which the substrate (such as a virulence factor) binds to the secretion pore and is released *via* an 'auto-transportation' mechanism (Costa *et al.*, 2015). In addition, the P pilus biogenesis system and the curli biogenesis systems also utilise a two-step secretion mechanism. Initial transfer of the substrate across the inner membrane for these systems is usually facilitated by the SecYEG translocon or, less commonly, the twin-arginine translocation (Tat) system (Costa *et al.*, 2015). The actual mechanism is dependent on the folding state and signal sequence of the substrate (Natale, Brüser, & Driessen, 2008). In contrast, double-membrane spanning secretion systems identified so far include the T1SS, T2SS, T3SS, T4SS, type IV pilus assembly system (T4PS), and the filamentous phage assembly-secretion system (FFSS) (Figure 2). These large, *trans*-envelope organelles vary in complexity, mode of action, and substrate (Korotkov, Gonen, & Hol, 2011).

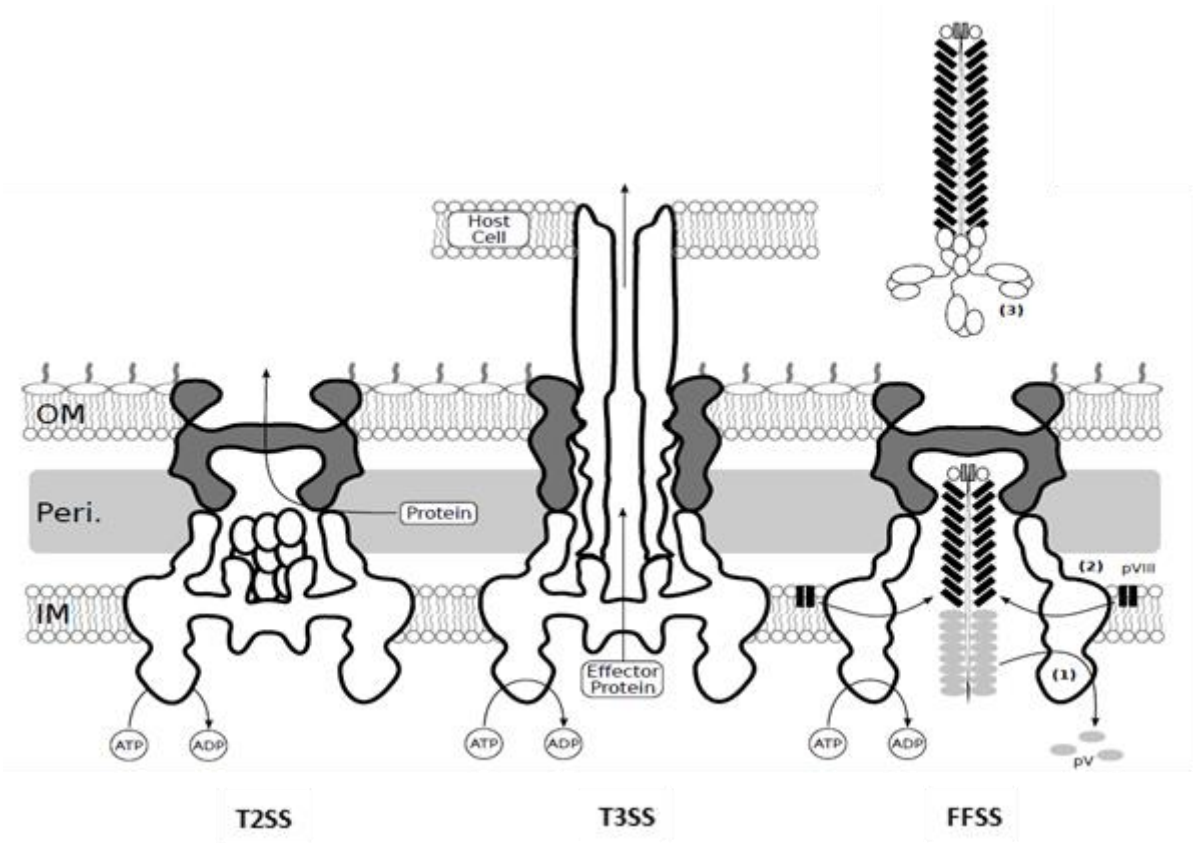

Figure 2: The type 2 (T2SS) and 3 (T3SS) secretion systems and the filamentous phage assembly secretion system (FFSS).

Substrate export is ATP-dependent, and each contains the secretin channel (dark grey). **Type 2** secretion system substrates enter the apparatus in the periplasm for release to the extracellular environment. **Type 3** secretion system substrates enter the needle complex through the middle of the apparatus for transport directly into the host cell. **Filamentous phage** assembly is initiated when the ssDNA phage genome is targeted to the IM pI/pXI complex, and pV is removed **(1)**. pVIII (coat protein) is assembled onto the phage filament **(2)** as it is moved through the open pIV secretin channel (not shown). The phage is released into the extracellular environment upon addition of pIII **(3)**. Reproduced from Spagnuolo (2015) with permission.

1.1.1 Pathogenicity and secretion systems

The double-membrane-spanning T2SS, T3SS, and T4PS are used for a pathogenic effect by many Gram-negative bacteria. The T2SS (Figure 2) is made up of 12-14 different proteins that form an outer membrane (OM) complex, a filamentous pseudopilus (in the periplasm), and inner membrane (IM) platform. Toxins and hydrolytic enzymes enter the T2SS secretion apparatus in the periplasm for transfer outside the bacterial cell. *Vibrio cholerae* (cholera) and enterotoxigenic *E. coli* (ETEC) (diarrhoea) secrete the cholera toxin and enterotoxin, respectively, using this system (Johnson, Abendroth, Hol, & Sandkvist, 2006).

Gram-negative pathogens including *Salmonella typhimurium* (typhoid fever), enteropathogenic *E. coli* (EPEC) (diarrhoea), and *Pseudomonas aeruginosa* (pneumonia and wound infections) utilise the T3SS (Figure 2) to secrete virulence factors directly into host cells (Hueck, 1998). The T3SS is composed of the *trans*-membrane secretion apparatus and extracellular needle complex. Upon contact with host cells, the needle complex forms a pore in the host cell membrane through which virulence factors are transported to modulate host inflammatory responses, cytoskeleton modelling, apoptosis and phagocytosis (Tsai, Burkinshaw, Strynadka, & Tainer, 2015).

The T4PS consists of twelve or more proteins and consists of an IM complex, OM secretin, and pilus that extends through the periplasm to the outside of the bacterium (Korotkov *et al.*, 2011). It secretes pilin subunits for the assembly of extracellular pili on the surfaces of Gram-negative pathogens, such as *Neisseria gonorrhoeae* (gonorrhoea)*, P. aeruginosa*, and *V. cholerae*. This allows for several functions, which include; twitching motility, biofilm formation, DNA uptake, and host cell attachment (Pelicic, 2008).

1.1.2 The Filamentous phage assembly-secretion system

Filamentous bacteriophage Ff (F1, fd, and M13) that reproduce within F-positive *E. coli* are released without bacterial cell lysis *via* the filamentous phage assembly-secretion system (FFSS) (Figure 2) (Rakonjac, 2012). The filamentous bacteriophage is a virus of bacteria which has a characteristic long rod shape consisting of an inner core of single-stranded DNA (ssDNA) surrounded by several thousand identical coat protein subunits (Marvin, Symmons, & Straus, 2014). The FFSS is composed of only three proteins but is incorporated across the entire *E. coli* envelope. They include pI and pXI which form a multimer in the IM and pIV (a large channel called a secretin), in the OM. Within the periplasm, the periplasmic domains pI/pXI interact with that of pIV (Feng, Model, & Russel, 1999). The start and end of filamentous phage assembly and release has not been fully elucidated. However, it is likely to be linked to the opening and closing of the secretin, pIV, gate (Marciano, Russel, & Simon, 1999; Marciano, Russel, & Simon, 2001).

During replication, the plus strand of filamentous ssDNA genome enters the *E. coli* K-12 cytoplasm. Following which, the second (minus) strand of Ff DNA is replicated by host proteins, producing a circular double-stranded DNA (dsDNA) molecule. This dsDNA is used as a template for transcription of phage-encoded proteins, and for the replication of the plus strand. The ssDNA-binding protein, pV, and plus-strand ssDNA form a complex that becomes the substrate for the assembly-secretion process. The complex is targeted to the IM pI/pXI complex, and pV is removed. The pVIII (coat protein) is then assembled onto the phage filament before translocation through an open pIV secretin channel. A high number of filamentous phage are released ($\leq 10^{13}$ phage/mL) without causing cell death. However, production of phage slows bacterial growth, resulting in an increased generation time (Rakonjac, 2012). Filamentous phage assembly and secretion is dependent on proton motive force and ATP hydrolysis (Feng *et al.*, 1999). Therefore, despite its relative simplicity to other secretion systems, the lysis-independent Ff production still creates a physical and energetic burden on the bacterial cell due to the release of hundreds of virions, as well as virion protein integration across the cell envelope (Rakonjac, 2012).

1.2 Secretins

The T2SS, T3SS, T4PS, and the FFSS are particularly notable as each contains a secretin, which is a large, homologous outer membrane channel (Korotkov *et al.*, 2011). As several of these systems are involved in pathogenicity and are utilised by many animal, human, and plant pathogens, the secretin has been proposed to be a target for antibiotic development (Baron, 2010).

Secretins are a family of large, gated channels in the OM of Gram-negative bacteria. They provide a pathway to the extracellular environment by allowing the passage of DNA, and single or multi-subunit proteins (Korotkov *et al.*, 2011). Secretins have radial symmetry and are 12-, 13-, or 14-mers that have structural similarity (Gold, Salzer, Averhoff, & Kühlbrandt, 2015; Opalka *et al.*, 2003; Tosi *et al.*, 2014). The secretin internal channel is large (with diameters up to 10 nm) and is blocked by a plug or septum (Tosi *et al.*, 2014). Closed state secretins, as determined by physiological assays, contain pores that are smaller than porins (pIV, (Tosi *et al.*, 2014)), equal to porins (PulD, (Tosi *et al.*, 2014)), or larger than porins (YscC, (Burghout *et al.*, 2004)). All have a highly conserved C-terminal secretin homology domain and a less conserved periplasmic N-terminal domain (Daefler, Guilvout, Hardie, Pugsley, & Russel, 1997) (Figure 3). Some secretins have an additional S domain at the C-terminal end of the secretin homology domain, which is involved in the assembly and insertion of the secretin into the OM in conjunction with lipoprotein chaperones (pilotins) (Korotkov *et al.*, 2011).

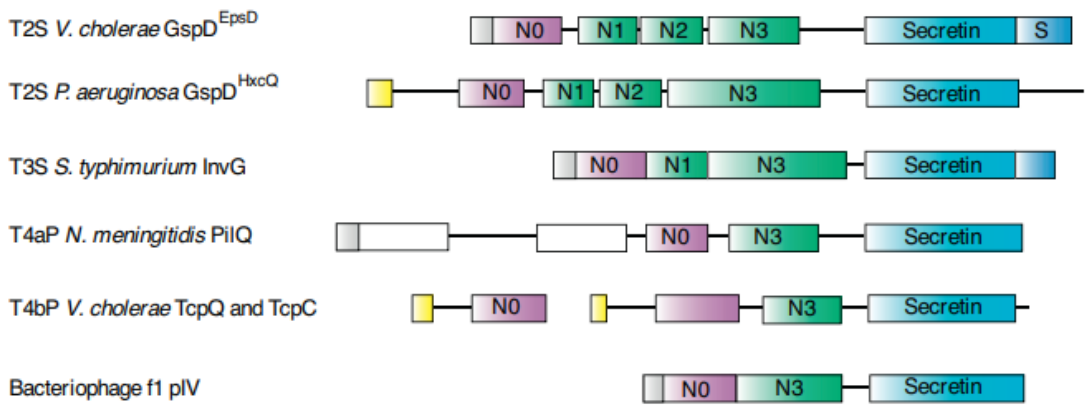

Figure 3: Domain organisation of secretins.

The N-terminal N0 domain (purple) is followed by one or more N1-N3 domains (green). These N-terminal signal sequences are cleaved off by a signal peptidase (grey) or a prolipoprotein (yellow) upon translocation across the inner membrane. The C-terminal secretin homology domain is shown in blue. Some secretins require the binding of lipoproteins, called pilotins, to target the channel to the outer membrane. Binding sites for pilotins are denoted by an 'S'. Secretin domains with unidentified topology are indicated in white. Reproduced with permission from Korotkov *et al.* (2011).

1.2.1 Outer membrane targeting and assembly

Mature monomers of secretins are transported across the IM by SecYEG translocons (Korotkov *et al.*, 2011). In the periplasm, the secretin is translocated to the OM (Korotkov *et al.*, 2011) by one of two ways. Secretins are either transported partially (T3SS secretin, InvG), or fully (T2SS secretin, PulD) to the OM, by cognate chaperones called pilotins, which bind to the C-terminal pilotin binding domain (S) (Figure 3) (Daefler & Russel, 1998; Guilvout, Chami, Engel, Pugsley, & Bayan, 2006). For some secretins which are lipoproteins, partial transport to the OM is facilitated by an N-terminal lipidation signal such is the case for HxcQ, a T2SS secretin (Viarre *et al.*, 2009). The targeting of the FFSS secretin, pIV, to the OM occurs by neither of these methods as it lacks a cognate chaperone, pilotin-binding domain, and an N-terminal lipidation signal. Rather, it is fractionated equally between the IM and OM (Russel & Kazmierczak, 1993). Fusing the pilotin-binding domain of PulD to the pIV C-terminus and co-expressing the pilotin, PulS, allows for pIV to be inserted into the OM almost exclusively (Daefler *et al.*, 1997).

1.2.2 Secretin structure and channel gating

Up until very recently, structural analysis of secretin channels had only been carried out at low resolution, primarily *via* electron microscopy (EM)-based techniques. For example, Chami *et al.* (2005) showed that the T2SS secretin, PulD, from *Klebsiella oxycota* was organised as a cylindrical, 12-mer, with two rings on either side of a central disc or plug. One ring was inserted into the periplasm, and the other was inserted into the OM. Based on these observations, a mechanism was proposed in which the substrate (pullulanase) binds to the ring within the periplasm allowing displacement of the plug and subsequent secretion through the remainder of the secretin. This was supported by a cryo-EM study which identified the symmetrical 12-meric structure of T2SS secretin, EpsD, from *V. cholerae* (Reichow, Korotkov, Hol, & Gonen, 2010) (Figure 4). The EspD channel also features a periplasmic gate, and therefore a similar secretion mechanism to PulD was proposed.

In addition, the three-tiered ring structure of FFSS secretin, pIV, has been elucidated by cryo-electron microscopy (cryo-EM) and single particle analysis (SPA) (Figure 5) (Opalka *et al.*, 2003). The N- and C-terminal entrances to the channel are large, at 6.0 nm and 8.8 nm in diameter, respectively. This size allows the entrance of antibiotics and bulky proteins that are too large to cross the lipopolysaccharide (LPS), yet, pIV does not render the cell sensitive to these due to the presence of the septum which closes the channel. Other evidence in support of the existence of a gate opening mechanism is the discovery that the pore size of pIV in its closed state is smaller than the filamentous phage it secretes (Opalka *et al.*, 2003).

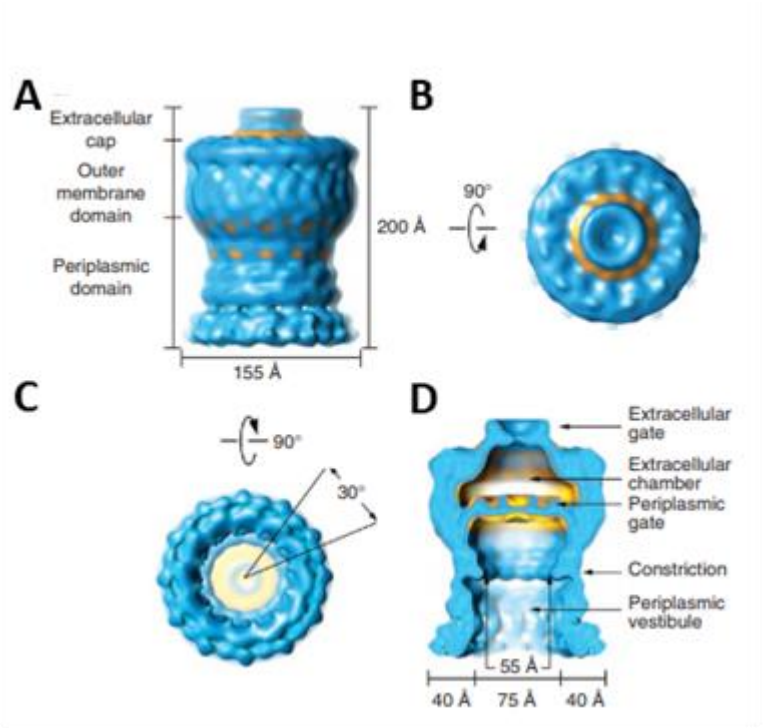

Figure 4: Three-dimensional cryo-EM model of T2SS EspD from *Vibrio cholerae.*

(A) Side, **(B)**, top, **(C)**, and bottom views at 19 Å resolution. **(D)** A slice view shows the internal structure of the channel featuring the extracellular gate and chamber, periplasmic gate, constriction, and periplasmic vestibule. Taken with permission and modified from Reichow *et al.* (2010).

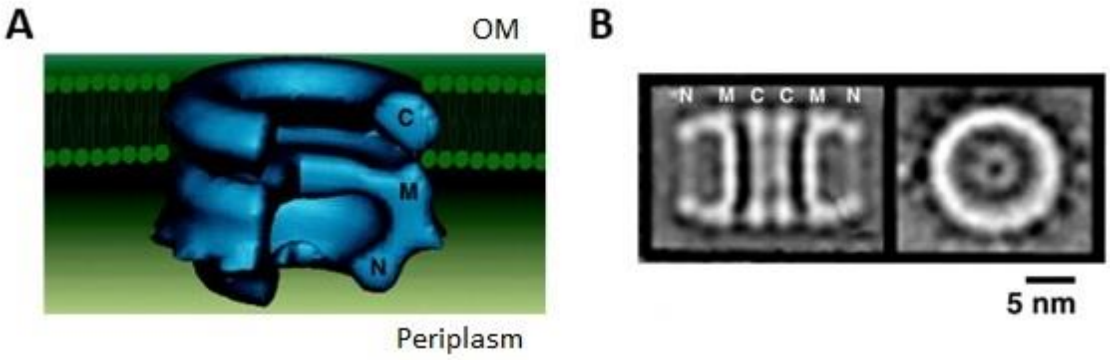

Figure 5: Model and electron micrograph of FFFS secretin, pIV.

(A) pIV secretin in the context of the outer membrane. The C-terminal domain (C) is inserted into the outer membrane (OM), and the M-ring (M) and N-terminal domain (N) are in the periplasm. The secretin is shown with a segment removed to show the septum that blocks the channel at the M-ring. **(B)** A single particle electron micrograph reconstruction of pIV with a side (left) and top (right) view showing the N-terminal domain (N), M-ring forming the septum (M), and C-terminal domain **(C)**. Both images are taken with permission and modified from Opalka *et al.* (2003).

The N-terminal domain of the secretin is comprised of independently folded subdomains; N0 and one or more of N1-N3 (Figure 3). The N0 subdomain has previously been shown to interact with other periplasmic and IM secretion system components leading to the suggestion that it allows for specificity in substrate secretion (Reichow *et al.*, 2010). A crystallographic study of the N-terminal domain of T2SS secretin, GspD, from enterotoxigenic *E. coli* (ETEC) revealed the presence of two globular lobes: N0 and N1 (Korotkov, Pardon, Steyaert, & Hol, 2009). These N-subdomains, which form rings, are believed to form the periplasmic portion of the secretin where the rest of the channel is inaccessible due to the periplasmic gate. As it was suggested by Reichow *et al.* (2010), perhaps, upon docking of the appropriate substrate at the N-subdomain, a conformational change in the periplasmic gate occurs, allowing translocation of the substrate to the extracellular environment.

In the absence of active secretory activity, secretion systems are generally regulated so they remain closed until the appropriate condition arises. The T3SS, which injects effector proteins into host cells (Figure 2), only becomes functional upon contact with host cell membranes (Nans, Kudryashev, Saibil, & Hayward, 2015). It would make sense that such large channels remain closed when non-functional to avoid negatively impacting OM integrity. A study of T4PS secretin, PilQ, from *Thermus thermophilus,* showed that the N-terminal periplasmic 5-ring (N0-5) opened up and the N0-N3 subdomains moved towards the IM for the secretion of pilin subunits (Gold *et al.*, 2015). In addition, when the T3SS secretin, CdsC, from *Chlamydia trachomatis,* makes contact with the host cell, it compresses, allowing for translocation of effector proteins (Nans *et al.*, 2015). Although these exact mechanisms are likely secretion system specific, it is plausible that the existence of a conformational change to regulate the channel is conserved between secretins.

It is only very recently that near-atomic resolution structures of secretins InvG from *S. typhimurium* T3SS and GspD from the T2SS of *V. cholerae* and pathogenic *E. coli* were elucidated (Worrall *et al.*, 2016; Yan, Yin, Xu, Zhu, & Li, 2017). These structures show that the secretin homology domain forms a double-barrel channel.

Furthermore, the secretin homology domain of GspD shows high sequence similarity to those of the FFSS secretin, pIV, and T2SS secretin, PulD (Figure 6A) (Yan *et al.*, 2017). The higher resolution structures have also enabled insights into the long-elusive gate opening mechanism. Worrall *et al.* (2016) showed the secretin homology domain of GspD comprises several β-strands between unstructured linker loops and a cap gate, which is also a β-hairpin. They proposed that the unstructured linker loops might pivot, allowing the cap gate to uncover the channel. Indeed, when Yan *et al.* (2017) solved the structure for GspD mutant G453A (glycine substituted for alanine at position 453), the mutation caused the tilting of the β-hairpin towards the channel wall by 25° (Figure 6D). Many residues within the secretin homology domain (including G453) are highly conserved between secretins (such as PilQ of T4PS, and pIV of FFSS) indicative of a similar gate-opening mechanism (Reichow *et al.*, 2010; Worrall *et al.*, 2016; Yan *et al.*, 2017).

Figure 6: Alignment and structural features of the secretin homology domain.

(A) InvG-PulD-pIV alignment showing regions of sequence homology. Only the C-terminal secretin homology domain is shown. Red boxes below the PulD sequence and yellow boxes below the pIV sequence show mutations that result in a leaky (open) channel phenotype (see 1.2.4 Leaky pIV mutants, (Khanum, 2015; Spagnuolo *et al.*, 2010)). Reproduced with permission from Khanum (2017) (Unpublished). **(B)** pIV secretin homology domain multimer modelled on the T2SS secretin, GspD, from *E. coli* (Yan *et al.*, 2017). Model created using SWISS-MODEL (Waterhouse *et al.*, 2018) **(C)** Topological model showing GspD secretin protomer secondary structure in the context of the outer membrane. Dashed lines indicate unsolved parts of the structure. Reproduced with permission from Yan *et al.* (2017). **(D)** Density maps in section view of wildtype GspD (left) and G453A mutant (right) (low-pass filtered to 7Å) in section view. The gate of the G453A mutant is open (red lines) and rotated upward by approximately 25°. In comparison, the gate of wild-type GspD remains closed (green lines). Reproduced with permission from Yan *et al.* (2017).

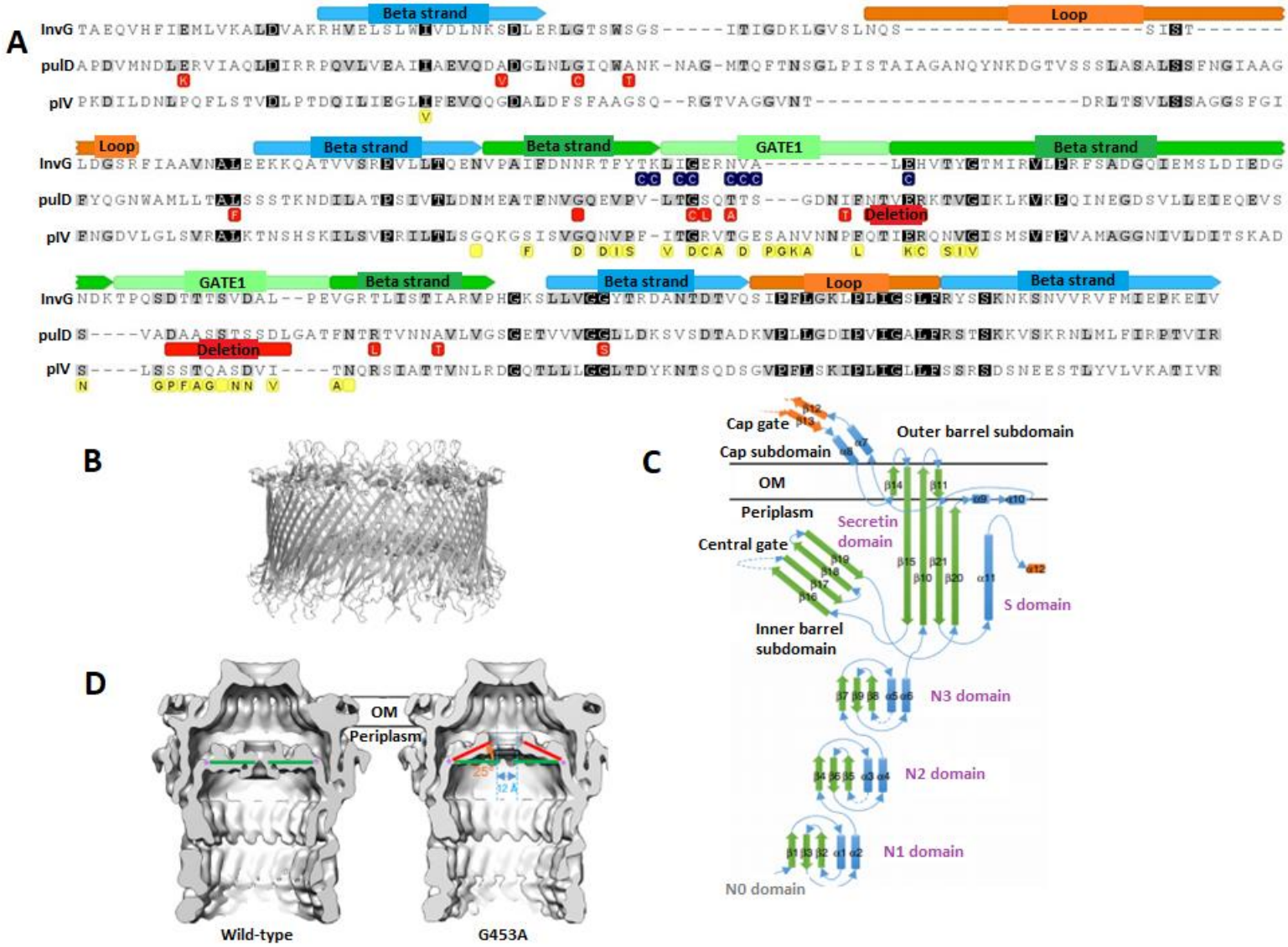
A
InvG
pulD
pIV
Beta strand
Loop
GATE1
Deletion
B
C
Cap gate
Outer barrel subdomain
Cap subdomain
OM
Periplasm
Secretin domain
Central gate
Inner barrel subdomain
S domain
N3 domain
N2 domain
N1 domain
N0 domain
D
OM
Periplasm
Wild-type
G453A

1.2.3 The model secretin, pIV

The filamentous bacteriophage f1 genome encodes the pIV secretin of the FFSS. The pIV channel is a multimer composed of 14 identical subunits with 14-fold radial symmetry (Figure 6B). It inserts into the OM as part of the FFSS (Figure 2), where it translocates filamentous bacteriophage into the extracellular environment. The opening and closing of the channel is likely regulated *via* a yet to be characterised conformational change (Opalka *et al.*, 2003).

The pIV channel has been used as a model for the T2SS, T3SS, and T4PS as, being the smallest of the homologues, it is relatively simple and has genetic versatility (because the secretion substrate (virion) carries the coding sequence for its own secretion system) (Marciano *et al.*, 2001; Russel, 1998; Russel, Linderoth, & Sali, 1997). Although high-resolution structural studies have not been carried out on pIV, high sequence similarity in the secretin homology domain in comparison with other secretins (for example, T2SS secretin, GspD (Yan *et al.*, 2017)), allows the structure to be modelled *in silico* (Figure 6A & 6B).

1.2.4 Leaky pIV mutants

A study by Spagnuolo *et al.* (2010) used random mutagenesis followed by positive selection to determine the residues involved in the gating of pIV. This resulted in the creation of “leaky” protein channels, which retained the correct folding and sometimes secretory function but had lost the ability to be gated (Spagnuolo *et al.*, 2010). The residues were mapped to two central areas within the conserved C-terminal domain named GATE1 and GATE2 (Figure 7A & 7B). Examples of leaky pIV mutants include pIV-E292K, which has a GATE1 mutation and pIV-S324G which has a mutation in GATE2. pIV-E292K contains a missense mutation in which a glutamic acid residue has been substituted for lysine at position 292. Comparatively, the pIV-S324G mutant has a missense mutation in which a serine residue has been substituted for glycine at position 324 (Spagnuolo *et al.*, 2010). It was suggested that these GATE regions were flanked by transmembrane β-sheets, facilitating a gating mechanism (Spagnuolo *et al.*, 2010).

The aforementioned near-atomic resolution study by Yan *et al.* (2017) supports the mapping of GATE1 and GATE2 to the central region of the channel gate (Spagnuolo *et al.*, 2010). Where, GATE1 is a β-hairpin that forms most of the gate and GATE2 forms a smaller loop above it (Figure 7C). Furthermore, the crystal structure of the GATE1 mutant, G453A, showed that the mutation caused the tilting of the β-hairpin towards the channel wall by 25°, resulting in pore formation (Figure 6D) (Yan *et al.*, 2017). This provides further support that the pIV mutant is leaky and that the mutation affects the gate or septum without adversely affecting the channel assembly or function.

A


C
M
N

B

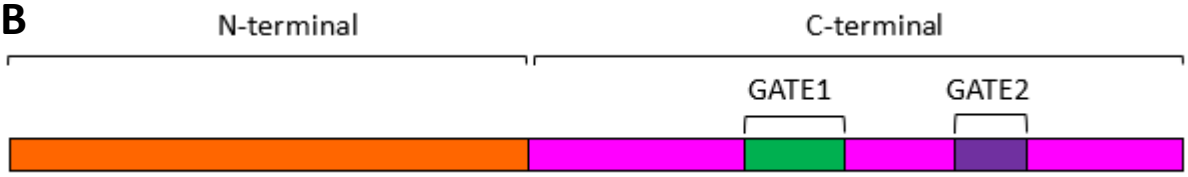
N-terminal
C-terminal
GATE1
GATE2

C

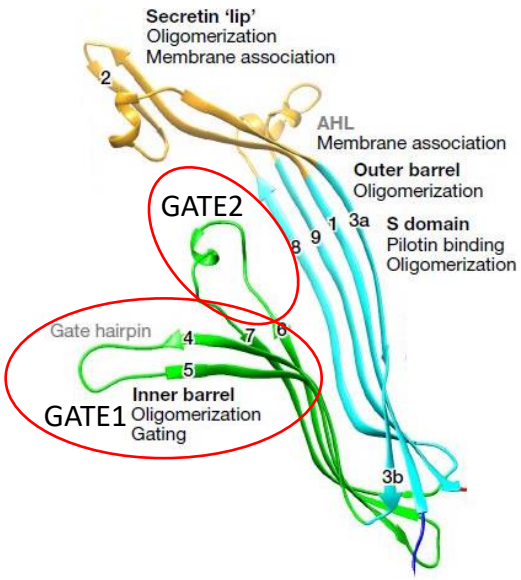
Secretin 'lip'
Oligomerization
Membrane association
2
AHL
Membrane association
Outer barrel
Oligomerization
GATE2
1
3a
S domain
Pilotin binding
Oligomerization
8
9
Gate hairpin
4
7
6
5
Inner barrel
GATE1
Oligomerization
Gating
3b

D

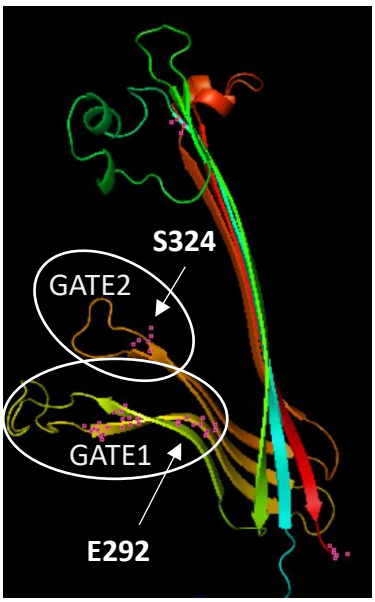
S324
GATE2
GATE1
E292

Figure 7: GATE1 and GATE2 domains of pIV and InvG secretins.

(A) Schematic representation of pIV and organisation of the C-terminal domain (C; light pink), M-ring (M; dark pink), and N-terminal domain (N; orange). Reproduced with permission from Spagnuolo *et al.* (2010). **(B)** A linear representation of pIV showing the N-terminal domain (orange) and C-terminal domain (pink) with the GATE1 (green) and GATE2 (purple) regions. Reproduced and modified with permission from Spagnuolo *et al.* (2010). **(C)** Secretin homology domain structure of InvG (T3SS secretin). Reproduced modified with permission from Worrall *et al.* (2016). The diagram shows N3 domain (blue), secretin domain outer β-sheet (cyan), secretin domain inner β –sheet (green), and secretin membrane association, AHL, and membrane insertion domain lip (gold). GATE regions (red circles), β-strand functional roles and numbers are indicated. **(D)** pIV secretin homology domain modelled on GspD (T2SS secretin) of *E. coli*. Positions of the mutations E292K and S324G (white arrows) which result in a leaky phenotype and GATE regions (white circles) are indicated.

Unlike wild-type pIV, leaky pIV mutants are also characterised by their permeability to maltopentaose, sensitivity to bile salts (deoxycholate), and/or sensitivity to vancomycin and bacitracin which would not normally penetrate the Gram-negative membrane (Spagnuolo *et al.*, 2010). Electrophysiology experiments revealed the increased permeability of leaky pIV in comparison with wild-type pIV. High voltage (200 mV) was required to open the wild-type pIV channel (Marciano *et al.*, 2001), while a significantly lower voltage of 80 mV was necessary to open the channel of leaky mutant, pIV-S324G (Marciano *et al.*, 1999).

Regarding the significance of these leaky mutants, it has been proposed that they are more representative of functioning secretin channels, because, in the absence of secretion, the wild-type secretin gate remains closed, in contrast to the leaky mutant, which remains open. Expression of the leaky mutant has been used as a method to examine the stress exerted on the Gram-negative cell during secretion when the channel is open (Spagnuolo, 2015).

1.3 Secretin-induced stress responses

Gram-negative bacteria utilise stress response pathways to maintain membrane integrity during secretin expression and virulence factor secretion. The insertion of large channels like secretins into the membrane disrupts membrane integrity and proton motive force (PMF) by allowing protons to leak across the inner membrane (IM) (Darwin, 2013). The three envelope stress responses include; Phage Shock Protein (Psp) response, Regulation of capsular synthesis (Rcs), and Conjugative plasmid expression (Cpx). In addition, Gram-negative bacteria also utilise the Superoxide stress response (Sox), which responds to oxidative stress in the cytoplasm. Upregulation of genes within these pathways and their corresponding regulons (groups of genes regulated by the same regulatory protein) in response to leaky or wild-type pIV expression in *E. coli* K-12 can be seen in Figure 8 (Spagnuolo, 2015).

It was originally thought that Cpx, Rcs, and Sox pathways were not induced by secretin stress (Bury-Mone *et al.*, 2009). However, the induction of Psp has previously been correlated with the mislocalisation of the secretin multimer into the IM. The secretin pIV induces Psp response as it inserts into both the IM and OM (Darwin, 2013). Moreover, all four pathways were recently shown to be upregulated in response to pIV-induced stress (Spagnuolo, 2015). To better understand Gram-negative bacterial pathogenesis, it would be useful to further elucidate the responses of these pathways to secretin-induced stress further.

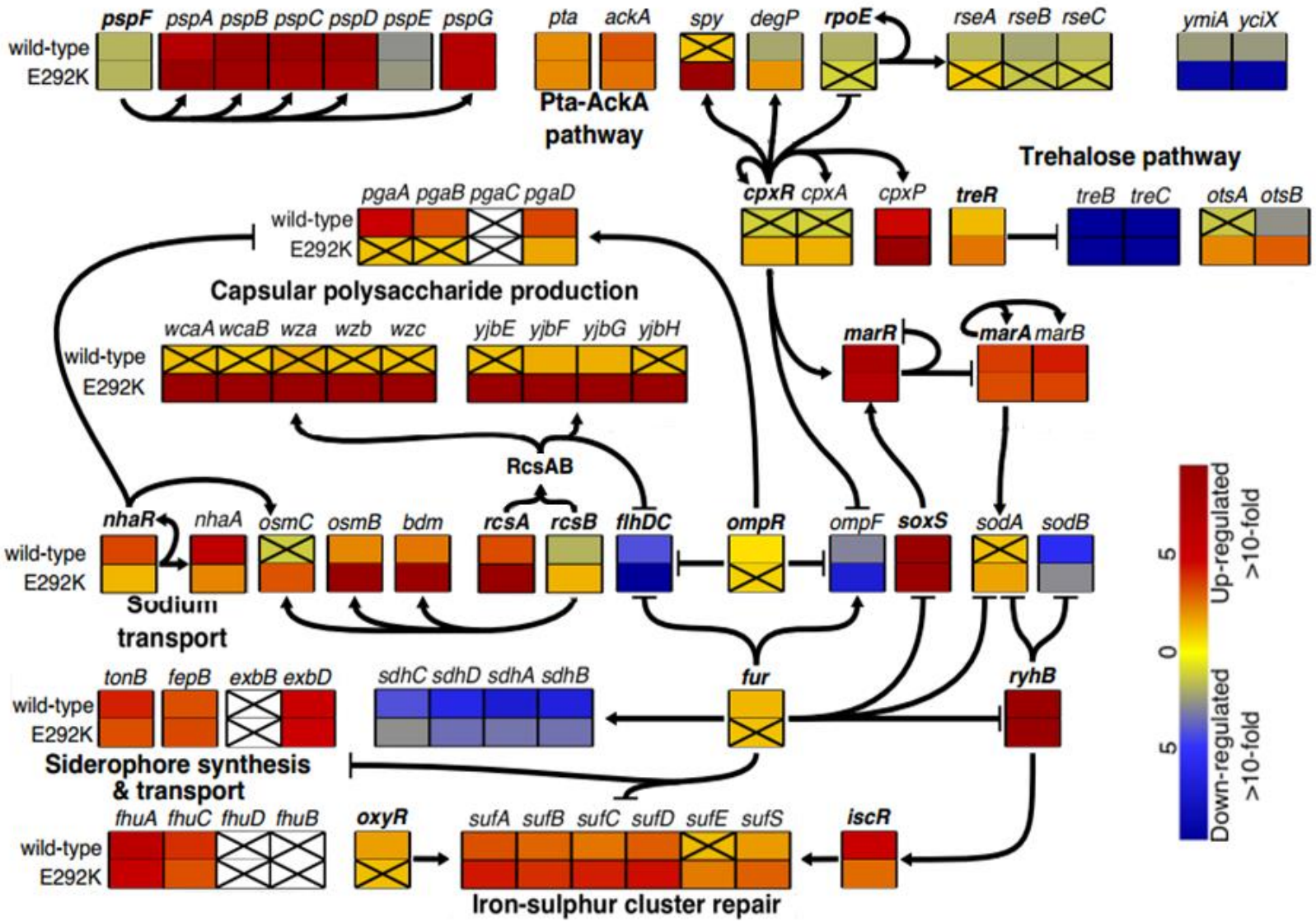
pspF pspA pspB pspC pspD pspE pspG
wild-type
E292K
pta ackA
Pta-AckA pathway
spy degP rpoE
rseA rseB rseC
ymiA yciX
Trehalose pathway
cpxR cpxA cpxP
treR
treB treC
otsA otsB
pgaA pgaB pgaC pgaD
wild-type
E292K
Capsular polysaccharide production
wcaA wcaB wza wzb wzc
yjbE yjbF yjbG yjbH
wild-type
E292K
marR
marA marB
RcsAB
nhaR nhaA osmC osmB bdm
rcsA rcsB
flhDC
ompR
ompF soxS
sodA sodB
wild-type
E292K
Sodium transport
tonB fepB exbB exbD
sdhC sdhD sdhA sdhB
fur
ryhB
wild-type
E292K
Siderophore synthesis & transport
fhuA fhuC fhuD fhuB
oxyR
sufA sufB sufC sufD sufE sufS
iscR
wild-type
E292K
Iron-sulphur cluster repair
5
0
5
Up-regulated >10-fold
Down-regulated >10-fold

Figure 8: Differential expression overview

Transcription factors are shown in bold; arrowhead shapes indicate the type of regulation according to published data; pointy and flat arrowheads indicate, respectively, positive and negative regulation. The expression of individual genes is shown as fold-change relative to the vector control. Cross-through boxes indicate non-significant differential expression (i.e. FDR > 0.05) (Spagnuolo, 2015). Reproduced with permission from Spagnuolo (2017) (Unpublished).

1.3.1 The phage shock protein (Psp) response

The Psp response (Figure 9) was initially discovered in response to filamentous phage infection of *E. coli* (Brissette, Russel, Weiner, & Model, 1990). Genes of the Psp response include the *pspABCDE* operon and *pspF*, which is located upstream from the pspABCDE operon and is divergently transcribed from a constitutive sigma-70-dependent promoter. The expression of an unlinked gene, *pspG*, is also induced and is co-regulated with the *pspABCDE* operon and *pspF*. In the absence of stress, PspA protein binds to and represses PspF, which prevents it from activating the other genes in the pathway. PspA is a negative regulator of the pathway, as in its absence, Psp expression is at high levels without inducing stimuli, and PspA null mutants don't have reduced survival in the presence of inducing stimuli (Jovanovic, Weiner, & Model, 1996). When induced, PspBC binds PspA by an unknown mechanism. This frees PspF, a sigma-54 transcriptional activator to interact with RNA polymerase holoenzyme allowing transcription of *pspA-E* and *pspG* (Yamaguchi, Reid, Rothenberg, & Darwin, 2013). PspE is a periplasmic rhodanese which has recently been shown to restore disulfide bonds in cell envelope proteins in conjunction with the protein DsbC (Chng *et al.*, 2012).

Several environmental conditions have been found that induce the Psp response to overcome membrane stress. This includes extreme heat shock (52°C), increased osmolarity, and ethanol treatment. Furthermore, the response is induced by expression of secretins and other large outer membrane channels that mislocalise into the inner membrane, most likely, dissipating proton motive force (PMF) (Brissette *et al.*, 1990; Jones, Lloyd, Tan, & Buck, 2003; Jovanovic *et al.*, 1996). The induction of Psp response due to secretin-induced stress has been documented (Darwin, 2013).

A recent study by Spagnuolo (2015) using RNA-Sequencing (RNA-Seq) analysis revealed that *pspA-D* and *pspG* transcription were upregulated 10-fold and 8-fold, respectively, upon induction of the leaky GATE1 mutant, pIV-E292K (Figure 8). In addition, *pspF* and *pspE* transcription was downregulated 2-fold (Spagnuolo, 2015), which has been mentioned previously (Lloyd *et al.*, 2004). Other stimuli that induce the expression of Psp genes include biofilm formation, bacterial protein secretion and translocation. Overload of the inner membrane protein translocation complex SecYEG, and mislocalised proteins in the membrane are also implicated (Beloin *et al.*, 2004; Jones *et al.*, 2003).

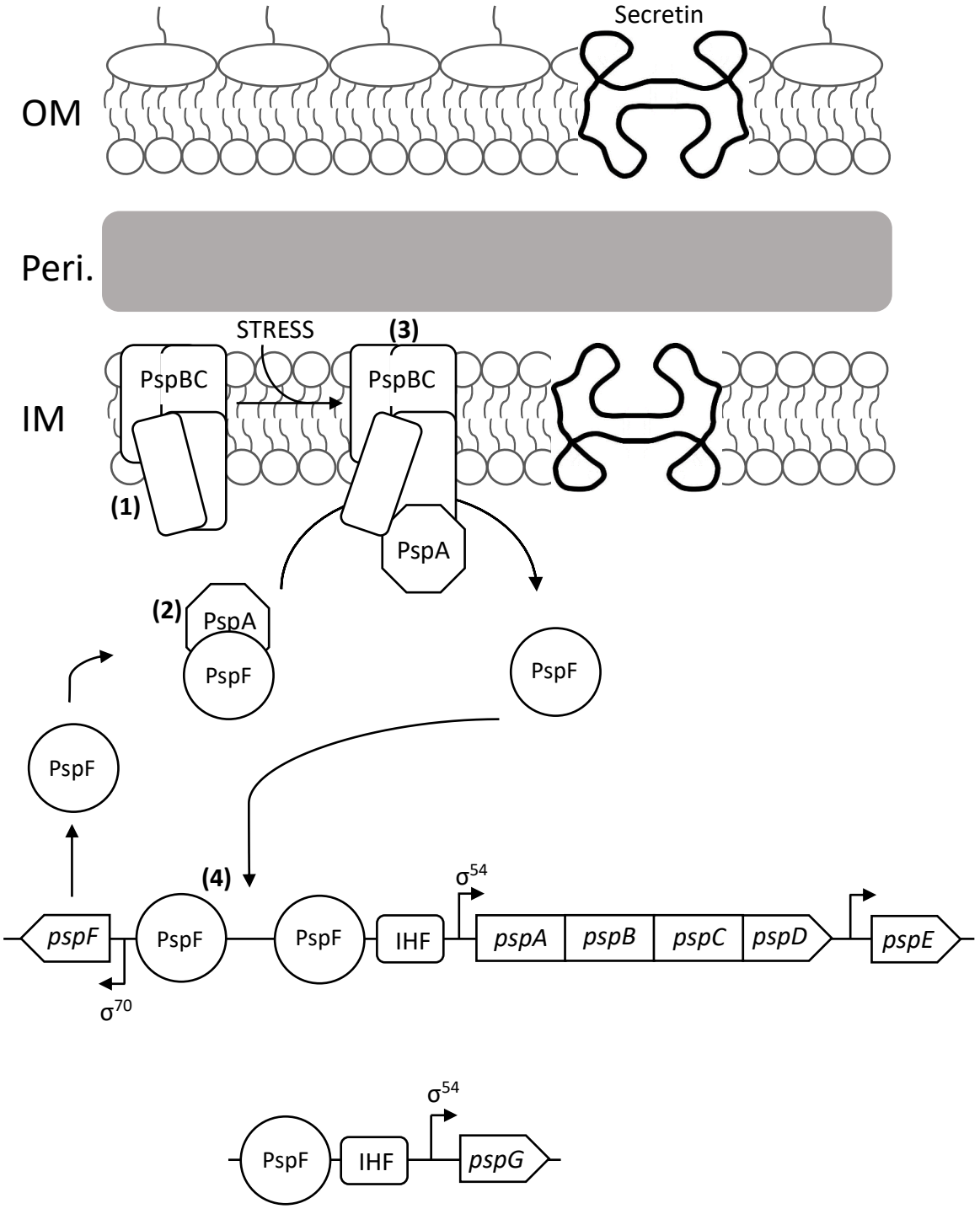
Secretin
OM
Peri.
IM
STRESS
(3)
PspBC
PspBC
(1)
PspA
(2)
PspA
PspF
PspF
PspF
(4)
σ54
pspF
PspF
PspF
IHF
pspA
pspB
pspC
pspD
pspE
σ70
σ54
PspF
IHF
pspG

Figure 9: Organisation and induction of the Phage Shock Protein response pathways.

(1) In the uninduced state, PspC covers the cytoplasmic domain of PspB which cannot bind PspA (the negative regulator). PspA binds to the response regulator PspF, inhibiting its activity. **(2)** In the event of membrane stress (e.g. mislocalisation of secretin into the inner membrane), PspC undergoes a conformational change and uncovers the cytoplasmic domain of PspB which then binds to PspA **(3)**. **(4)** PspF (a σ^{54} transcriptional activator) is then free to upregulate the *pspABCDE* operon, its own expression (the *pspF* gene under control of a σ^{70} dependent promoter), and unlinked gene *pspG*. The *pspA* and *pspG* promoters are σ^{54} dependent. Reproduced with modification and permission from Spagnuolo (2015).

1.3.2 The Rcs phosphorelay system

The Rcs response (Figure 10) is a phosphorelay system and is widely known to be involved in colanic acid capsular exopolysaccharide synthesis, which is considered to be important for biofilm formation (Laubacher & Ades, 2008; Pando, Karlinsey, Lara, Libby, & Fang, 2017). Known genes of the Rcs system include *rcsA, rcsB, rcsC, rcsD,* and *rcsF.* When induced by outer membrane and periplasmic stressors, the lipoprotein, RcsF, in the outer membrane, transmits a signal to the sensor kinase, RscC, in the inner membrane. RcsC then activates RcsB by phosphorylating one of its N-terminal aspartic acid residues. RcsD, a histidine-containing phosphotransmitter facilitates this activation of RcsB. RcsB is a transcriptional regulator that binds to DNA and upregulates target genes either as a homodimer or bound to RcsA as a heterodimer (Flores-Kim & Darwin, 2014). RcsA and RcsB both contain C-terminal helix-turn-helix motifs supporting their role as DNA binding proteins (Bury-Mone *et al.*, 2009).

It has been proposed that the Rcs system, directly and indirectly, affects the expression of up to 2.5% of the *E. coli* genome (Ferrieres, Aslam, Cooper, & Clarke, 2007). Target genes directly affected can be divided into two groups: RcsA-dependent (which typically induces the expression of capsular polysaccharide synthesis operons) and RcsA-independent. At RcsA-dependent targets, RcsB binds with RcsA 50-100 nucleotides upstream from the -35 promoter to a conserved RcsAB box, and RcsA is thought to enhance the regulatory activity of RcsB. RcsB homodimers ($RcsB_2$) can also regulate gene expression in the absence of RcsA (Pannen, Fabisch, Gausling, & Schnetz, 2016) by binding to a conserved box situated directly after the -35 promoter (Wehland & Bernhard, 2000). Targets for $RcsB_2$ binding include genes for cell division, protein folding and sorting, osmotic shock and acid resistance, and the alternative sigma factor, RpoS/σ^{38} (Francez-Charlot *et al.*, 2003; Krin, Danchin, & Soutourina, 2010). In addition, the genes *bdm* and *osmB* encoding a motility modulator, and osmotically inducible lipoprotein, respectively, were highly upregulated in response to leaky pIV-E292K expression (Figure 8) (Spagnuolo, 2015). These genes are controlled by $RcsB_2$ indicating an upregulation of the Rcs phosphorelay in the presence of secretin-induced stress (Spagnuolo, 2015).

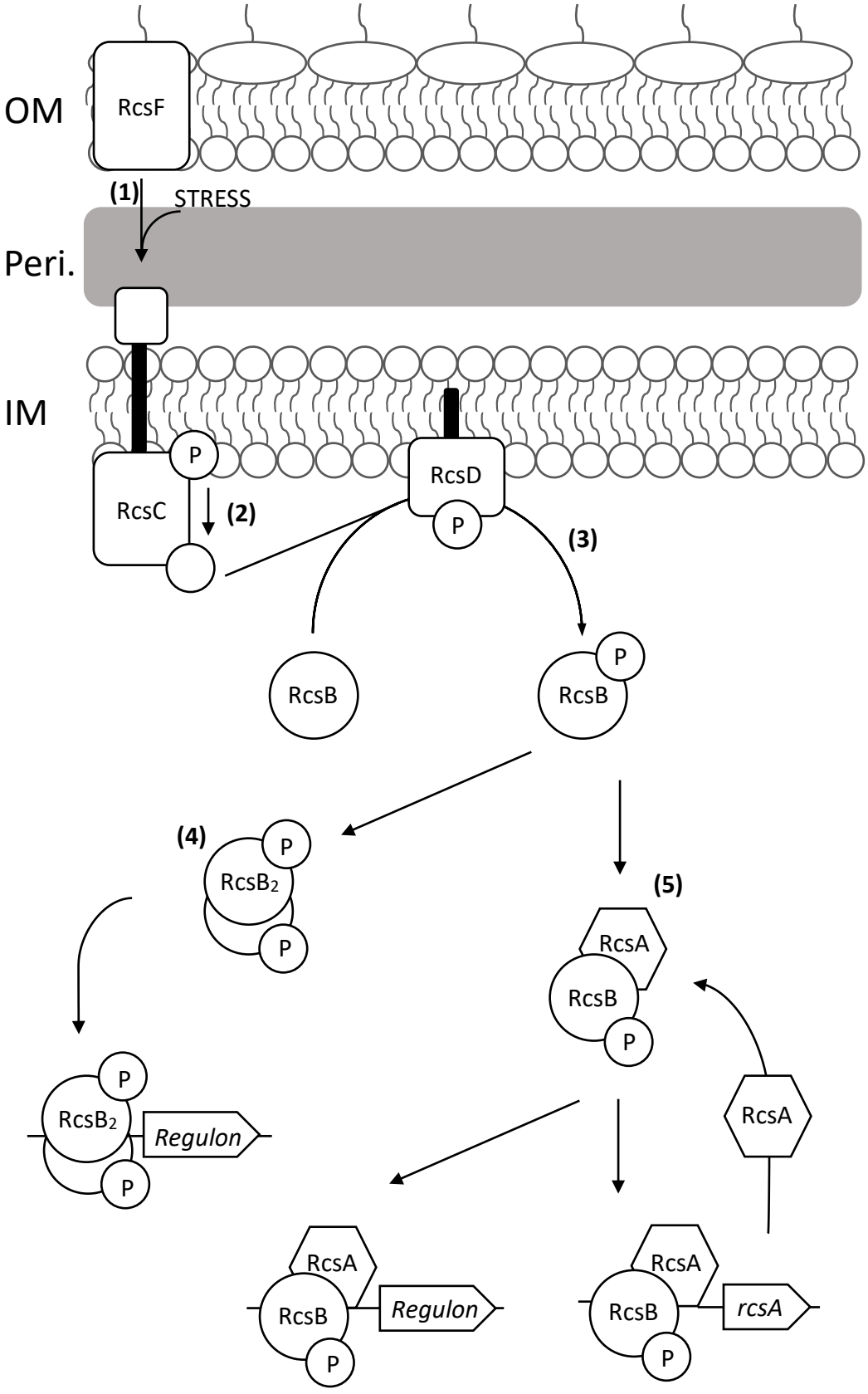
OM
RcsF
(1)
STRESS
Peri.
IM
P
RcsC
(2)
RcsD
P
(3)
RcsB
RcsB
P
(4)
P
RcsB2
P
(5)
RcsA
RcsB
P
P
RcsB2
Regulon
P
RcsA
RcsA
RcsB
Regulon
P
RcsA
RcsB
rcsA
P

Figure 10: Organisation and induction of the Rcs phosphorelay system.

Upon induction of the pathway **(1)**, RcsF, in the outer membrane, transmits a signal to RcsC sensor kinase in the inner membrane. Damage to the peptidoglycan may directly stimulate RcsC. RcsC transfers phosphate to RcsD **(2)** which phosphorylates and activates RcsB **(3)**. RcsB may then form a homodimer and regulate the expression of RcsA-independent genes **(4)** or form a heterodimer with RcsA to regulate the expression of RcsA-dependent genes and *rcsA* **(5)**. Reproduced with modification and permission from Spagnuolo (2015).

1.3.3 The Cpx two-component regulatory system

The Cpx regulatory system (Figure 11), encoded by the *cpxRA* operon, is often thought to be required for conjugal DNA transfer and controls the expression of 38 other transcriptional units (Raivio, Popkin, & Silhavy, 1999). Upon induction, CpxA, the inner membrane sensor kinase, is autophosphorylated. The signal is then transmitted by subsequent phosphorylation of the response regulator, CpxR, which targets down-stream stress-mediating genes. The gene *cpxP,* which encodes the periplasmic protein, CpxP, is located upstream of the *cpxRA* operon. CpxP inhibits the system during non-inducing conditions by binding phosphorylated CpxA to its operator. Structural studies show CpxP has a concave surface made up of positively charged residues that allow inhibitory activity by binding to the negatively charged residues of CpxA's periplasmic domain (Zhou *et al.*, 2011).

Since its discovery, the Cpx response has been implicated in responses to several different inducers, including; alkaline pH, overproduction of extracytoplasmic proteins, detection of cell adhesion to surfaces, misfolded proteins, and overproduction of the protein, NlpE. Genes upregulated by CpxR include *dsbA*, *degP*, *rotA, ppiA,* and *ppiD* which are all involved in protein folding (Duguay & Silhavy, 2004; Hunke, Keller, & Müller, 2011) Furthermore, a recent study by Spagnuolo (2015) found that *cpxP* is upregulated as a result of leaky pIV-E292K expression, suggesting an involvement of the pathway in mediation of secretin-induced stress (Figure 8).

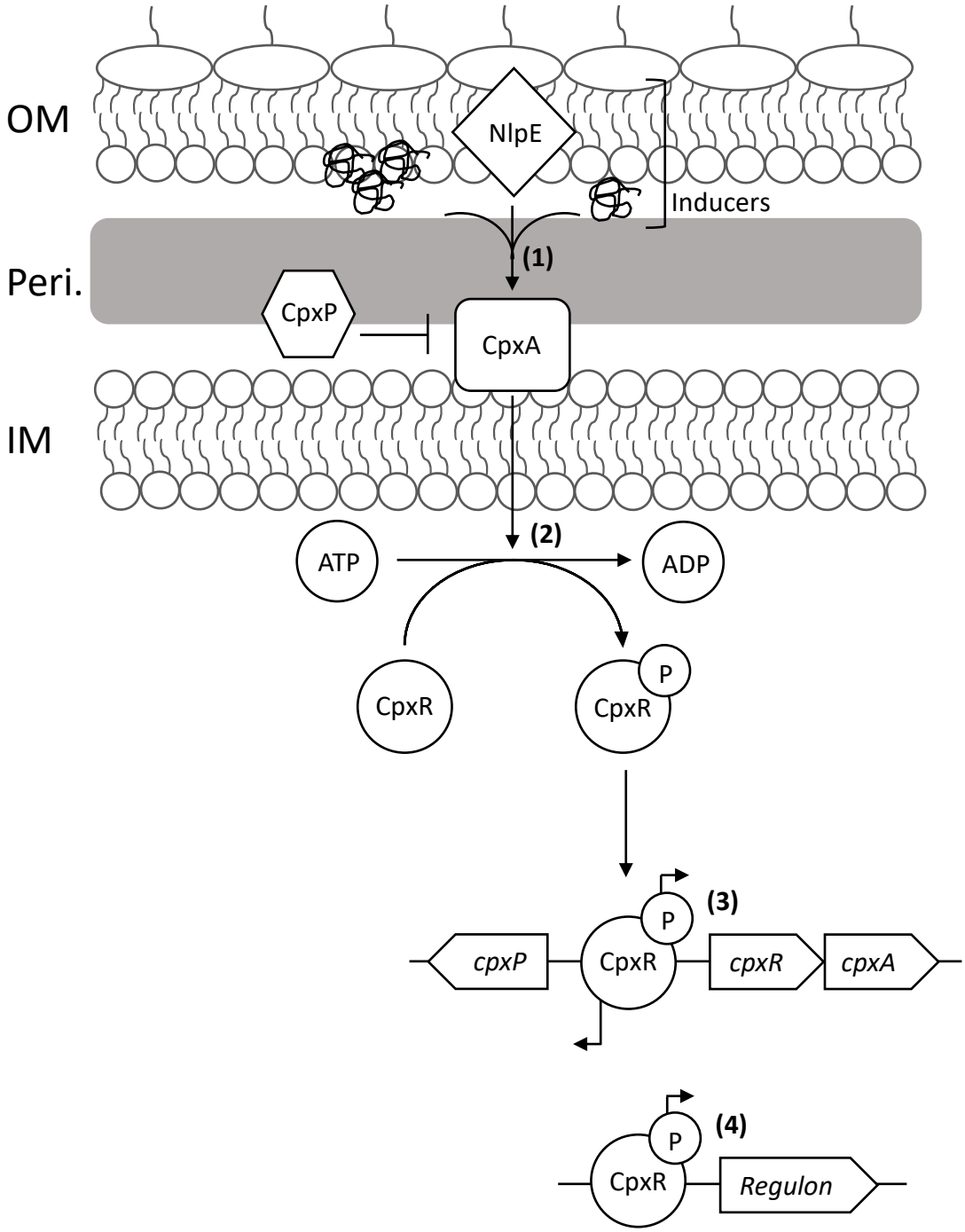
OM
Peri.
IM
NlpE
Inducers
(1)
CpxP
CpxA
(2)
ATP
ADP
CpxR
P
CpxR
(3)
P
cpxP
CpxR
cpxR
cpxA
(4)
P
CpxR
Regulon

Figure 11: Organisation and induction of the Cpx two component regulatory system.

In the absence of membrane stress, CpxP inhibits activation of CpxA and the pathway is uninduced. The cytoplasmic ATPase domain of CpxA is induced by aggregated or misfolded proteins, or the overproduction of specific protein NlpE (the inducers) **(1)**. The response regulator, CpxR, is then activated by phosphorylation **(2)** and regulates the expression of the *cpx* operon **(3)** and stress mediating genes (*Regulon*) **(4)**. Reproduced with modification and permission from Spagnuolo (2015).

1.3.4 The soxRS signal transduction pathway

The SoxRS pathway (Figure 12) upregulates genes to prevent and mitigate stress resulting from the presence of reactive oxygen species (ROS) in Gram-negative bacteria. Sources of oxidative stress include products of aerobic metabolism and oxidants produced as a result of the activation of the host immune response (Blanchard, Wholey, Conlon, & Pomposiello, 2007). The pathway is composed of two cytoplasmic proteins: SoxR (the redox-sensing transcriptional activator) and SoxS (a DNA-binding transcriptional activator). In both inducing and non-inducing conditions, SoxR binds to the operator of *soxS*. SoxR is a dimer that contains one [2Fe-2S] cluster per monomer and can only upregulate the expression of *soxS* when the cluster is in the oxidised, not reduced state. The reduction of the [2Fe-2S] cluster is NADPH dependent, however, during oxidative stress, NADPH is depleted in the cell. This prevents the reduction and inactivation of SoxR and allows the upregulation of *soxS* and subsequent expression of ROS-induced stress mediating genes including *sodA* (superoxide dismutase) and *katE* (catalase) (Srijaruskul *et al.*, 2015). Interestingly, it appears that open secretin channels do not increase ROS stress, as *soxS* transcription has been shown to be upregulated in response to wild-type pIV expression, not leaky pIV (Figure 8) (Spagnuolo, 2015).

Figure 12: Organisation and induction of the SoxRS signal transduction pathway.

The proteins SoxR and SoxS regulate the superoxide stress response. When uninduced, SoxR is reduced by NADPH-dependent activity **(1)**. In the presence of superoxide ($O_2^{-}\cdot$), SoxR is oxidised **(2)** allowing it to upregulate *soxS* expression and regulate its own expression. SoxS is a DNA-binding transcriptional regulator which controls the expression of superoxide stress-mediating genes (*Regulon*) **(4)**. Reproduced with modification and permission from Spagnuolo (2015).

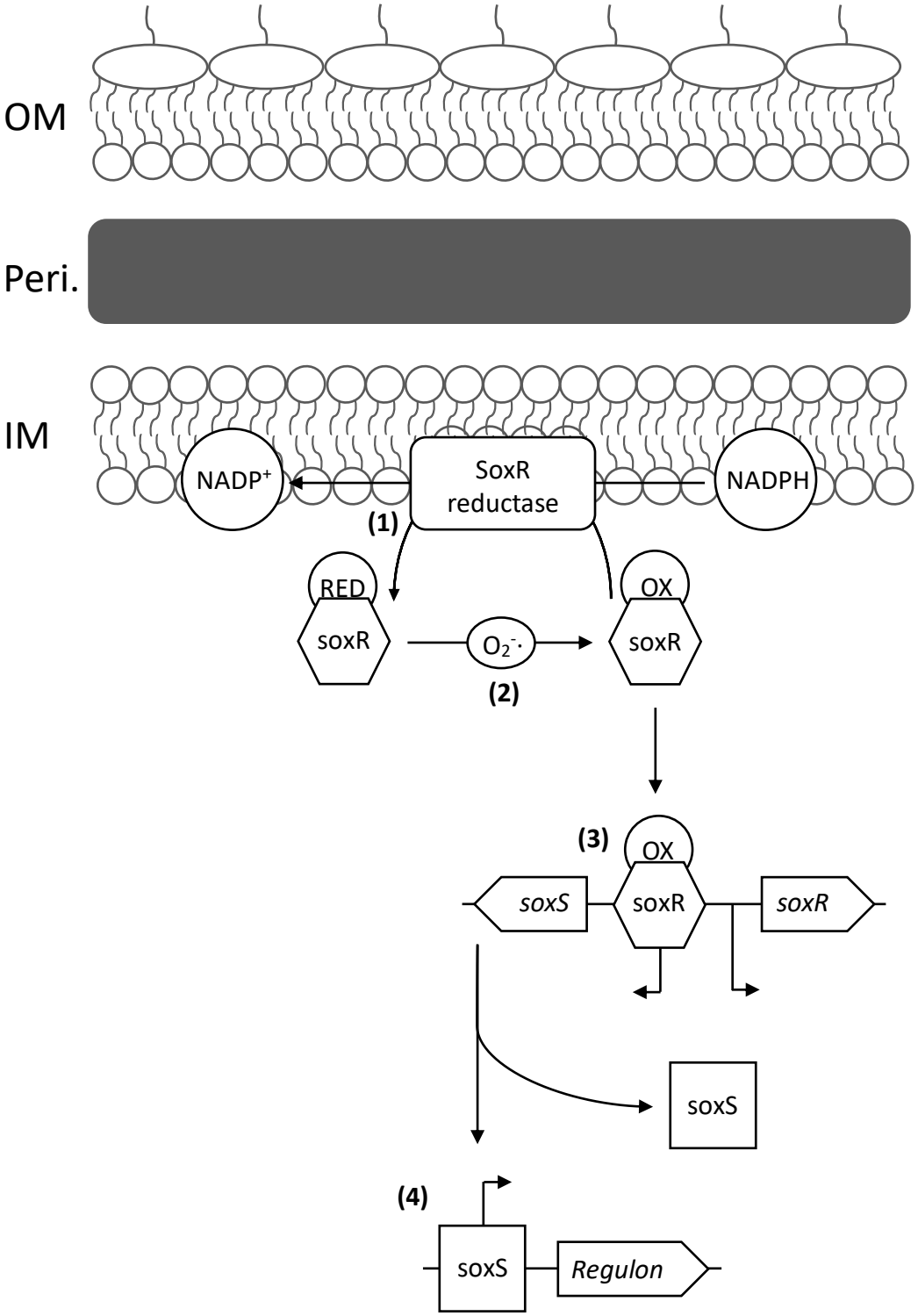
OM
Peri.
IM
NADP+
SoxR
reductase
NADPH
(1)
RED
soxR
O2-·
OX
soxR
(2)
(3)
OX
soxS
soxR
soxR
soxS
(4)
soxS
Regulon

1.3.5 Response pathways required for secretin-induced stress

The activation of these stress responses causes alterations in gene expression which allows for the preservation of membrane integrity in response to secretin-mediated stress (Spagnuolo, 2015). As the Psp, Rcs, Cpx, and Sox pathways regulate genes enabling a pathogenic phenotype (expression of a functional secretion system), a possible strategy against disease is to target components of these pathways (Worthington, Blackledge, & Melander, 2013). Microarray transcriptome analysis on cells expressing the wild-type FFSS secretin pIV, and the T3SS secretin, YsaC, from *Yersinia enterocolitica* showed induction of the Psp regulon but not the regulons of several other stress responses (Jovanovic, Lloyd, Stumpf, Mayhew, & Buck, 2006). If these pathways are required for the survival of Gram-negative bacteria secreting virulence factors, these pathways as a whole and specific effectors could be potential drug targets that when inactivated, allow the killing of pathogenic bacteria (Costa *et al.*, 2015). This, in turn, would provide a means to combat infections by Gram-negative bacteria, some of which urgently require the discovery of new antibiotics for treatment (Bonomo *et al.*, 2017; Karaiskos & Giamarellou, 2014; Wellington *et al.*, 2013; Zowawi *et al.*, 2015).

1.4 Aims

This aims of this project are to:

1. Identify the stress response pathways that are required for the survival of leaky pIV secretin expression, and
2. Use transmission electron microscopy (TEM) to determine the effect of leaky secretin on the bacterial cell membrane.

Chapter Two: Materials and Methods

2.1 Bacterial strains, Plasmids, and growth conditions

All bacterial strains are laboratory *E. coli* K-12 strains and are shown in Table 1. The plasmids used in this work are listed in Table 2.

All cultures were grown in 2xYT (Difco™, Bectone-Dickinson) liquid media with shaking or on 2xYT solid media (1% v/v bacteriological agar (Neogen)) at 37°C for 18 hours (Sambrook, Fritsch, & Maniatis, 1989) unless otherwise specified. Dilutions were performed in 2xYT liquid media unless otherwise stated.

The liquid or solid media was supplemented with the appropriate antibiotic for selection based on antibiotic resistance markers; tetracycline (Tet, 10 µg/mL), chloramphenicol (Cm, 25 µg/mL), kanamycin (Km, 50 µg/mL), or ampicillin (Amp, 100 µg/mL). Plasmids containing the *tac* promoter were induced on 2xYT solid media by the addition of isopropyl β-*D*-1-thiogalactopyranoside (IPTG) at 0.1 mM or 1 mM. Plasmids containing the araBAD promoter were induced on solid media containing arabinose (2 g per litre) or repressed with the addition of glucose (2 g per litre). All antibiotics and IPTG were purchased from GoldBio (USA). All analytical grade chemicals were sourced from Sigma Aldrich unless otherwise stated.

Table 1: Bacterial strains.

Strain	Parent	Genotype	Reference
K1822	MC1061	MC1061, Hfr	(Feng *et al.*, 1999)
BW25113		F-, Δ(*araD-araB*)*567*, Δ*lacZ4787*(::*rrnB-3*), λ$^-$, *rph-1*, Δ(*rhaD-rhaB*)*568*, hsdR514	(Baba *et al.*, 2006)
JW2205-2	BW25113	BW25113, Δ*rcsB::kan*	(Baba *et al.*, 2006)
JW1296-5	BW25113	BW25113, Δ*pspF::kan*	(Baba *et al.*, 2006)
JW3883-1	BW25113	BW25113, Δ*cpxR::kan*	(Baba *et al.*, 2006)
JW4023-5	BW25113	BW25113, Δ*soxS::kan*	(Baba *et al.*, 2006)
K1508	MC4100	MC4100, *ΔlamB106*	(Baneyx & Georgiou, 1991)
K2384	K1508	K1508, *ΔcpxR772*	(Rehm, 2016)
K2385	K1508	K1508, *ΔrcsB770*	(Rehm, 2016)
K2386	K1508	K1508, *ΔsoxS756*	(Rehm, 2016)
K2388	K1508	K1508, *ΔpspF739*	(Rehm, 2016)
K2458	K1508	K1508, *ΔrcsA726*	(Khanum, 2015) KnR marker removed by FLP recombination by expression of FLP recombinase from plasmid pCP20 (Cherepanov & Wackernagel, 1995).
K2459	K1508	K1508, *ΔsoxR757*	(Khanum, 2015) KnR marker removed by FLP recombination using by expression of FLP recombinase from plasmid pCP20 (Cherepanov & Wackernagel, 1995).

Table 2: Plasmids.

Plasmid	Description	Reference
pGZ119EH	Contains a Cm^R marker and *colD* origin of replication; protein expression cassette is driven by the *tac* promoter.	(Lessl *et al.*, 1992)
pPMR132	A derivative of pGZ119EH; expresses *gIV* wild-type under the control of the *tac* promoter.	(Linderoth, Model, & Russel, 1996; Linderoth, Simon, & Russel, 1997)
pPMR132-E292K	Mutant of pPMR132 encoding pIV containing E292 → K missense mutation.	(Spagnuolo, 2015)
pGZ119EHt	pGZ119EH containing the Tet^R marker instead of the Cm^R marker.	(Spagnuolo, 2015)
pPMR132t	pPMR132 containing the Tet^R marker instead of the Cm^R marker.	(Spagnuolo, 2015)
pPMR132t-E292K	pPMR132-E292K containing the Tet^R marker instead of the Cm^R marker.	(Spagnuolo, 2015)
pSB-RcsB	Kan^R marker and ColA origin of replication; driven by the araBAD promoter with corresponding regulator gene, *araC*. Constructed to contain the gene, *rcsB.*	This study

Table 2: Plasmids (Continued).

Plasmid	Description	Reference
pCA24N-RcsB[a]	pCA24N*::rcsB, Δgfp.* Complementation vector for K2385.	(Kitagawa *et al.*, 2005)
pBAD/gIII	Contains an expression cassette (encoding an N-terminal gIII signal sequence, and C-terminal polyhistidine (6xHis) tag and *c-myc* epitope) containing an *ara*BAD promoter (araBAD) regulated *via* the *araC* gene, Amp^R marker, and pBR322 origin of replication.	(Guzman, Belin, Carson, & Beckwith, 1995)
pCOLADuet™-1	Contains two multiple cloning sites (encoding a His-tag or S-tag) regulated by a *T7-lac* promoter, Kn^R marker, and ColA origin of replication.	(Tolia & Joshua-Tor, 2006)

[a]pCA24N vector (Kitagawa *et al.*, 2005) contains an expression cassette (encoding an N-terminal His-tag and a C-terminal GFP tag) controlled by *T5-lac* promoter, Cm^R marker and pUC (high-copy-number) origin of replication. For the plasmid used in this work, the sequence encoding the C-terminal GFP tag was deleted from all pCA24N-derived plasmids, as described by Spagnuolo (2015).

2.2 Construction of a novel expression plasmid containing a Kan^R marker and the araBAD promoter

Construction of the vector, named pSB-RcsB, was carried out by PCR and by Gibson Assembly (Gibson *et al.*, 2009) using the NEBuilder HiFi DNA Assembly master mix (New England Biolabs). The PCR was used for amplifying three sections in three reactions with primer pairs listed in Table 3 (Integrated DNA Technologies, US). Primers were designed to amplify the araBAD promoter and *araC* of the pBAD/gIII vector (Invitrogen); *rrnB-T1* terminator and *rcsB* of pCA24N-RcsB; and, Kan^R and ColA origin of replication from pCOLA-Duet^{TM}-1 (Novagen). For the construction of pSB-RcsB, primer pairs include; SB001 and SB002; SB003 and SB004; and SB005 and SB006. The template for the three reactions were pBAD/gIII, pCA24N-RcsB, and pCOLAduet^{TM}-1, respectively. Polymerase PRIMESTAR (Takara, Japan) was used for all PCR amplifications, according to the T_m of the specific primers, processivity of polymerase, and the manufacturer's instructions. The PCR products were joined, without purification, with NEBuilder HiFi DNA Assembly master mix (New England Biolabs), according to the manufacturer's instructions. The mixture was used for transformation by electroporation (see 2.4.2) into electrocompetent K1822 cells. Individual colonies from agar plates containing kanamycin were isolated and the plasmid DNA purified (see 2.5). The plasmid was purified from the transformants and analysed by restriction endonuclease analysis (enzyme was from New England Biolabs) and sequenced (BigDye® Terminator V3.1 Chemistry; Massey Genome Service, NZ) using two primers (SBSeq1 and SBSeq2) that flanked the promoter region and *rcsB* (Table 3).

Table 3: List of primers.

Primer	Sequence (5'–3')	Details
SB001 [a]	ctagatttcagtgcaatttatctCAAATGGACGAAGCAGGGAT	pBAD/gIII, forward, Gibson Assembly
SB002 [a]	tcatattgttggccctcagggccggCATGGTTAATTCCTCCTGTTAG	pBAD/gIII, reverse, Gibson Assembly
SB003 [a]	gctaacaggaggaattaaccatgCCGGCCCTGAGGGCCAACA	pCA24N(rcsB), forward, Gibson Assembly
SB004 [a]	ttctaagaattaattcatgagcACCTATAAAAATAGGCGTATCACG	pCA24N(rcsB), reverse, Gibson Assembly
SB005 [a]	tcgtgatacgcctatttttataggtGCTCATGAATTAATTCTTAGA	pCOLAduet™-1, forward, Gibson Assembly
SB006 [a]	cagaatccctgcttcgtccatttgaGATAAATTGCACTGAAATCTA	pCOLAduet™-1, reverse, Gibson Assembly
SBSeq1	CGA ATG GTG AGA TTG AGA ATA	pSB-RcsB, forward, sequencing
SBSeq2	TCA CCG TCA TCA CCG AAA C	pSB-RcsB, reverse, sequencing

[a]Overhang regions used for cloning by NEBuilder HiFi DNA Assembly Cloning Kit are indicated by lowercase letters.

2.3 Generation of competent cells

2.3.1 Generation of chemically competent cells

Chemically competent cells were generated as described previously by (Sambrook *et al.*, 1989), with modification. Overnight cultures were diluted 100-fold in 100 mL of 2xYT medium and grown at 37°C with shaking. The subcultures were incubated on ice for 20 minutes once an optical density of 0.15-0.2 at 600 nm (OD_{600}) was reached (Multiskan GO spectrophotometer, Thermo Scientific). Following this, the cells were pelleted by centrifugation at 3,000 x g for 10 minutes at 4°C and the supernatant was discarded. The individual pellets were then gently re-suspended with 20 mL 0.1 M $CaCl_2$ and centrifuged once more at 3,000 x g for 5 minutes at 4°C. The supernatants were again discarded, and the individual pellets re-suspended in 2 mL of a 10% v/v glycerol and 0.1 M $CaCl_2$ solution. Aliquots of 50 µL were then dispensed into separate 1.7 mL Eppendorf tubes and either stored at -80°C or used immediately for transformation.

2.3.2 Generation of electrocompetent cells

Electro-competent cells were generated as described previously by Jacobsson, Rosander, Bjerketorp, and Frykberg (2003), with modification. Overnight cultures were diluted 100-fold in 100 mL of 2xYT medium and grown at 37°C with shaking. The subcultures were incubated on ice for 30 minutes once an optical density of 0.5-0.6 at 600 nm (OD_{600nm}) was reached (Multiskan GO spectrophotometer, Thermo Scientific). Following this, they were pelleted by centrifugation at 4,000 x g for 20 minutes at 4°C, and the supernatant was discarded. The individual pellets were then gently re-suspended with 50 mL of 10% v/v glycerol. These centrifugation and resuspension steps were repeated two more times; the pellet was then resuspended in an equal volume of 10% glycerol. The cells were distributed into 1.7 mL Eppendorf tubes in 50 µL aliquots and used immediately for transformation or stored at -80°C.

2.4 Transformation

2.4.1 Transformation by heat-shock

Transformation of chemically competent cells by heat-shock was carried out as previously described by Sambrook *et al.* (1989), with modification. Plasmid DNA was added to aliquots of chemically competent cells (30 µL) for a final concentration of 10 ng/µL. The cells were incubated on ice for 45 minutes before being heat shocked in a 42°C water bath for 1 minute. Following this, the cells were placed on ice for a further 2 minutes and then mixed with 1 mL of 2xYT liquid media before being incubated at 37°C for 1 hour, with shaking. The transformants were selected by plating on 2xYT agar plates supplemented with the appropriate antibiotic and incubated for 18 hours at 37°C.

2.4.2 Transformation by electroporation

Transformation of electrocompetent cells by electroporation was carried out as previously described by Sambrook *et al.* (1989), with modification. Plasmid DNA was added to 50 µL aliquots of electrocompetent cells in an electroporation cuvette for a final concentration of 10 ng/µL. The resultant mixture was mixed and then incubated on ice for 1 minute. A brief 2.5 kV pulse was applied using a MicroPulser™ electroporator (Bio-Rad) before the addition of 950 µL SOC broth (2% w/v tryptone, 0.5% w/v yeast extract, 10 mM NaCl, 2.5 mM KCl, 10 mM $MgCl_2$, 20 mM glucose). The cells were then incubated, with shaking, for 1 hour at 37°C. The transformants were selected for by plating on 2xYT agar plates supplemented with the appropriate antibiotic and incubated for 18 hours at 37°C.

2.5 Plasmid isolation and purification

Plasmids were isolated using the High Pure Plasmid Isolation Kit (Roche) from 4 mL overnight liquid cultures, according to the manufacturer's instructions. Quantification of plasmid DNA was then carried out using the NanoDrop ND-1000 UV-Vis spectrophotometer, according to the manufacturer's instructions. All plasmid DNA was stored at -20°C.

2.6 Phenotypic Characterisation of Mutant Strains

2.6.1 Synthetic lethality assay

The ability of K1508 and the chromosomal deletion mutants (*ΔcpxR, ΔrcsB, ΔsoxS, ΔpspF, ΔrcsA,* and *ΔsoxR*) to form colonies was assessed when each expressed either wild-type pIV or the leaky variant, pIV-E292K. Chemically competent cells of K1508, K2384, K2385, K2386, K2388, K2458, and K2459 were transformed *via* heat-shock (see 2.4.1) with wild-type pIV (pPMR132t or pPMR132), pIV-E292K (pPMR132-E292Kt or pPMR132-E292K), or a vector control with no pIV (pGZ119EHt or pGZ119EH) (see 3.2.1 & 3.1.2). Alternatively, chemically competent cells of BW25113, JW2205-2, JW1296-5, JW3883-1, and JW4023-5 were transformed *via* heat shock with wild-type pIV (pPMR132), pIV-E292K (pPMR132-E292K), or the vector control (pGZ119EH) (see 3.1.1). Three colonies from each transformation plate were picked to inoculate separate 3 mL overnight cultures, supplemented with the appropriate antibiotic. The cultures were then serially diluted up to 10^6-fold in triplicate (that is, three biological and technical replicates). Dilutions were plated on a quarter plate of 2xYT solid media (referred to as titration plates) containing the appropriate antibiotic and either 0.1 mM or 1 mM IPTG for plasmid gene induction, or no IPTG. Plates were then incubated at 37°C for 18 hours. Colonies were counted at a dilution that produced between 100 and 500 colonies. Plating efficiency of transformants in the presence or absence of IPTG was calculated relative to the vector control.

2.6.2 Complementation

The single gene deleted in K2385 was reintroduced to determine cell viability when expression of wild-type pIV or leaky variant, pIV-E292K, occurred. Chemically competent cells of K2385 were transformed *via* heat-shock with complementing plasmid, pSB-RcsB, and plated on solid, non-inducing media. A single colony was selected to inoculate separate 3 mL overnight cultures, supplemented with the appropriate antibiotic. Following which, chemically competent cells were generated of the transformants (see 2.3.1). These competent cells were subsequently transformed *via* heat-shock with wild-type pIV (pPMR132), pIV-E292K (pPMR132-E292K), or a vector control with no pIV (pGZ119EH). Three colonies from each transformation plate were picked to inoculate separate 3 mL overnight cultures, supplemented with the appropriate antibiotics. The cultures were then serially diluted up to 10^6-fold in triplicate (that is, three biological and technical replicates). Dilutions were plated on a quarter plate of 2xYT solid media that induces (contains arabinose) or represses expression (contains glucose) of the complementing plasmid. The agar also contained the appropriate antibiotics and either 0.1 mM or 1 mM IPTG, or no IPTG. After incubation at 37°C for 18 hours, the colonies were counted at a dilution that produced between 100 and 500 colonies. Plating efficiency of transformants containing the complementing plasmid in the presence or absence of IPTG was calculated relative to the vector control.

2.6.3 Vancomycin susceptibility assay

Vancomycin susceptibility was assayed on 2xYT solid media using ETest® strips (BioMèrieux) that provide a concentration gradient of 0.016 to 256 µg/mL of vancomycin. The plates contained the appropriate antibiotic for plasmid maintenance and 0.1 mM IPTG for plasmid expression. Fresh overnight cultures of transformants (inoculated separately from transformant plates and titration plates containing 1 mM IPTG) were diluted 100-fold. Once dry, a single ETest® strip was added per plate followed by incubation at 37°C for 18 hours.

Each plate was then observed for either resistance (no zone of growth inhibition) or sensitivity (zone of growth inhibition present) to vancomycin. If sensitive, the minimum inhibitory concentration (MIC) was recorded.

2.6.4 Mucoidy

Overnight cultures of transformants (inoculated with a single colony from the transformation plates and synthetic lethality plates containing 1 mM IPTG) were diluted 10^4-fold. Then, 100 µL was plated onto solid inducing media and incubated for 18 hours at 37°C to visualise any mucoid phenotype.

2.6.5 Transmission Electron Microscopy

To prepare bacteria for visualisation *via* transmission electron microscopy (TEM), the overnight cultures of fresh transformants were diluted 10^4-fold and plated on 2xYT solid media supplemented with the appropriate antibiotic and 0.1 mM IPTG. These were incubated for 18 hours at 37°C. Colonies were then scratched off the plate and suspended in 1 mL of primary fixative consisting of 3% v/v glutaraldehyde (Merck) and 0.25% w.v Ruthenium Red (ProSciTech, Aus) in 0.1 M pH 7.2 phosphate buffer. The suspension was then left at room temperature for 2 hours followed by centrifugation at 4,000 rpm (Heraeus Pico 17, Thermo Scientific) for 4 minutes. The supernatant was then discarded and 1 mL of molten, yet cooled, 3% low temperature melting agarose was added and mixed. This suspension was then centrifuged as prior and allowed to set. Following this, the sediment was removed from the tube and any excess agarose cut off and discarded. The sediment was thinly sliced and washed with 0.1 M phosphate buffer (pH 7.2) for 30 minutes, replacing the buffer at 10-minute intervals. Subsequently, the slices were post-fixed in 0.1 M phosphate buffer containing 1% OsO_4 for 1 hour at room temperature. The slices were washed with 0.1 M phosphate buffer (pH 7.2) as described above, then dehydrated through a graded acetone series (25%, 50%, 75%, 95%, 100%) for 15 minutes each, followed by 2 hours at 100% with an exchange of the acetone after 1 hour. The samples were then put into a 50:50 resin (Procue 812, ProSciTech, Aus): acetone mixture and stirred overnight.

The next day this mixture was replaced with 100% resin and left stirring for 8 hours after which the resin was renewed and left stirring overnight. Once again, the resin was renewed and left stirring for 8 hours. The samples were then embedded in moulds with new resin and left to cure at 60°C for 48 hours. The resultant blocks were trimmed to an appropriate area before cutting with a diamond knife (Diatome, Austria) at 100 nm. These were then stretched with chloroform and mounted on a grid using a Quick Coat G pen (Saiko, Japan). Grids were strained in saturated uranyl acetate in 50% ethanol for 4 minutes, washed with 50% v/v ethanol in MilliQ water and then stained in lead citrate for another 4 minutes. Lastly, the samples were washed with MilliQ water and viewed using an FEI Tecnai G^2 Spirit BioTWIN Transmission Electron Microscope.

2.7 Statistical Analysis

Survivability for the synthetic lethality assays was analysed by using colony counts to determine the plating efficiency in colony forming units per mL (CFU/mL) of each strain. This relative plating efficiency was then expressed as a ratio of *E. coli* producing pIV secretin (wild-type or leaky mutant, pIV-E292K) to cells not producing pIV (the vector control) using the exact Poisson test (see Tables A1, A2, & A3). The 95% confidence intervals of these ratios were also calculated using the exact Poisson test. The one-tailed Welch's T-Test was used to determine the significance of the relative plating efficiency. *P* values of less than 0.05 determined that the mean of the plate counts for the parental *E. coli* strain or the isogenic deletion mutant expressing secretin (either variant) is less than the mean of the wild-type *E. coli* or deletion mutant expressing the vector control. Note that the one-tailed Welch's T-Test was used for hypothesis testing instead of the exact Poisson test in order to use *P* values that were more conservative.

Chapter Three: Results

3.1 Requirements of *E. coli* K-12 to survive secretin-induced stress

It was revealed, through differential gene expression analysis, that expression of the secretin, wild-type pIV, induces the Psp, Cpx, Rcs, and Sox stress responses (Spagnuolo, 2015). Upon expression of a leaky mutant, pIV-E292K, induction of Rcs and Cpx responses is more prominent. In contrast, cells producing either pIV variant resulted in similar induction levels of Psp and Sox responses (Spagnuolo, 2015). In this thesis, the importance of these differentially expressed regulons for the survival of *E. coli* expressing wild-type or leaky pIV secretin was investigated. The viability of wild-type *E. coli* and cells containing single gene deletions of a positive master regulator of each of these responses (obtained from the Keio collection; (Baba *et al.*, 2006)), was assessed using a synthetic lethality assay. A master regulator from each of Psp, Rcs, Cpx, and Sox stress response pathways, when not present, prevents the activation of all downstream genes within the pathway or regulon. Cell survival was determined by calculating the ratio of relative plating efficiency (in colony forming units per mL (CFU/mL)) of *E. coli* producing pIV secretin (wild-type or leaky mutant, pIV-E292K) to cells not producing pIV (the vector control). Colony formation was evaluated on agar plates containing either 0 mM, 0.1 mM, or 1 mM of the gene *pIV* expression inducer, IPTG. This results in low levels of expression from a leaky *tac* promoter (Linderoth *et al.*, 1996; Linderoth *et al.*, 1997), intermediate levels, or high levels of pIV expression, respectively.

3.1.1 Synthetic lethality with BW25113 wild-type *E. coli* background

Individual knockout mutants containing a gene deletion of *cpxR* (Cpx regulatory system)*, rcsB* (Rcs phosphorelay)*, soxS* (Sox signal transduction pathway), or *pspF* (Psp response) and the parental *E. coli* strain, BW25113, were transformed with a plasmid containing leaky pIV-E292K (pPMR132-E292K), wild-type pIV (pPMR132), or a vector control with no pIV (pGZ119EH). The plating efficiency, which is dependent on the level of pIV in the cell for each of these newly obtained strains, was determined by counting colonies on solid media, enabling increasing levels of the *tac*-promoter-driven expression (with no IPTG or 0.1 mM or 1 mM IPTG). The ability of *E. coli* K-12 to form colonies producing leaky pIV-E292K at 1 mM IPTG was reduced by over 95% upon deletion of *cpxR*, *rcsB*, *soxS*, and *pspF*. In comparison, plating efficiency was decreased in cells producing wild-type pIV by ≥80% in the absence of the *cpxR, rcsB,* and *pspF* genes, and by ~60% in the the absence of *soxS* (Figure 13 & Table A1).

Figure 13: Relative plating efficiencies of BW25113 and isogenic single gene deletion mutants producing wild-type pIV or leaky pIV-E292K.

Single gene deletion mutants; *ΔcpxR, ΔpspF, ΔrcsB, ΔsoxS*, and wild-type *E. coli* K-12 (BW25113) (wt) were transformed with a plasmid encoding wild-type pIV (pPMR132), leaky pIV mutant (pPMR132-E292K), or a vector control with no pIV (pGZ119EH). Fresh overnight cultures of transformants were plated on 2xYT solid media containing IPTG for plasmid induction and 25 µg/mL chloramphenicol (Cm). IPTG concentrations include 0 mM (allowing for weak pIV induction from the leaky *tac* promoter (Linderoth *et al.*, 1996; Linderoth *et al.*, 1997; Spagnuolo, 2015), 0.1 mM (intermediate expression levels), or 1 mM (expression). Plating efficiencies (expressed as a percentage) were determined by calculating the ratio of relative plating efficiency (in colony forming units per mL (CFU/mL)) of *E. coli* producing pIV secretin (wild-type or leaky mutant, pIV-E292K) to cells not producing pIV (the vector control). The bars show the mean plating efficiency of three technical replicates. In all cases, error bars are within the 95% confidence intervals derived from exact Poisson tests. Welch's one-tailed T-test was used to determine whether colony counts were significantly lower than that of the vector controls. * denotes $p < 0.01 – 0.05$, ** denotes $p < 0.001 – 0.01$, *** denotes $p < 0.001$. Dataset shown in Table A1.

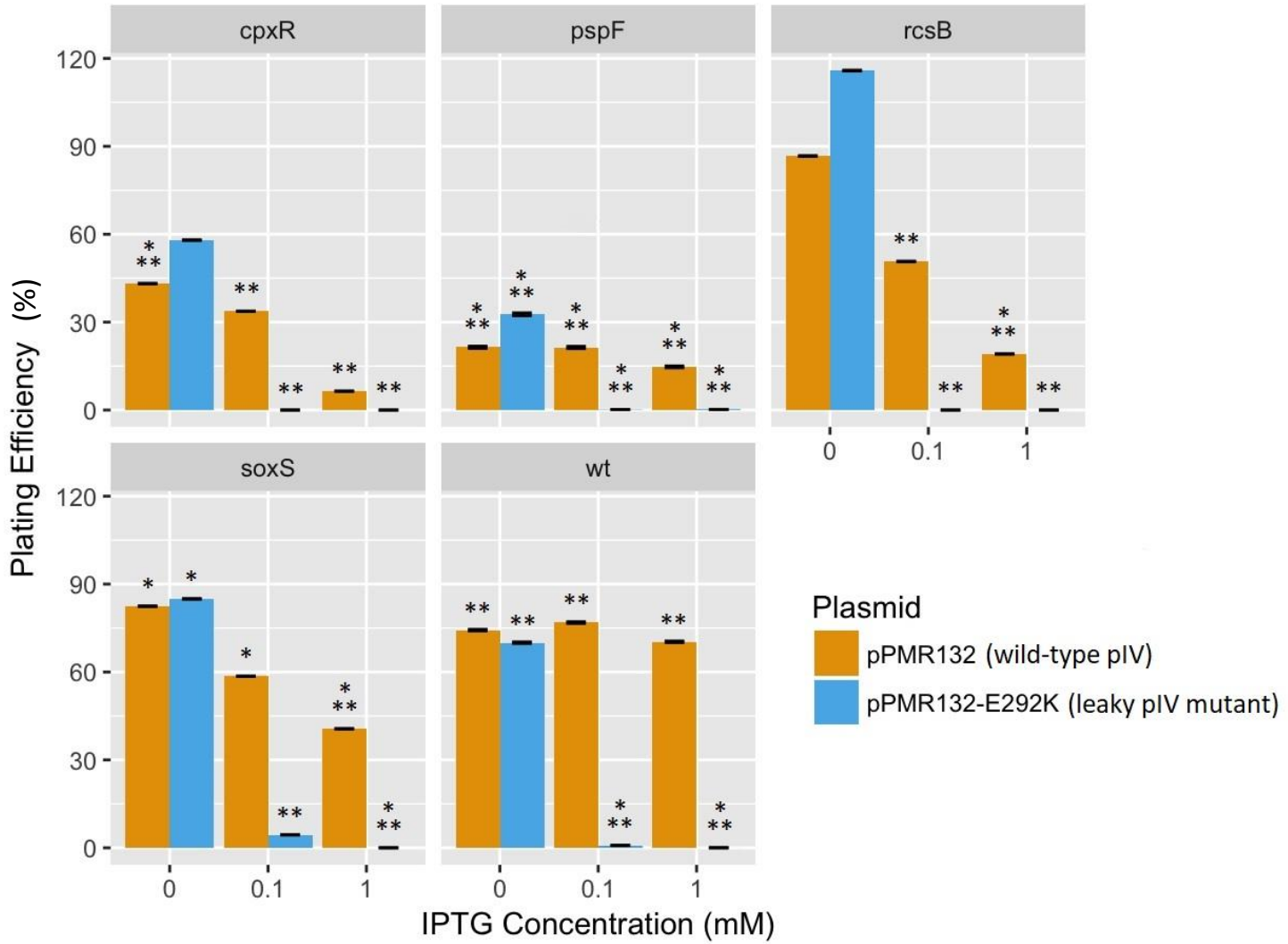
cpxR
pspF
rcsB
soxS
wt
Plating Efficiency (%)
120
90
60
30
0
0
0.1
1
IPTG Concentration (mM)
Plasmid
pPMR132 (wild-type pIV)
pPMR132-E292K (leaky pIV mutant)

In the absence of CpxR (*ΔcpxR* mutant), cells producing leaky pIV-E292K showed a ~99% reduction in plating efficiency relative to the vector control (Welch's T-Test; *P* value ≤ 0.01). The absence of CpxR was slightly less prominent in cells producing wild-type pIV with a ~94% reduction in plating efficiency (Welch's T-Test; *P* value ≤ 0.01).

In the *ΔrcsB* background, the ability of cells to form colonies when producing leaky pIV-E292K or wild-type pIV was not significantly affected by weak pIV expression (0 mM IPTG). However, the plating efficiency was reduced by ~99% with leaky pIV production at 0.1 mM and 1 mM IPTG (Welch's T-Test; *P* value ≤ 0.01). Production of wild-type pIV in the absence of RcsB at 0.1 and 1 mM IPTG showed a smaller yet significant ~50% and ~80% decrease in plating efficiency relative to the vector control, respectively (Welch's T-Test; *P* value ≤ 0.01).

Plating efficiency decreased in the *ΔsoxS* background by ~99% and ~60% in cells producing leaky pIV-E292K and wild-type pIV, respectively (Welch's T-Test; *P* value ≤ 0.05). Induction of leaky pIV or wild-type pIV had similar effects on cell viability (a decrease in plating efficiency of ~15%) at weak levels of pIV induction (Welch's T-Test; *P* value; ≤ 0.05).

Cells producing leaky pIV-E292K in the absence of PspF (*ΔpspF* mutant) showed a decreased plating efficiency of ~98% with pIV induction by 0.1 and 1 mM IPTG (Welch's T-Test; *P* value ≤ 0.001). Wild-type pIV production in the *pspF*-null background resulted in a ~85% decrease in plating efficiency, relative to the vector control (Welch's T-Test; *P* value ≤ 0.001).

Furthermore, the ability of wild-type *E. coli* (BW25113) to form colonies when producing leaky pIV-E292K (with 1 mM IPTG) decreased by ~99% (Welch's T-Test; *P* value ≤ 0.001). This is comparable to the reduction in cell viability observed in the *ΔcpxR, ΔrcsB, ΔsoxS,* and *ΔpspF* mutants upon production of pIV-E292K. Therefore, expression of pIV-E292K is lethal to the strain BW25113 in which all four stress response regulons were intact, precluding examination of the role of these pathways in the ability of *E. coli* to survive secretin-induced stress.

3.1.2 Synthetic lethality assay with K1508 wild-type *E. coli* background

The analyses in the previous section used a strain, BW25113, which has intact envelope and cytoplasmic stress responses found to be induced by pIV expression (Spagnuolo, 2015). This strain was initially used because the Keio knock-out collection was constructed in it (Baba *et al.*, 2006). Hence 'off-the-shelf' mutants from the collection could be ordered and used directly. A much more appropriate strain to use in these assays is K1508, in which the original transcriptome analysis was carried out (Spagnuolo, 2015) and where leaky pIV-E292K production was not toxic. To carry out the synthetic lethality analysis in this strain, the knock-out mutations of the genes of interest were introduced into this strain by generalised (P1) transductions using the kanamycin resistance (Kn^R) marker for selection as described by Rehm (2016). This marker is flanked by the *frt* sites (recognised by the site-specific recombinase FLP). The Kn^R marker in each of the transductants was removed by transient FLP expression leaving nearly complete deletions (Baba *et al.*, 2006). Synthetic lethality analyses were performed in the same manner and using the same methodology as described in the previous section.

As expected, the plating efficiency of the wild-type strain, K1508, producing leaky pIV-E292K or wild-type pIV was less than ~45% relative to the cells transformed with the vector control (Welch's T-Test; *P* value < 0.001) (Figure 14 & Table A2).

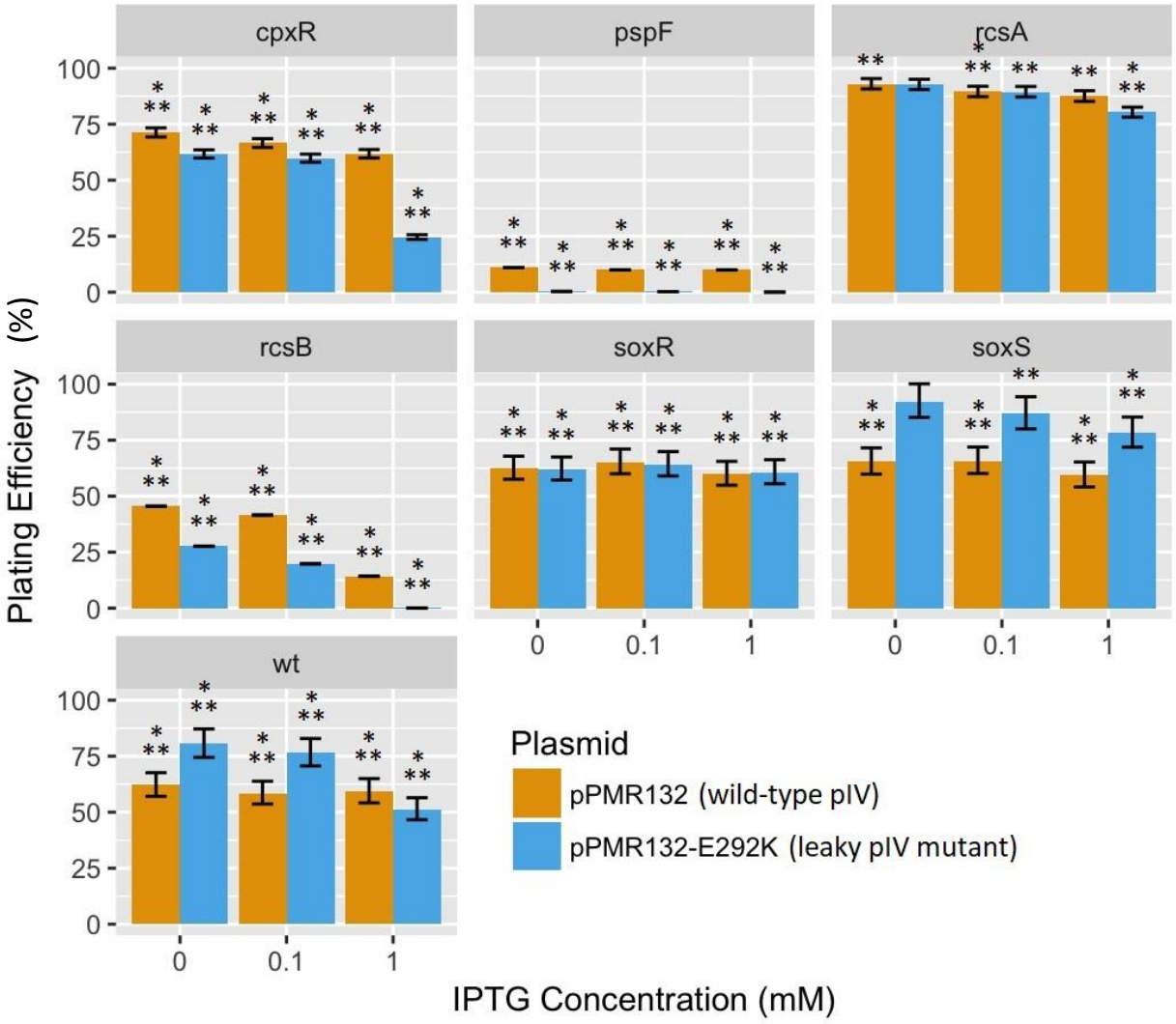
cpxR
pspF
rcsA
rcsB
soxR
soxS
wt
Plating Efficiency (%)
100
75
50
25
0
0
0.1
1
IPTG Concentration (mM)
Plasmid
pPMR132 (wild-type pIV)
pPMR132-E292K (leaky pIV mutant)

Figure 14: The requirement of secretin-induced stress response genes.

Single gene deletion mutants; *ΔcpxR, ΔpspF, ΔrcsA, ΔrcsB, ΔsoxR, ΔsoxS*, and wild-type *E. coli* K-12 (K1508) (wt) were transformed with a plasmid encoding wild-type pIV (pPMR132), leaky pIV mutant (pPMR132-E292K), or a vector control with no pIV (pGZ119EH). Fresh overnight cultures of transformants were plated on 2xYT solid media containing IPTG for plasmid induction and 25 µg/mL chloramphenicol (Cm). IPTG concentrations include 0 mM (allowing for weak pIV induction from the leaky *tac* promoter (Linderoth *et al.*, 1996; Linderoth *et al.*, 1997; Spagnuolo, 2015), 0.1 mM (intermediate expression levels), or 1 mM (expression). Plating efficiencies (expressed as a percentage) were determined by calculating the ratio of relative plating efficiency (in colony forming units per mL (CFU/mL)) of *E. coli* producing pIV secretin (wild-type or leaky mutant, pIV-E292K) to cells not producing pIV (the vector control) The bars show the mean plating efficiency of three technical replicates. In all cases, error bars are the 95% confidence intervals derived from exact Poisson tests. Welch's one-tailed T-test was used to determine whether colony counts were significantly lower than that of the vector controls. * denotes $p < 0.01 – 0.05$, ** denotes $p < 0.001 – 0.01$, *** denotes $p < 0.001$. Dataset shown in Table A2.

Plating efficiency of the *ΔcpxR* cultures producing leaky pIV-E292K decreased by ~75% relative to the vector control on the plates with 1 mM IPTG. Lower levels of pIV induction with 0.1 mM IPTG and no IPTG resulted in a decrease in plating efficiency of ~40% (Welch's T-Test; *P* value < 0.001). Plating efficiency reduced by 30 – 40% in *ΔcpxR* cultures producing wild-type pIV (Welch's T-Test; *P* value < 0.001).

Deletion of *soxR* in cells producing wild-type pIV or leaky pIV-E292K reduced the ability of *E. coli* K-12 to form colonies relative the vector control by ~35 – 40% regardless of IPTG concentration (Welch's T-Test; *P* value < 0.001). Deletion of *soxS* in cells reduced plating efficiency by ~35 – 40% and ~8 – 22% with the production of wild-type pIV or leaky pIV-E292K, respectively across all IPTG concentrations (Welch's T-Test; *P* value < 0.01). An exception exists where the plating efficiency of the *ΔsoxS* mutant was not affected upon weak induction of pIV-E292K (0 mM IPTG) (Welch's T-Test; *P* value ≥ 0.05). The plating efficiency in the ΔsoxS mutant producing leaky pIV-E292K was consistantly higher than those producing wild-type pIV which occurs at all levels of pIV induction. It is unclear why this is, however, induction of *soxS* was consistantly higher with the production of wild type pIV and not leaky pIV as observed from RNA-Seq studies (Spagnuolo, 2015).

A very severe (~99%) reduction in plating efficiency was observed in the *ΔrcsB* mutant producing pIV-E292K (Welch's T-Test; *P* value < 0.001). Viability of *ΔrcsB* mutant decreased as induction of leaky pIV-E292K increased. Please note that the tiny colonies in Figure 15D were difficult to photograph however, there are more colonies at 0.1 mM IPTG compared with 1 mM IPTG when the plates are observed up close. A significant reduction (~85%) in the ability of *ΔrcsB* mutant to form colonies when producing wild-type pIV (Welch's T-Test; *P* value < 0.001). In comparison, a much smaller reduction of ~20% and ~13% was observed in *ΔrcsA* mutant producing pIV-E292K or wild-type pIV, respectively. However, the colonies were smaller for *ΔrcsA* mutant producing pIV-E292K in comparison with wild-type pIV production (Figure 15C), indicative of a reduced growth rate.

The ability of the *ΔpspF* mutant to form colonies was also severely reduced (~99%) with the production of leaky pIV-E292K, which occurred at all levels of pIV induction (Welch's T-Test; *P* value < 0.001). Production of wild-type pIV in *ΔpspF* mutant reduced plating efficiency relative to the vector control by ~90% (Welch's T-Test; *P* value < 0.001).

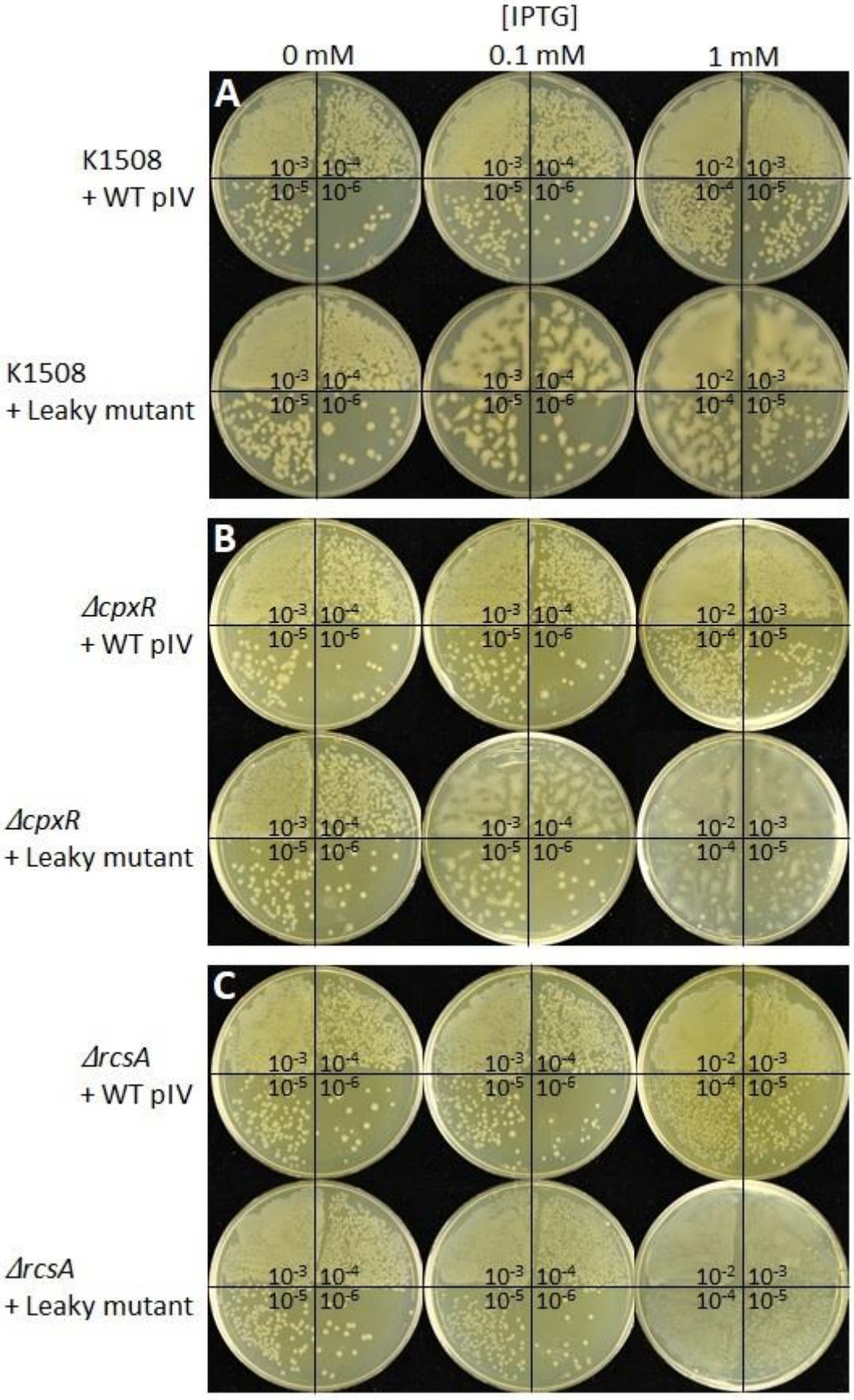
[IPTG]
0 mM
0.1 mM
1 mM
A
K1508
+ WT pIV
K1508
+ Leaky mutant
B
ΔcpxR
+ WT pIV
ΔcpxR
+ Leaky mutant
C
ΔrcsA
+ WT pIV
ΔrcsA
+ Leaky mutant
10-3 10-4
10-5 10-6
10-2 10-3
10-4 10-5

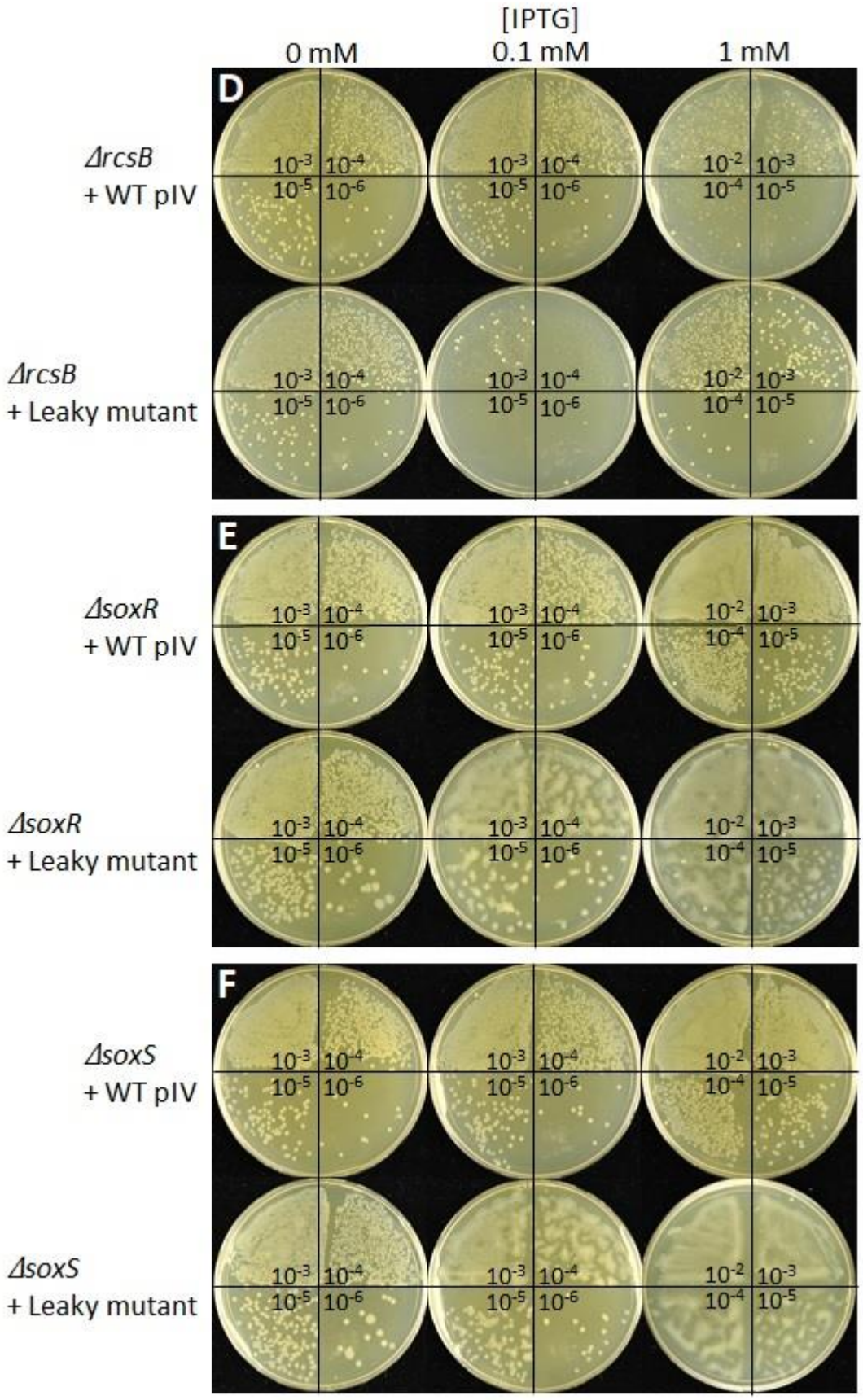
[IPTG]
0 mM
0.1 mM
1 mM
D
ΔrcsB
+ WT pIV
ΔrcsB
+ Leaky mutant
E
ΔsoxR
+ WT pIV
ΔsoxR
+ Leaky mutant
F
ΔsoxS
+ WT pIV
ΔsoxS
+ Leaky mutant
10-3 10-4
10-5 10-6
10-2 10-3
10-4 10-5

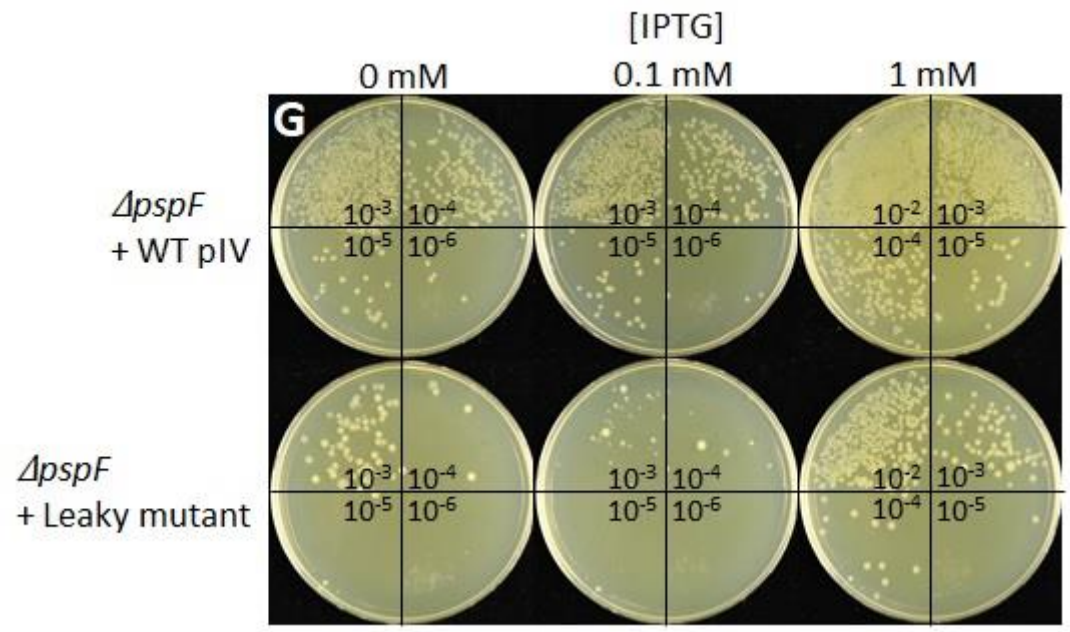

Figure 15: Synthetic lethality assay plates of K1508 and isogenic single gene deletion mutants producing pIV secretin.

Wild-type *E. coli* K-12 strain, K1508 **(A)**, and isogenic deletion mutants *ΔcpxR* **(B)**, *ΔrcsA* **(C)**, *ΔrcsB* **(D)**, *ΔsoxR* **(E)**, *ΔsoxS* **(F)**, and *ΔpspF* **(G)** were transformed with a plasmid encoding wild-type pIV (WT pIV) or leaky pIV-E292K (Leaky mutant). Fresh overnight cultures of transformants were diluted (10-fold serial dilutions) and plated on 2xYT solid media containing 25 µg/mL Cm for plasmid maintenance and IPTG for induction of pIV expression at 0, 0.1, or 1 mM.

Overall, smaller decreases in plating efficiency (≤40%) were observed for *ΔrcsA*, *ΔsoxR,* or *ΔsoxS* producing wild-type pIV or leaky pIV-E292K. The values were similar (or higher in the case of *ΔrcsA*) to the plating efficiency of wild-type *E. coli* expressing either variant of pIV. The cultures of the *ΔcpxR* mutant showed a decrease in plating efficiency that was <40% when expressing wild-type pIV at all three levels of induction and at two lower levels of induction for the pIV-E292K mutant. The difference was ~75% for the leaky mutant at the highest level of induction (1 mM IPTG).

In the two other knockout mutants, *ΔrcsB,* and *ΔpspF*, however, a remarkable decrease in plating efficiency (up to ~99%) was observed for the leaky pIV-E292K-producing cultures. This drastic reduction of plating in the *ΔpspF* mutant was observed at all levels of pIV induction, whereas it was only observed at 1 mM in the *ΔrcsB* mutant. The plating efficiency of the *ΔpspF* cultures producing wild-type pIV was ~90% at all levels of pIV induction, while the reduction of the *ΔrcsB* mutant expressing the wild-type pIV was about 55 – 60% at 0 and 0.1 mM IPTG, and ~85% at 1 mM IPTG. These findings show that the Rcs and Psp stress responses likely have a pivotal role in the survival of the stress caused by the pIV secretin, and PspF is essential even at very low levels of pIV production.

3.1.2.1 Vancomycin susceptibility test

Expression of the leaky pIV-E292K mutant has been shown to increase the proportion of clones in which a mutation in pIV has been acquired, such that the pIV channel can no longer be assembled (Spagnuolo *et al.*, 2010). The elimination of the pIV channel, in turn, abolishes the secretin stress in such mutants and is, therefore, a selective advantage. Given that pIV-E292K confers vancomycin sensitivity to its host (Spagnuolo *et al.*, 2010), loss of the expression can be evaluated phenotypically by monitoring the vancomycin minimal inhibitory concentration (MIC).

The status of pIV was observed at two points in the experiment; in the culture directly derived from the cells transformed by a pIV-expressing plasmid that was analysed for synthetic lethality (spread on the plates to determine the plating efficiency; hereby referred to as “transformant”) and also in the cultures seeded from colonies obtained from the synthetic lethality assay plates containing 1 mM IPTG (referred to as “titre”). The vancomycin MIC was determined on plates using an ‘E-strip’ containing a vancomycin concentration gradient of 0.016 – 256 µg/mL. Fresh overnight cultures from a transformant colony and a colony selected from the synthetic lethality assay titre plate containing 1 mM IPTG were diluted 100-fold and plated on solid 2xYT inducing media (containing 0.1 mM IPTG) with a vancomycin strip (Figure 16). The negative control for this experiment was the wild-type *E. coli* K-12 (K1508) producing wild-type pIV (Figure 16A), which does not confer vancomycin sensitivity due to a closed gate or septum (Spagnuolo *et al.*, 2010). The cultures of K1508 and isogenic *ΔsoxR, ΔcpxR, ΔsoxS,* and *ΔrcsA* mutants derived from the original transformant and seeded from the assay (titre) plate showed a zone of vancomycin sensitivity (Figure 16B). In contrast, the original pPMR132-E292K transformants of *ΔrcsB* and *ΔpspF* mutants did not form a lawn on the vancomycin assay plates, in agreement with their poor plating efficiency (reduction of >80% relative to the vector control (Figure 14 & Table A2)) in the presence of 0.1 mM IPTG. Furthermore, colonies from the synthetic lethality plate containing 1 mM IPTG gave rise to cultures that did not show a zone of vancomycin sensitivity. This shows that leaky pIV-E292K expression has been lost, which is in agreement with the intolerance to secretin-induced stress in the absence of RcsB and PspF. It appears that the colonies growing in the presence of 1 mM IPTG are not the genuine pIV-E292K-expressing cells, but rather, pIV-negative mutants. Plasmid loss is unlikely as PspF- and RcsB-null mutants grew uninhibited on plates supplemented with chloramphenicol for plasmid maintenance (Figure 15D & 15G).

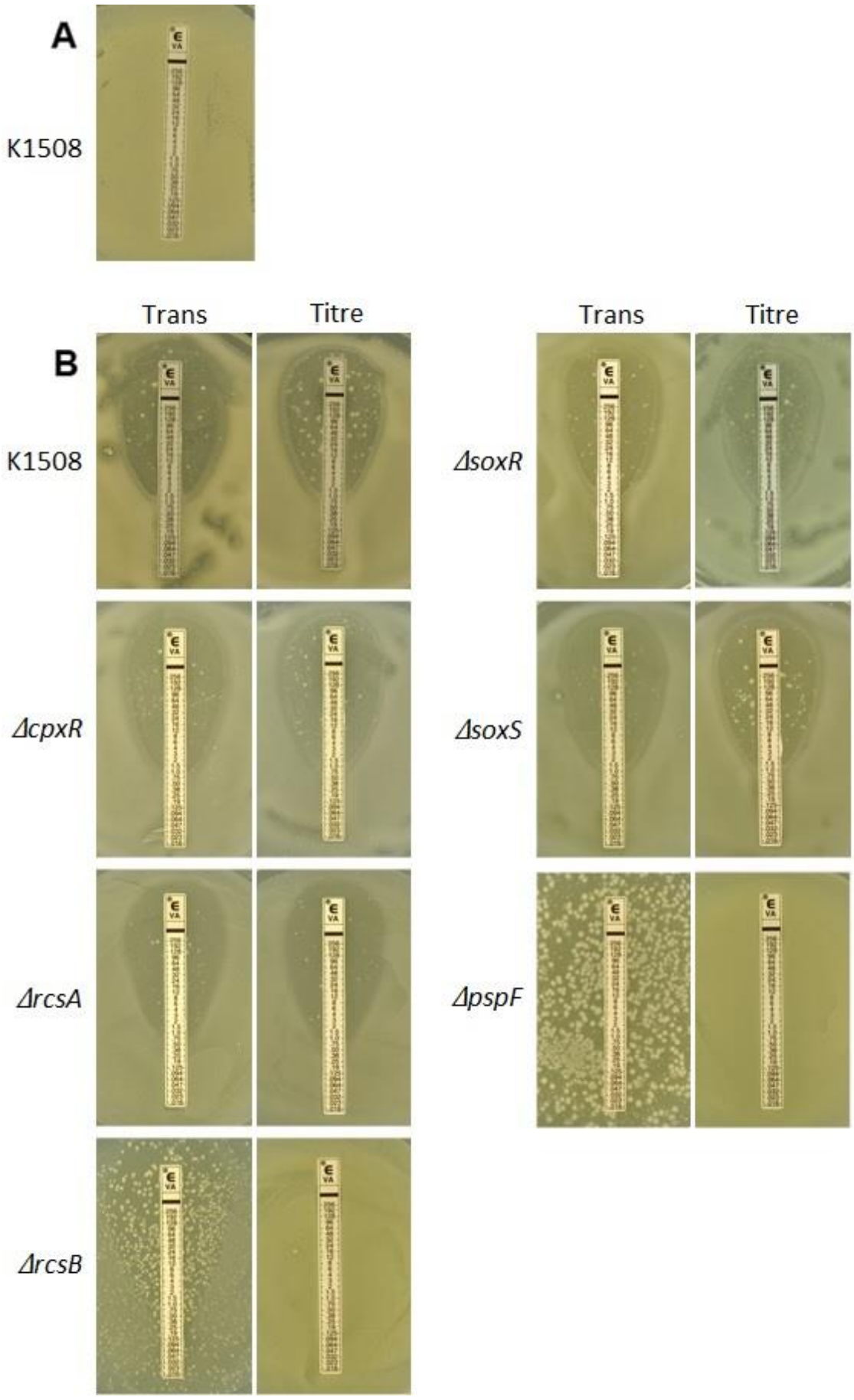
A
K1508
Trans
Titre
Trans
Titre
B
K1508
ΔsoxR
ΔcpxR
ΔsoxS
ΔrcsA
ΔpspF
ΔrcsB

Figure 16: Vancomycin sensitivity of *E. coli* K-12 strain K1508 and isogenic deletion mutants producing pIV.

Wild-type *E. coli* K-12 (K1508) is transformed with wild-type pIV **(A)**. K1508 and isogenic deletion mutants *ΔcpxR*, *ΔrcsA*, *ΔrcsB*, *ΔsoxR*, *ΔsoxS*, and *ΔpspF* are transformed with leaky pIV-E292K **(B)**. Fresh overnight cultures from a transformant colony (Trans) and a colony selected from the synthetic lethality plate (Titre) containing 1 mM IPTG were diluted 100-fold and plated on solid 2xYT inducing media containing 25 µg/mL chloramphenicol (Cm) and 0.1 mM IPTG with a vancomycin strip.

3.1.2.2 Rcs-dependent mucoid phenotype

It was observed in the synthetic lethality assay that the colony morphology of *E. coli* K-12 and several isogenic deletion mutants producing pIV-E292K had a mucoid phenotype (Figure 15). This is characteristic of overproduction of capsular polysaccharide (Markovitz, 1964) and indicates a dramatic upregulation of the *wza-wzb-wzc-wcaABO* and *yjbEFGH* extracellular polysaccharide synthesis and export operons in the cells expressing the leaky mutant, pIV-E292K (Figure 8) (Spagnuolo, 2015). To further investigate this phenotype, dilutions of overnight cultures of fresh transformants (giving 500 to 1000 colonies per plate) were spread on 2xYT solid inducing media (containing 0.1 mM IPTG) (Figure 17). K1508 and isogenic deletion mutants *ΔcpxR*, *ΔsoxR*, and *ΔsoxS* exhibited mucoidy. Colonies of the *ΔpspF* mutant transformed with leaky pIV-E292K produced a mixture of mucoid and non-mucoid colonies. As a lack of pIV-E292K expression is signaled by a non-mucoid phenotype, this is in agreement with the mutation and loss of pIV-E292K production due to its toxicity. However, this phenotype did not extend to *ΔrcsA* and *ΔrcsB* producing leaky pIV. It could be argued that the pIV-E292K was lost from the *ΔrcsB* strain due to the toxicity, whereas the leaky mutant was not toxic to the *ΔrcsA* mutant in the synthetic lethality assay and pIV-E292K was expressed in this strain according to the vancomycin sensitivity assay (Figure 14 & 16). No mucoidy was observed for wild-type *E. coli* or any deletion mutant producing wild-type pIV. These results are in agreement with the role of the RcsA/RcsB heterodimer as a master regulator of the two capsular exopolysaccharide expression operons that are highly upregulated in the pIV-E292K-expressing K1508. RcsA and RcsB are both required for expression of these two capsular biosynthesis and secretion operons (Ferrieres *et al.*, 2007; Spagnuolo, 2015; Wehland & Bernhard, 2000).

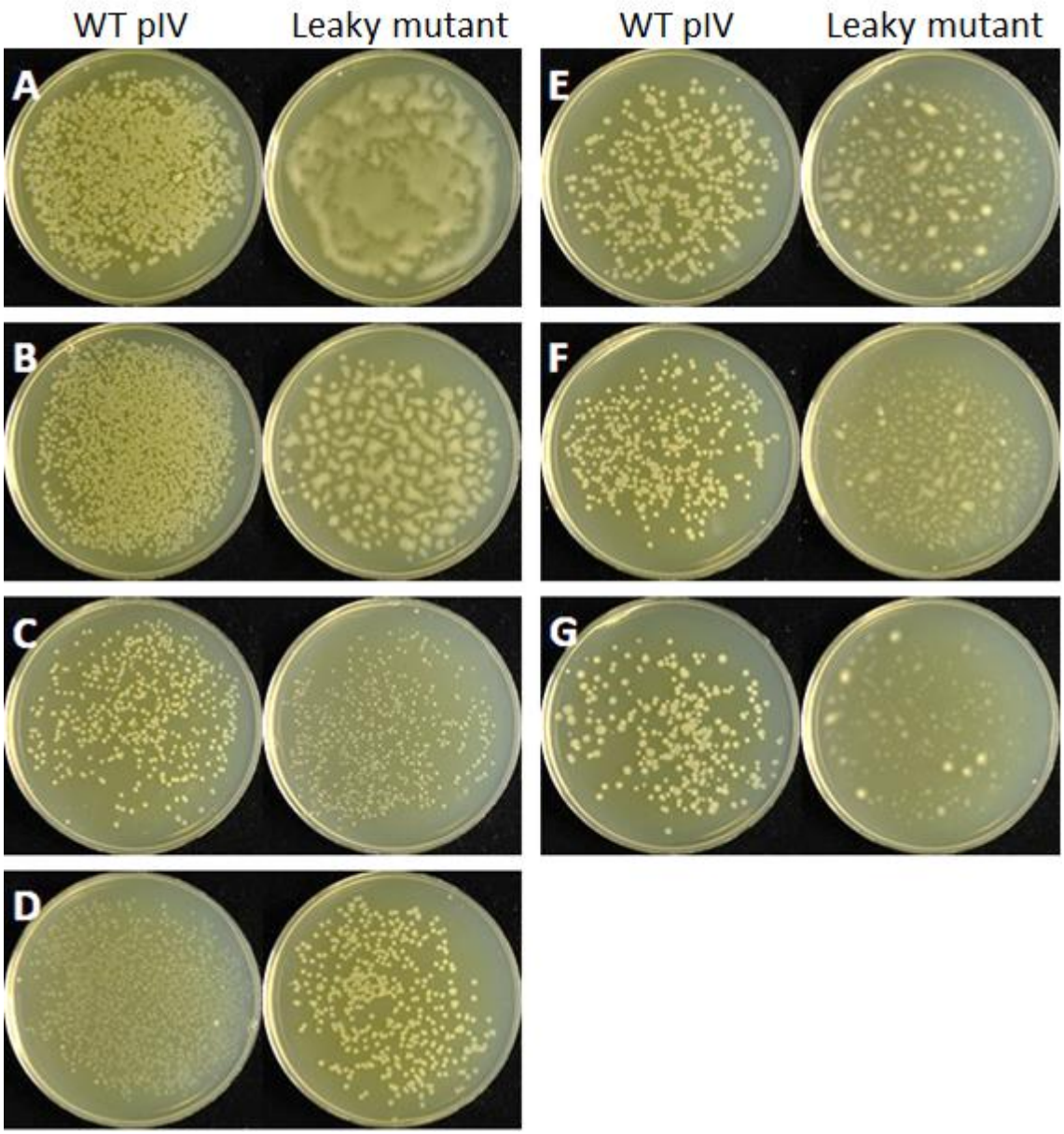

Figure 17: Rcs-dependent mucoid phenotype of *E. coli* K-12 and isogenic deletion mutants producing pIV.

Wild-type *E. coli* K-12 strain K1508 **(A)** and isogenic deletion mutants *ΔcpxR* **(B)**, *ΔrcsA* **(C)**, *ΔrcsB* **(D)**, *ΔsoxR* **(E)**, *ΔsoxS* **(F)**, and *ΔpspF* **(G)** were transformed with a plasmid encoding wild-type pIV or leaky pIV mutant, pIV-E292K. Fresh overnight cultures of transformants were diluted and plated on 2xYT solid inducing media containing 0.1 mM IPTG.

To examine whether the mucoid phenotype correlates with the presence of extracellular polysaccharides, the cells were observed using electron transmission microscopy (TEM) (Figure 18). Wild-type *E. coli* (K1058), *ΔrcsA,* and *ΔrcsB* were transformed with wild-type pIV (pPMR132) and leaky pIV-E292K (pPMR132-E292K), and overnight cultures of transformants were plated on solid inducing media. After incubation, colonies were scraped off the plates, embedded in resin, and sectioned (see 2.6.5). As expected, wild-type *E. coli* producing leaky pIV-E292K appeared to have developed an Rcs-dependent capsule which was absent from *ΔrcsA* and *ΔrcsB* mutants. In the *ΔrcsA* and *ΔrcsB* mutants, production of leaky pIV-E292K has resulted in plasmolysis of the cell membrane, of which visual indicators include an uneven cell membrane and increased thickness of the periplasm due to retraction of the inner membrane from the outer membrane (Cook, MacAlister, & Rothfield, 1986). Visual identification of plasmolysis has been implicated previously as an indicator of membrane integrity or the lack thereof, and hence cell viability (Korber, Choi, Wolfaardt, & Caldwell, 1996). Such disruption of membrane integrity is greater in *ΔrcsB* mutant than *ΔrcsA* producing leaky pIV-E292K (Figure 18B & 18C). This is consistent with the synthetic lethality assay result where *ΔrcsB* producing pIV-E292K had a much greater reduction in cell viability (~99%), relative to the vector control (Figure 14). Interestingly, some *ΔrcsB* cells observed did not have extensive plasmolysis and cell membranes were mostly intact, comparable to wild-type *E. coli* (Figure 18D). This is likely to be visual evidence of revertants (first observed as vancomycin resistant colonies (Figure 16)), in which the leaky pIV expression was eliminated by mutation (Spagnuolo, 2015).

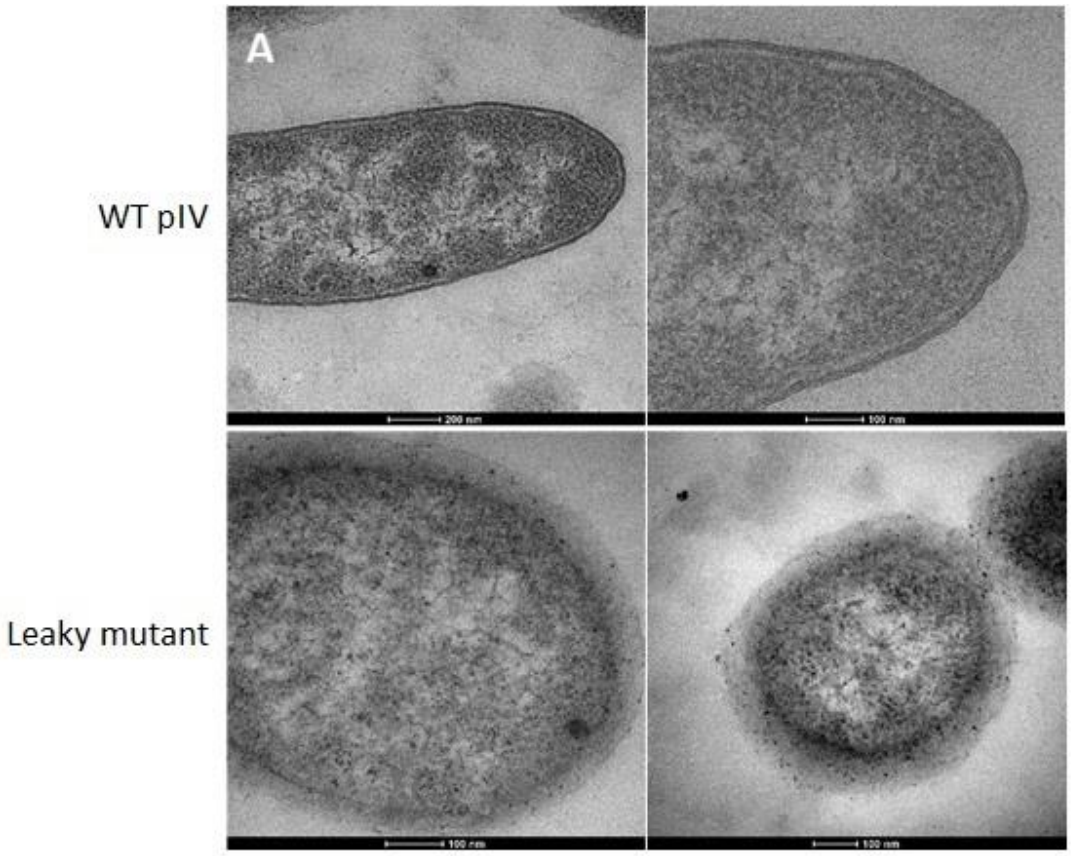
A
WT pIV
Leaky mutant

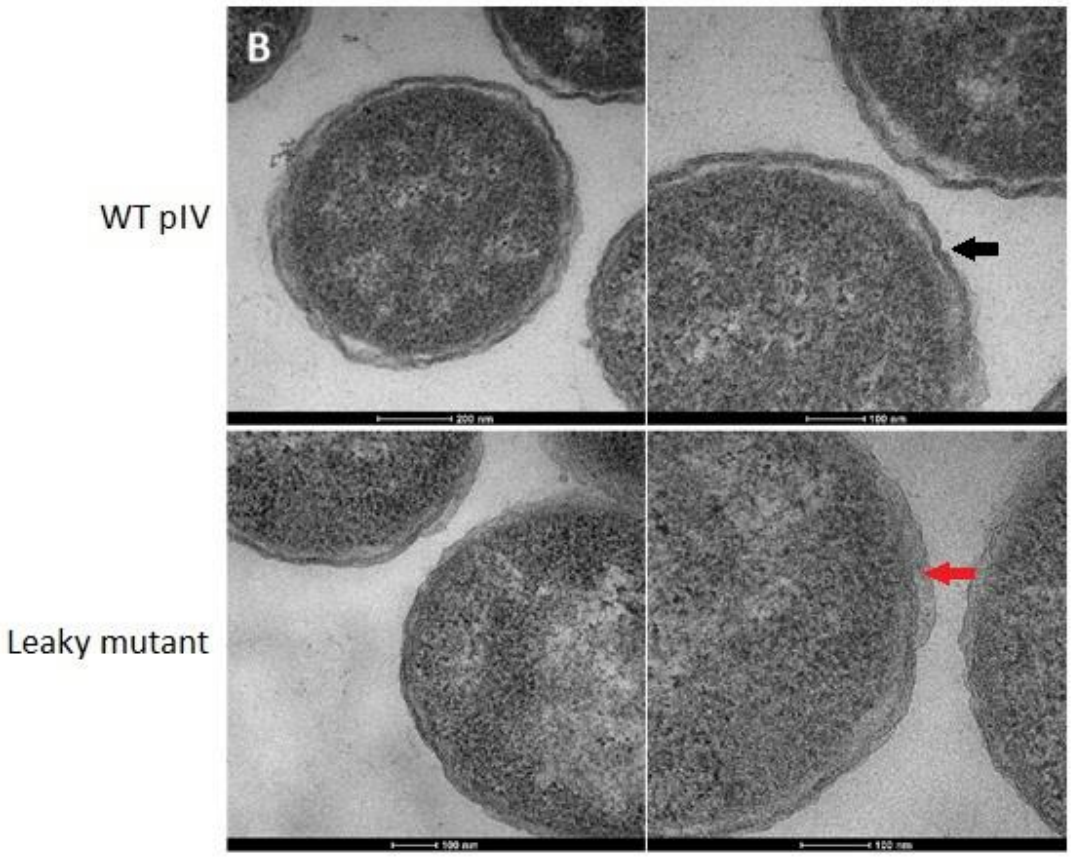
B
WT pIV
Leaky mutant

WT pIV

Leaky mutant

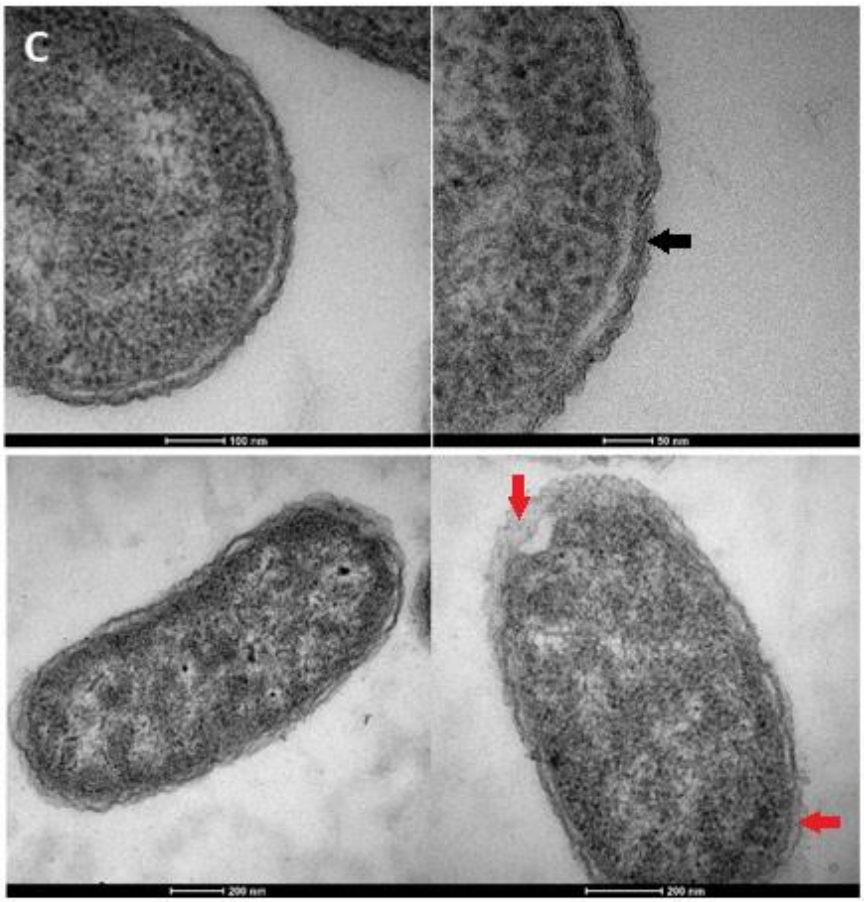

Leaky mutant

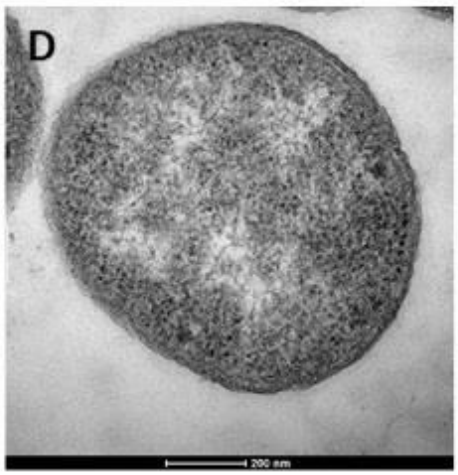

Figure 18: Rcs-dependent capsule layer in K1508 expressing leaky mutant pIV-E292K visualised by transmission electron microscopy.

Wild-type *E. coli* K-12 strain K1508 **(A)** and isogenic deletion mutants *ΔrcsA* **(B)**, and *ΔrcsB* **(C and D)**, were transformed with a plasmid encoding wild-type pIV (WT pIV) or pIV-E292K (leaky mutant). Fresh overnight cultures of transformants were diluted and plated on 2xYT solid inducing media containing 0.1 mM IPTG. After overnight incubation, the cells were scraped off the plates and the sections, embedded in resin, were prepared for examination by the transmission electron microscope (TEM). In the ΔrcsA and ΔrcsB mutants, production of pIV has resulted in plasmolysis seen by uneven cell membranes (black arrows) and increased thickness of the periplasm (red arrows).

3.2 Complementation of the synthetic lethality phenotype by expression of deleted genes *in trans*

3.2.1 Synthetic lethality assay: Expressing pIV from a plasmid expressing tetracycline resistance marker

The synthetic lethality assay confirmed previously published findings that the Psp response is required for survival of leaky secretin expression (Darwin, 2013). However, the finding that the RcsB master regulator is required for the survival of *E. coli* K-12 experiencing secretin-induced stress is novel. To confirm that the synthetic lethality is due to a lack of RcsB, rather than an indirect effect, it was necessary to carry out complementation by *in trans* expression of RcsB *via* a complementing plasmid. The ASKA collection of *E. coli* expressed proteins is available in a vector called pCA24N. This vector has the same selectable marker as pPMR132 (chloramphenicol resistance (Cm^R)), and hence the two plasmids could not be transformed into the same *E. coli* cell. To overcome this technical issue, the three plasmids used in the synthetic lethality assays in 3.1 were modified to replace the Cm^R with the Tet^R marker, to obtain pGZ119EHt, pPMR132t, and pPMR132t-E292K (Spagnuolo, 2015).

The synthetic lethality assay was repeated with the same set of strains as in 3.1.2 above; the parental wild-type *E. coli* K-12 strain, K1508, and derived single knockout mutants *ΔcpxR, ΔrcsA, ΔrcsB, ΔsoxR, ΔsoxS,* and *ΔpspF*. Each strain was transformed with a plasmid containing leaky pIV-E292K (pPMR132t-E292K), wild-type pIV (pPMR132t), or a vector control that does not contain any cloned insert (pGZ119EHt). All three plasmids carried a tetracycline (instead of chloramphenicol) resistance marker (Tet^R). Again, survivability was determined by evaluating colony formation and calculating the ratio of relative plating efficiency of *E. coli* producing pIV secretin (wild-type or leaky mutant, pIV-E292K) to cells not producing pIV (the vector control) (Figure 19 & Table A3).

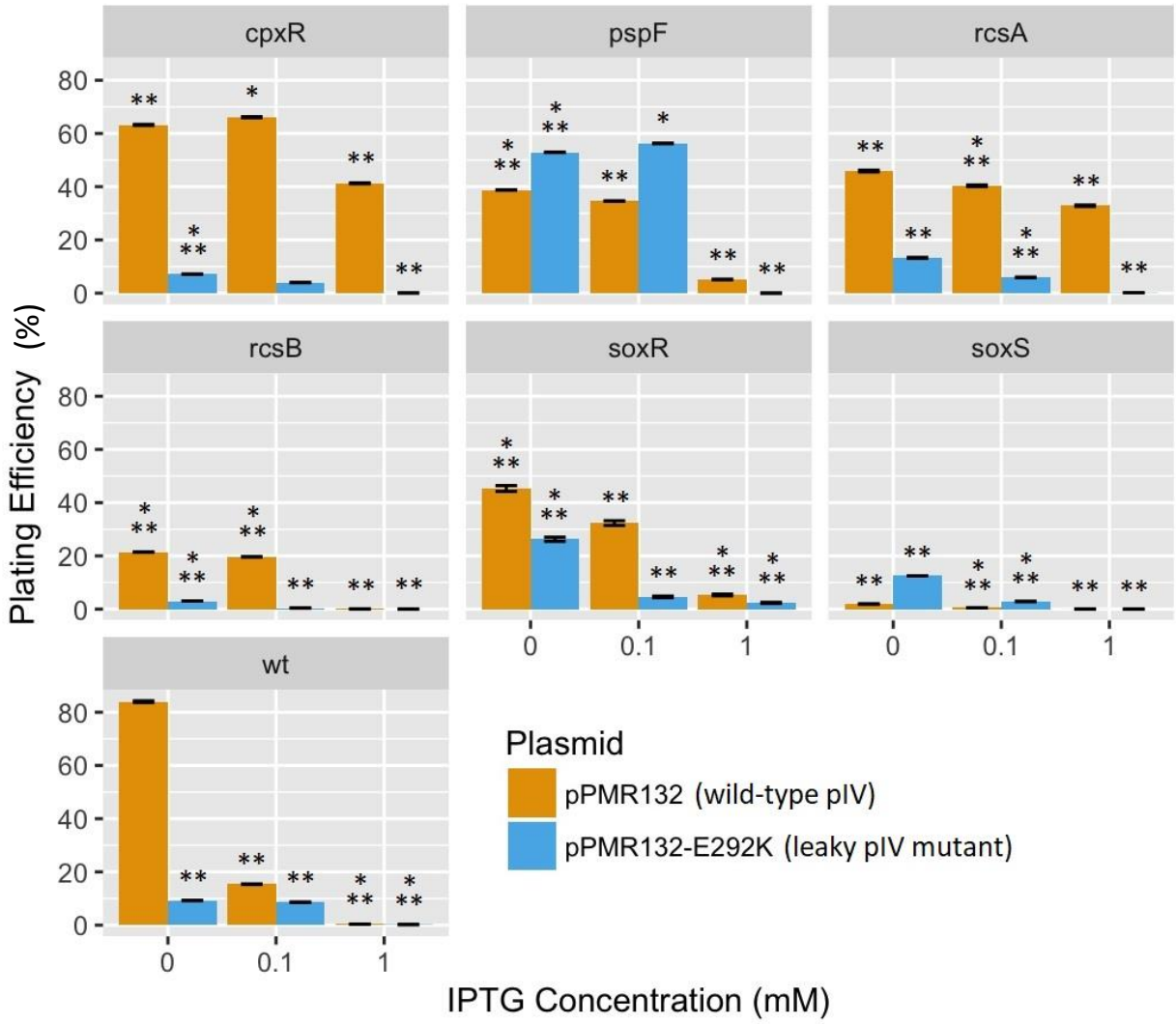
cpxR
pspF
rcsA
rcsB
soxR
soxS
wt
Plating Efficiency (%)
0
20
40
60
80
0
0.1
1
IPTG Concentration (mM)
Plasmid
pPMR132 (wild-type pIV)
pPMR132-E292K (leaky pIV mutant)

Figure 19: Relative plating efficiencies of K1508 and isogenic single gene deletion mutants co-producing wild-type or leaky pIV-E292K and Tet^{R}.

Single gene deletion mutants; *ΔcpxR, ΔpspF, ΔrcsA, ΔrcsB, ΔsoxR , ΔsoxS*, and wild-type *E. coli* K-12 (K1508) (wt) were transformed with a plasmid encoding wild-type pIV (pPMR132t), leaky pIV mutant (pPMR132t-E292K), or a vector control with no pIV (pGZ119EHt). Fresh overnight cultures of transformants were plated on 2xYT solid media containing IPTG for plasmid induction and 10 μg/mL tetracycline (Tet). IPTG concentrations include 0 mM (allowing for weak pIV induction from the leaky *tac* promoter (Linderoth *et al.*, 1996; Linderoth *et al.*, 1997; Spagnuolo, 2015), 0.1 mM (intermediate expression levels), or 1 mM (expression). Plating efficiencies (expressed as a percentage) were determined by calculating the ratio of relative plating efficiency (in colony forming units per mL (CFU/mL)) of *E. coli* producing pIV secretin (wild-type or leaky mutant, pIV-E292K) to cells not producing pIV (the vector control). The bars show the mean plating efficiency of three technical replicates. In all cases, error bars are the 95% confidence intervals derived from exact Poisson tests. Welch's one-tailed T-test was used to determine whether colony counts were significantly lower than that of the vector controls. * denotes $p < 0.01 – 0.05$, ** denotes $p < 0.001 – 0.01$, *** denotes $p < 0.001$.

The ability of *E. coli* K-12 to form colonies producing leaky pIV-E292K and Tet^R protein was reduced by ~90% in wild-type host K1508 and deletion mutants *ΔcpxR*, *ΔrcsA*, *ΔrcsB*, *ΔsoxR*, *ΔsoxS*, and *ΔpspF* (Welch's T-Test; *P* value < 0.01). A striking reduction was also observed for *ΔrcsA*, *ΔrcsB*, *ΔsoxR*, *ΔsoxS*, and *ΔpspF* mutants co-producing wild-type pIV with Tet^R, and toxicity of this plasmid to K1508 was similar to that of the pPMR132t-E292K.

Plating efficiency of cells producing wild-type pIV in the presence of Tet^R relative to the vector control in the *ΔcpxR* background decreased by ~60% (Welch's T-Test; *P* value < 0.01). In comparison, production of leaky pIV-E292K in the absence of CpxR decreased viability by ~99% (Welch's T-Test; *P* value < 0.01).

A ~99% reduction in plating efficiency was observed in *ΔrcsB* and *ΔrcsA* mutants producing pIV-E292K in the presence of Tet^R (Welch's T-Test; *P* value < 0.01). Striking reductions in the viability of *ΔrcsB* mutant occurred at all levels of leaky pIV-E292K induction. The reduction in the ability of *ΔrcsB* mutant to form colonies when producing wild-type pIV was also observed to be ~99% (Welch's T-Test; *P* value < 0.01). In comparison, *ΔrcsA* mutant had a decreased plating efficiency of ~68% upon wild-type pIV production (Welch's T-Test; *P* value < 0.01).

ΔsoxR cultures producing leaky pIV-E292K or wild-type pIV in the presence of Tet^R reduced the ability of *E. coli* K-12 to form colonies relative the vector control by ≥95% (Welch's T-Test; *P* value < 0.001). A striking reduction in the ability of the *ΔsoxS* mutant to form colonies was observed with the production of pIV-E292K and wild-type pIV in the presence of Tet^R of ~99% (Welch's T-Test; *P* value < 0.01).

Production of wild-type pIV (in the presence of Tet^R) in *ΔpspF* mutant reduced plating efficiency by ~95% (Welch's T-Test; *P* value < 0.01). The ability of the *ΔpspF* mutant to form colonies decreased by up to ~99% as the level of pIV-E292K induction increased (while Tet^R stayed constant). Only a ~45% reduction was noticed for this strain at low (no IPTG) and intermediate (0.1 mM IPTG) pIV expression levels (Welch's T-Test; *P* value < 0.05).

The ability of wild-type *E. coli* K-12 (K1508) to form colonies when producing leaky pIV-E292K and wild-type pIV (in the presence of Tet^R) decreased in parallel with that of other mutants, as the induction level increased (Welch's T-Test; *P* value ≤ 0.01). Cell viability of wild-type *E. coli* K-12 producing pIV at 1 mM IPTG decreased more than those of *ΔcpxR, ΔrcsA,* and *ΔpspF* mutants producing wild-type pIV, and *ΔsoxR* mutant producing leaky and wild-type pIV (all in the presence of the same amount of Tet^R). Furthermore, the ability of K1508 to form colonies was comparable to all mutants producing pIV-E292K at 1 mM IPTG. The toxicity of the wild-type pIV and the leaky pIV-E292K mutant when co-expressed with the *Tet*^{R} gene means this lowered plating efficiency cannot be attributed to the absence of any of the stress response pathways controlled by the deleted regulators. For this reason, biological repeats and further technical repeats were not carried out.

3.2.2 Vancomycin susceptibility test for the pIV-E292K and Tet^R co-expressing plasmid

To understand why such a reduction in cell viability was occurring in wild-type *E. coli* producing pIV, in the presence of the Tet^R protein (TetA efflux pump), a vancomycin sensitivity assay was carried out (Figure 20). The cultures derived from the colonies of freshly transformed wild-type *E. coli* showed a zone of clearance and a very weak lawn. The transformation plate contains 0 mM, and therefore pIV is produced at low levels from a leaky *tac* promoter even in the absence of IPTG (the plasmid can complement a *ΔgIV* mutation in phage in the absence of IPTG, in an F'derivative of K1508). This indicates that leaky pIV production is not lost when pIV-E292K production is weakly induced in the wild-type (K1508) culture. In contrast, all isogenic *E. coli* deletion mutants from cultures seeded from the transformation plate (no IPTG) showed no lawn, but rather some vancomycin resistant colonies; depending on the level of toxicity that the plasmid has on a particular mutant. When the cultures were seeded from the titre plate containing 1 mM IPTG, all strains formed thick lawns of vancomycin-resistant bacteria, indicating an absence of pIV-E292K (from the Tet^R-containing plasmid) (Figure 20B).

Lack of pIV production is not due to plasmid loss as all strains grow uninhibited on media containing tetracycline (Tet) for plasmid maintenance (Figure 20 and 21), but rather due to the selection of plasmids which acquired mutations in gene *IV*, as has been previously observed (Spagnuolo, 2015).

Toxicity of the leaky pIV-E292K in the presence of Tet^R becomes apparent in the vancomycin sensitivity assay where there is no apparent lawn, (for plates labeled 'Trans'), apart from a thin lawn for K1508 and *ΔsoxS* mutant (Figure 20B). Instead, varying numbers of vancomycin-resistant colonies can be observed on the plate. Furthermore, in agreement with the low plating efficiency at 1 mM IPTG, cultures derived from the synthetic lethality assays (labeled 'Titre'; Figure 20B), are completely resistant to vancomycin, reflecting the loss of pIV-E292K.

Figure 20: Vancomycin sensitivity of *E. coli* K-12 and isogenic deletion mutants co-expressing pIV-E292K and Tet^R.

Wild-type *E. coli* K-12 (K1508) is shown transformed with wild-type pIV in the presence of Tet^R (negative control; resistant to vancomycin) **(A)**. K1508 and isogenic deletion mutants *ΔcpxR*, *ΔrcsA*, *ΔrcsB*, *ΔsoxR*, *ΔsoxS*, and *ΔpspF* are shown transformed with leaky pIV-E292K in the presence of Tet^R **(B)**. Fresh overnight cultures from a transformant colony (Trans) and a colony selected from the synthetic lethality plate (Titre) containing 1 mM IPTG were diluted 100-fold and plated on solid 2xYT inducing media containing 10 µg/mL tetracycline for plasmid maintenance and 0.1 mM IPTG with a vancomycin strip.

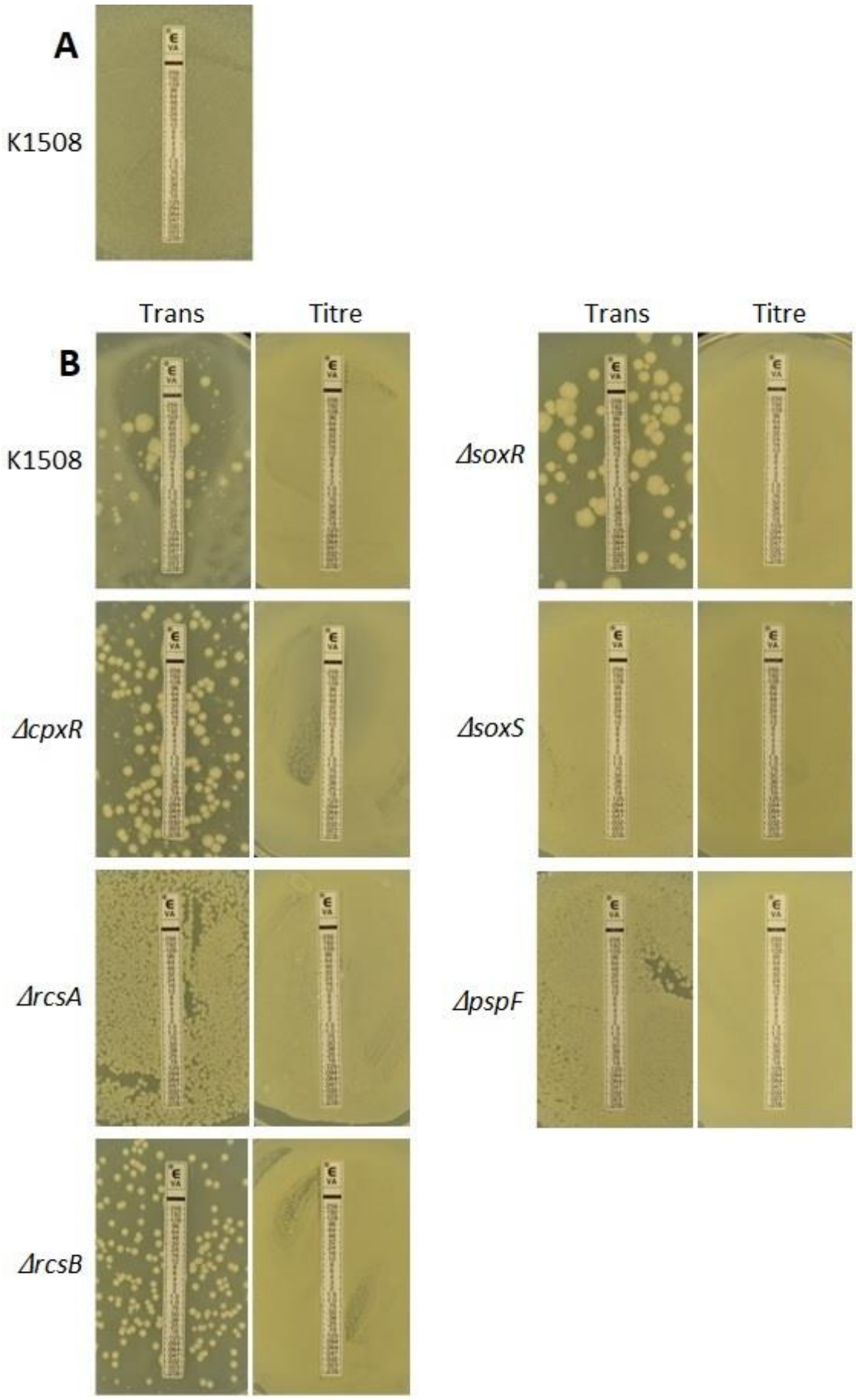
A
K1508
Trans
Titre
Trans
Titre
B
K1508
ΔsoxR
ΔcpxR
ΔsoxS
ΔrcsA
ΔpspF
ΔrcsB

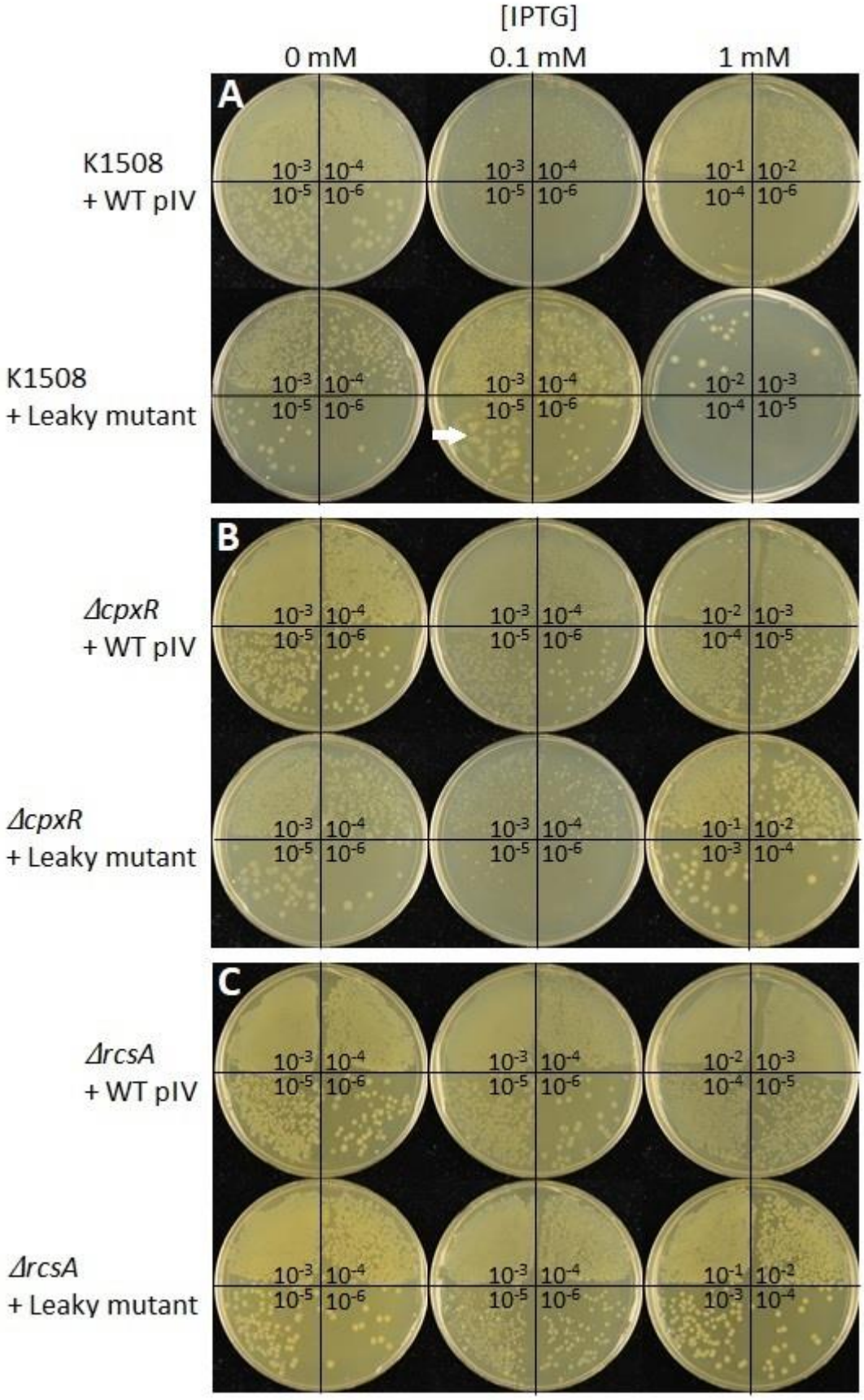
[IPTG]
0 mM
0.1 mM
1 mM
A
K1508
+ WT pIV
K1508
+ Leaky mutant
B
ΔcpxR
+ WT pIV
ΔcpxR
+ Leaky mutant
C
ΔrcsA
+ WT pIV
ΔrcsA
+ Leaky mutant

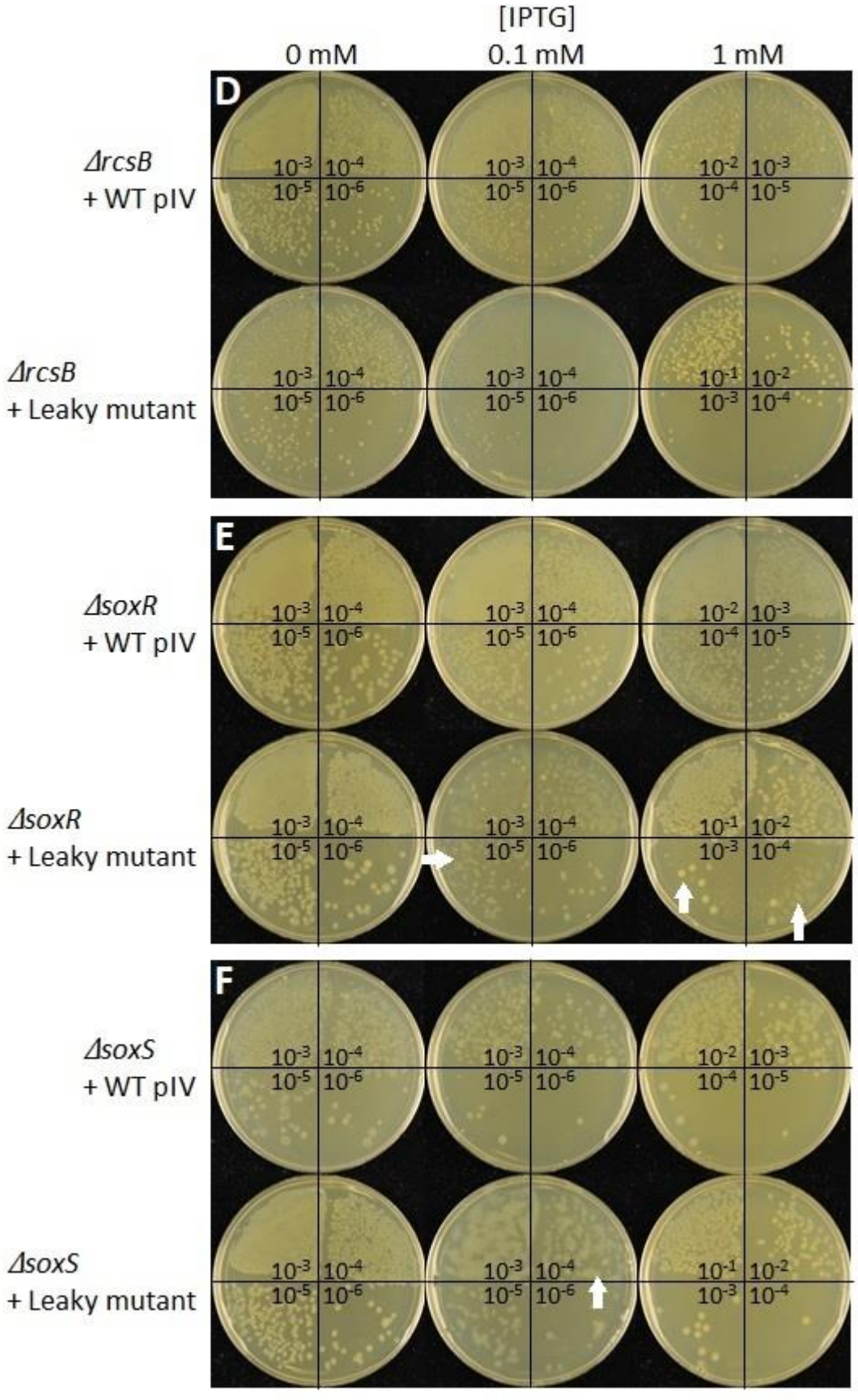
[IPTG]
0 mM
0.1 mM
1 mM
D
ΔrcsB
+ WT pIV
ΔrcsB
+ Leaky mutant
E
ΔsoxR
+ WT pIV
ΔsoxR
+ Leaky mutant
F
ΔsoxS
+ WT pIV
ΔsoxS
+ Leaky mutant

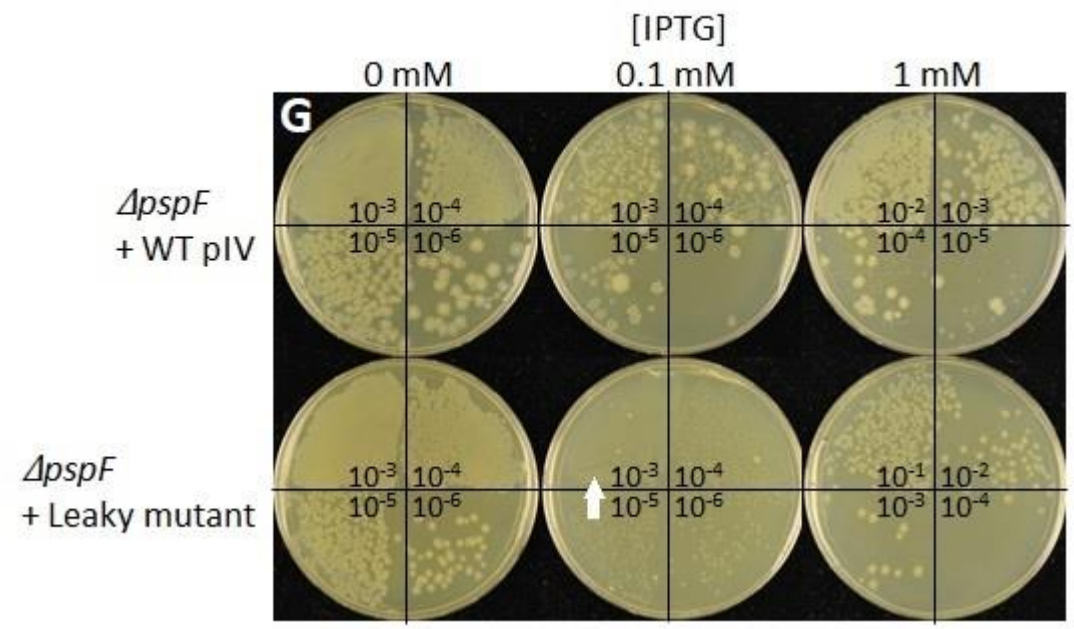

Figure 21: Synthetic lethality assay plates of K1508 and isogenic single gene deletion mutants producing pIV secretin (with Tet^R).

Wild-type *E. coli* K-12 strain K1508 **(A)** and isogenic deletion mutants *ΔcpxR* **(B)**, *ΔrcsA* **(C)**, *ΔrcsB* **(D)**, *ΔsoxR* **(E)**, *ΔsoxS* **(F)**, and *ΔpspF* **(G)** were transformed with a plasmid encoding wild-type pIV (WT pIV) or leaky pIV-E292K (Leaky mutant). Fresh overnight cultures of transformants were diluted (10-fold serial dilutions) and plated on 2xYT solid media containing 10 µg/mL tetracycline for plasmid maintenance and IPTG for induction of pIV expression at 0, 0.1, or 1 mM. White arrows indicate the presence of mucoid colonies.

3.2.3 Mucoid phenotype in the pIV-E292K and Tet^R co-expressing cultures

A mucoid phenotype is indicative of pIV-E292K production (see 3.1.2.2). Wild-type *E. coli* and *ΔcpxR*, *ΔsoxS,* and *ΔpspF* mutants containing the Tet^R plasmid are mucoid at intermediate levels of pIV-E292K (0.1 mM IPTG) but not with 1 mM IPTG (and a constant level of Tet^R). The plating efficiencies determined at 1 mM IPTG are likely derived from the cells that no longer produced pIV-E292K, based on the observed vancomycin resistance (Figure 20). The vancomycin sensitivity assay (Figure 20) showed a loss of pIV-E292K production in all deletion mutants even with weak pIV induction (transformants seeded from plates with no IPTG) due to the presence of resistant colonies. This can be explained where cells selected from the transformant plates were grown in an overnight culture before exposure to vancomycin strips. Any revertants would grow faster in an overnight culture to outnumber pIV-E292K-producing cells resulting in a resistant phenotype.

Colony size was noticeably smaller for wild-type K1508 strain and the isogenic deletion mutants containing the Tet^R plasmid producing pIV-E292K at 0.1 mM IPTG, indicative of a slower growth rate and therefore an increase in generation time (Figure 21). pIV-E292K expression in mutants other than *ΔrcsA* and *ΔrcsB* mutants was reflected by the presence of mucoidy (Figure 17 & Figure 21). The size of colonies on the 1 mM IPTG titration plates increased (in comparison with those on the 0.1 mM IPTG plates), and the mucoidy was lost for all strains producing pIV-E292K but *ΔsoxR* mutant (Figure 21). Cultures seeded from the colonies on these titration plates (with 1 mM IPTG) showed the vancomycin-resistant phenotype (Figure 20B). Therefore, the titration plate colonies contain mutant Tet^R plasmids that have a mutated gene *IV* that does not produce a pIV channel. Note that *ΔrcsA* and *ΔrcsB* mutants do not have a mucoid phenotype even with pIV-E292K production (Figure 17) because they are required for expression of genes encoding the capsular polysaccharide biosynthesis and secretion pathways induced by leaky secretin expression.

In summary, colonies on plates containing 1 mM IPTG derived from transformants of the Tet^R-containing pPMR132t-E292K plasmid in K1508 and isogenic knockout mutants have selectively acquired mutations that abolish leaky pIV-E292K channel assembly or production. All assays using TetA (Tet^R) expression vectors show a strong toxic effect in combination with wild-type and leaky pIV, making them unsuitable for use in complementing assays.

3.2.4 Construction of a novel complementing plasmid

Findings in section 3.1 using the Cm^R-containing pPMR132 and pPMR132-E292K plasmids showed that *rcsB* or *pspF* genes are required for overcoming pIV-E292K-induced stress. Given the body of research on PspF that has already confirmed its essentiality for the survival of secretin stress, the finding that RcsB is also essential for survival was the object of further research. The first step towards understanding how RcsB acts in preventing cell death from secretin stress was to confirm that it is directly, rather than indirectly, involved in the protection from secretin-induced stress. Part of this effort involved the construction of Tet^R-containing variants of the pIV-expression plasmids, given that complementing with the RcsB-expressing plasmid from the ASKA collection has a Cm^R marker, the same as in pPMR132 and its derivatives. However, due to the toxicity of pIV in combination with the Tet^R marker, the pPMR132t, and pPMR132t-E292K plasmids could not be used for a complementation experiment. Instead, the Cm^R-containing pPMR132 variants had to be used.

As a result, the new strategy was developed, which involved the construction of a new complementation vector containing a kanamycin resistance marker (Km^R) instead of the Tet^R marker. The construction of a novel vector allowed the opportunity to include an additional improvement; replacement of the T5-*lac* promoter (which drives the expression of RcsB in pCA24N) with the araBAD promoter. This change allowed independent control of the expression of pIV (by IPTG) and RcsB (by arabinose). This novel RcsB complementing plasmid was named pSB-RcsB (Figure 22).

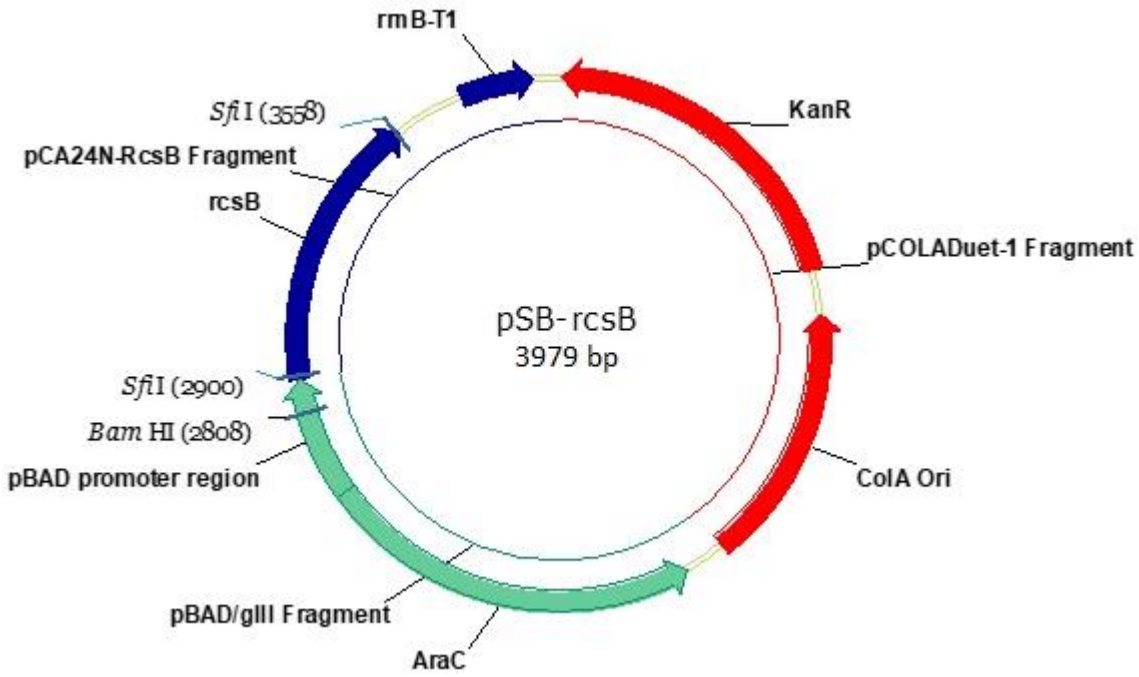

Figure 22: pSB-RcsB plasmid map.

pSB-RcsB is designed to be composed of sequences derived from three plasmids. It contains the *araC* regulatory gene and araBAD promoter from pBAD/gIII (Guzman *et al.*, 1995). Immediately after that is the *rcsB* gene flanked by two SfiI sites and rrnB-T1 transcription terminator from pCA24N-RcsB (Kitagawa *et al.*, 2005). The plasmid also contains a ColA origin of replication and kanamycin resistance gene derived from pCOLADuet™-1 (Tolia & Joshua-Tor, 2006).

The AraC protein (which itself is positively regulated by 3',5'-cyclic adenosine monophosphate (cAMP)), positively and negatively regulates expression from the araBAD promoter (Carra & Schleif, 1993; Lobell & Schleif, 1990). Expression from the araBAD promoter is induced in the presence of arabinose and repressed in the presence of glucose which reduces cellular cAMP levels (Miyada, Stoltzfus, & Wilcox, 1984). Use of this promoter allows clear differentiation of plating efficiency in *ΔrcsB* mutants producing pIV (either variant) in both the presence and absence of RcsB. The plasmid, pSB-RcsB, was constructed by using PCR to amplify a section from each of pBAD/gIII, pCA24N-RcsB, and pCOLADuet^{TM}-1 (see Table 2 for plasmid details & Figure 23). The PCR products were joined without purification and according to manufacturer's instructions using Gibson Assembly, (with NEBuilder HiFi DNA Assembly master mix by New England Biolabs). Full details on the construction of pSB-RcsB can be found in section 2.2. The resulting ~3.9-Kb pSB-RcsB plasmid was expected to contain the *araC* regulatory gene and araBAD promoter (of pBAD/gIII (Guzman *et al.*, 1995)), immediately preceding *rcsB* flanked by two SfiI sites and a rrnB-T1 transcription terminator (from pCA24N-RcsB (Kitagawa *et al.*, 2005)). The plasmid was also designed to contain a ColA origin of replication and kanamycin resistance gene (from pCOLADuet^{TM}-1 (Tolia & Joshua-Tor, 2006)). Restriction analysis of the construct with the enzyme, BamHI, which has a single cut site (Figure 22) revealed a fragment that was a smaller size than expected; ~3.2 Kb instead of ~3.9 Kb (Figure 24).

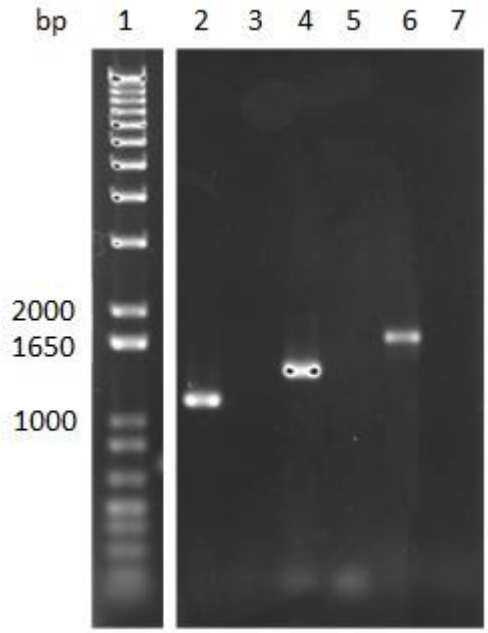

Figure 23: PCR products from templates pCA24N-RcsB, pBAD/gIII, and pCOLADuet^{TM}-1.

1% agarose DNA gel electrophoresis run at 50 volts for 2 hours showing 1 Kb+ DNA ladder **(1)**, pCA24N-RcsB PCR product (1059 bp) **(2)** with no template control **(3)**, pBAD/gIII PCR product (1221 bp) **(4)** with no template control **(5)**, and pCOLADuet^{TM} PCR product (1561 bp) **(6)** with no template control **(7)**. All bands are of the approximate expected size.

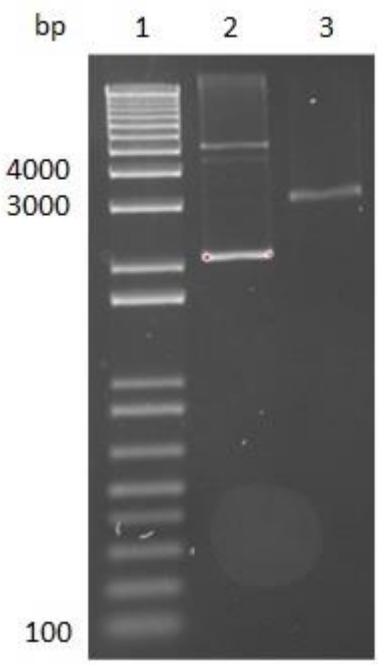

Figure 24: BamHI restriction digestion of pSB-RcsB.

1% agarose DNA gel electrophoresis run at 80 volts for 70 minutes showing 1 Kb+ DNA ladder **(1)**, uncut pSB-RcsB **(2)**, and pSB-RcsB digested with BamHI for 1 hour at 37°C **(3)**.

A sequencing reaction (BigDye® Terminator V3.1 Chemistry; Massey Genome Service, NZ) was carried out spanning 100 nucleotides (nt) upstream of the pBAD/gIII promoter region to 100 nt downstream of *rcsB* revealing that the pSB-RcsB sequence was not as expected (Figure 25). Alignment of pSB-RcsB with the forward sequence showed that the 5' portion corresponds to the araBAD promoter as intended, and the 3' portion of the sequence is identical to the beginning of the fragment derived from pCOLADuet™-1. However, there is a segment in the middle (161 nt) that did not align with the *in silico* engineered plasmid. Instead, use of the Basic Alignment Search Tool (BLAST) revealed that the 161 nt segment aligned to a segment from pCA24N that encompasses parts of the *T5-lac* promoter and the His-tag in the opposite orientation to the araBAD promoter.

It is likely that the rest of the plasmid is correct as the transformation of pSB-RcsB into *ΔrcsB* mutant gave rise to transformants that were kanamycin resistant (data not shown). Therefore, as only the fragment derived from pCA24N-RcsB is incorrect, this is an empty vector for one-step cloning of RcsB. Once the plasmid is constructed to contain *rcsB*, and complementation is carried out, it will be determined whether RcsB is directly, rather than indirectly, required for *E. coli* K-12 to survive pIV-induced stress.

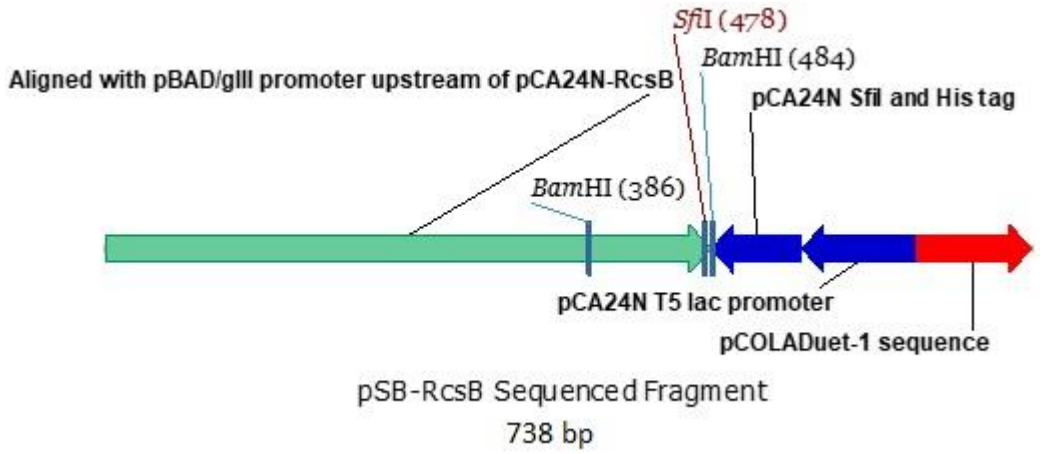

Figure 25: Map of a sequenced fragment of pSB-RcsB.

The araBAD promoter (from pBAD/gIII) and the pCA24N-RcsB derived fragment of pSB-RcsB was sequenced. The 5' and 3' portion of the sequence corresponds to the correct sequence of the araBAD promoter and 5' end of the pCOLA-Duet™-1 fragment, respectively. In the opposite orientation to the araBAD promoter is two fragments corresponding to the pCA24N *T5-lac* promoter and SfiI site and His tag instead of the desired *rcsB* gene.

Chapter Four: Discussion and Conclusions

4.1 Discussion

This thesis set out to determine the requirement of key master regulators within the stress response pathways Psp, Rcs, Cpx, and Sox for the survival of *E. coli* experiencing leaky pIV-induced stress. Synthetic lethality assays show that the Psp regulon and RcsB-dependent branch of the Rcs regulon, as well as CpxR (though to a lesser extent) is essential to maintain membrane integrity. It was also determined by TEM that expression of leaky pIV leads to the production of an Rcs-dependent capsule and plasmolysis of the cell membrane in the absence of RcsB. However, there were a few obstacles and limitations encountered which will be discussed first.

Synthetic lethality assays undertaken in the BW25113 parental *E. coli* K-12 strain and isogenic deletion mutants as well as with plasmids containing pIV with a Tet^R marker are invalid (Figure 13 & 19, respectively). This is because of the apparent loss in cell viability in wild-type *E. coli*, and therefore, the reduction in plating efficiency of any isogenic single gene deletion mutant cannot be attributed to an incomplete stress response. This is not the case for K1508 which tolerated expression of the leaky pIV rather well.

Genomes of both wild-type strains (BW25113 and K1508) have been sequenced (V, Le., personal communication, July 16th, 2018). The strain, K1508 that endures the leaky secretin stress carries several mutations in genes involved in motility and energy metabolism, which may confer a greater tolerance to secretin expression. The gene for the positive flagellar transcriptional activator, *flhD*, contains a frameshift mutation. A lack of functional FlhD protein may result in reduced motility in the K1508 strain (Horne *et al.*, 2016). It is plausible that a lack of active flagella on the bacterial surface, (creating a demand on PMF to drive flagella activity (Fung & Berg, 1995; Gosink & Häse, 2000)), allows K1508 to better tolerate lowered PMF from pIV production.

K1508 was also found to contain a missense and in-frame insertion mutations in the gene *spoT* (which are also noted by Spira, Hu, and Ferenci (2008)). The enzyme, SpoT, which is involved in the stringent response, has both synthetase and hydrolase (degradative) activity for the alarmone guanosine 5',3' bispyrophosphate (ppGpp) (Hernandez & Bremer, 1991). The first 203 amino acids of SpoT are involved in degradation of ppGpp (Gentry & Cashel, 1996) and an in-frame insertion mutation has been found to occur between amino acids 82 and 83 in K1508 (V, Le., personal communication, July 16th, 2018; (Spira *et al.*, 2008)). This may reduce SpoT ppGpp degradative activity and has been shown to result in increased levels of this alarmone in K1508 (Spira *et al.*, 2008). The missense mutation (histidine to tyrosine) occurs in the region of the protein likely responsible for synthetase activity (V, Le., personal communication, July 16th, 2018; (Gentry & Cashel, 1996)). As it is a substitution between two polar amino acids, it may have less of an effect on synthetase function (and as mentioned above, ppGpp levels are elevated in K1508). SpoT synthetase activity has been shown to increase ppGpp levels in response to intracellular conditions including limitations in fatty acid synthesis, phosphate starvation, and iron starvation (Battesti & Bouveret, 2006; Bougdour & Gottesman, 2007; Vinella, Albrecht, Cashel, & D'Ari, 2005). It was found that production of wild-type and leaky pIV resulted in significant upregulation of a small regulatory RNA, *rhyB* (Spagnuolo, 2015). Transcription of *rhyB* is negatively regulated by iron-sensing master regulator Fur in a complex with Fe^{2+} (Fur-Fe^{2+}). Strong upregulation of *rhyB* is a sign of Fur-Fe^{2+} depletion which can occur under iron starvation conditions (Boyd, Thomas, Dai, Boyd, & Outten, 2014; Zheng, Doan, Schneider, & Storz, 1999), which suggests that pIV production may lower intracellular iron (Spagnuolo, 2015). ppGpp influences gene expression such that general stress response genes and energy metabolism is upregulated, and subsequently, generation of PMF (Durfee, Hansen, Zhi, Blattner, & Jin, 2008; Traxler *et al.*, 2008). Therefore, perhaps this mutation in K1508 confers greater tolerance to secretin-induced stress as the cell is better able to maintain PMF (due to higher ppGpp levels) despite the production of a membrane channel which depletes it. However, further experiments to elucidate how *spoT* function is affected by the mutations and how this function relates to secretin-induced stress is necessary here.

In the K1508 background, on the other hand, plasmids expressing pIV was incompatible with the Tet^R marker that was encoded on the same plasmid. The Tet^R marker encodes the *tetA* tetracycline-resistance gene, (a TetA efflux pump), which confers resistance to tetracycline by the expulsion of this antibiotic from the bacterial cytoplasm (Bolivar *et al.*, 1977; Hellweger, 2013). This pump is powered by PMF (Li, Kromann, Olsen, Svenningsen, & Olsen, 2017). Expression of large channels, like pIV, depletes PMF by allowing protons to leak across the IM (Darwin, 2013). Yet, PMF is required to energise transport of tetracycline through the TetA efflux pump, to maintain resistance to tetracycline (Levy, 2002; Nikaido, 1996). It is plausible then, that leaky pIV expression becomes highly toxic in combination with Tet^R expression, resulting in dramatic loss of plating efficiency (>97%) on plates containing tetracyline and 1 mM IPTG. This occurs even in the wild-type K1508 strain, (Figure 19 & Table A3; Welch's T-Test; *P* value < 0.01), that is otherwise tolerant to leaky secretin expression (Figure 14 & Table A2; Welch's T-Test; *P* value < 0.001).

In contrast to the Tet^R marker, the Cm^R marker encodes chloramphenicol acetyltransferase, the enzyme that chemically modifies and thereby inactivates chloramphenicol, without affecting the cellular physiology (Kehrenberg, Schwarz, Jacobsen, Hansen, & Vester, 2005; Yong-Seok, Joong-Soo, & Jai-Kyung, 1987). In agreement with this mechanism of resistance, expression of pIV (wild-type or leaky variant) from a plasmid containing a Cm^R marker, did not result in a striking loss in cell viability (<45%) in the wild-type K1508 strain, even under maximal induction of leaky pIV-E292K expression (Figure 14 & Table A2; Welch's T-Test; *P* value < 0.001). Therefore, any further discussion regarding gene requirements in *E. coli* K-12 experiencing secretin-induced stress refers to the synthetic lethality assay using K1508 and isogenic single deletion mutants transformed with plasmids carrying a Cm^R marker.

Significant, though small (≤40%) decreases in plating efficiency was observed for *ΔrcsA*, *ΔsoxR*, and *ΔsoxS* mutants, and a ~75% decrease for *ΔcpxR* mutant, producing leaky pIV-E292K at maximal secretin induction (1 mM IPTG) (Figure 14 & Table A2).

However, more striking decreases in plating efficiency of ~99% were observed in *ΔrcsB* and *ΔpspF* producing leaky pIV, and ≥85% for these mutants producing wild-type pIV (Figure 14 & Table A2). In the absence of each, activation of the corresponding pathway and regulon is inhibited (Spagnuolo, 2015). This effect was achieved at 0.1 mM IPTG in the *ΔpspF* mutant, whereas in the *ΔrcsB* mutant, higher expression of the secretin was required (1 mM IPTG). Therefore, RcsB and PspF responses likely have a pivotal role in regulating gene expression in response to secretin-induced stress. This is suggestive of a requirement of the capsular polysaccharide (Rcs) and phage-shock (Psp) regulons for the survival of *E. coli* K-12 experiencing secretin-induced stress. This conflicts with several previous findings that show a requirement of only the PspF regulon, but not RcsB regulon (Jovanovic *et al.*, 2006; Lloyd *et al.*, 2004; Seo, Savitzky, Ford, & Darwin, 2007). Furthermore, a study on *E. coli* K1508 *ΔpspF* mutant showed decreased survival of cells when expressing the T3SS secretin, InvG, which is leaky in the absence of secretion (Khanum, 2015). The findings presented in this thesis, however, are in agreement with the most recent transcriptome analysis of the stress induced by expression of the wild-type pIV and the pIV-E292K leaky mutant using RNA-Seq, (Figure 8) (Spagnuolo, 2015), which is much more accurate and has a much wider dynamic range of quantification in comparison to the microarrays used before this work was published (Jovanovic *et al.*, 2006; Seo *et al.*, 2007). Ultimately, effectors within each pathway that are required for secretin expression could be poteintial drug targets that when inactivated, prevent the expression of stress-mediating genes, or inhibit secretin expression, and therefore the secretion of virulence factors.

4.1.1 Leaky phenotype of the pIV-E292K mutant

The near-atomic resolution structures of the InvG secretin from *S. enterica* (Worrall *et al.*, 2016) and the T2SS GspD secretins from *V. cholerae* and pathogenic *E. coli* (Yan *et al.*, 2017) have recently been published. This has allowed modeling of the pIV secretin domain which is homologous to InvG and GspD, to show the placement of the leaky-channel mutation, E292K, in the central region of the channel gate loop which is comprised of a β-hairpin (Figure 7D).

In particular, the structure of a *V. cholerae* GspD leaky mutant, showed that the GATE1 region corresponds to the channel gate, where the point mutation, G453A, resulted in a conformational change (Figure 6D) so that the β-hairpin tilted 25° towards the channel wall, effectively opening the gate (Yan *et al.*, 2017). This supports the idea that the gate of the pIV-E282K is open and is, therefore, representative of an actively secreting wild-type pIV channel. Further evidence that the gate is open is that the E292K mutation renders the secretin channel permissible to vancomycin and deoxycholate (a detergent), while the wild-type channel does not (Spagnuolo *et al.*, 2010). Yet the pIV-E292K mutant is functional in filamentous phage assembly (Spagnuolo *et al.*, 2010). However, it is plausible that the location of the mutation results in slower folding in comparison with wild-type pIV (Figure 7; (Spagnuolo, 2015; Yan *et al.*, 2017). This data supports the conclusion that the E292K mutation affects the channel gate, (and therefore confers a leaky phenotype), but does not disrupt the structure and function of the other domains of the channel as the mutation is mapped to the inner gating β-loops. Furthermore, the location of the mutation is in the same position within the GATE1 hairpin structure as the G453 residue whose mutation was structurally demonstrated to cause tilting and opening of the gating loop (Yan *et al.*, 2017). This suggests that the leaky phenotype is due to an inability of the gate to close, rather than the destabilisation of the OM by disrupting the interaction between the channel and the membrane in which it is inserted.

4.1.2 Cpx Response

Induction of the Cpx response has been known to be stimulated by protein accumulation in the periplasm (specifically OM lipoprotein, NlpE), and misfolded subunits of Pap or Bfp pili (Price & Raivio, 2009). Upregulation of the Cpx response pathway requires the positive regulator, CpxR, which is phosphorylated by CpxA kinase (Figure 11) (DiGiuseppe & Silhavy, 2003). A statistically significant ~40% and ~75% decrease in plating efficiency is observed in *ΔcpxR* mutants producing wild-type pIV and leaky pIV-E292K, respectively, relative to the vector control (Figure 14 & Table A2). These data indicate that the Cpx response is required for *E. coli* K-12 to mitigate pIV-induced stress (Welch's T-Test; *P* value < 0.001).

The pIV secretin (more so the leaky pIV-E292K variant than wild-type pIV) has been shown to stimulate upregulation of the CpxR regulon (Spagnuolo, 2015). The Cpx response has also been shown to have involvement in the expression of the type IV bundle-forming pilus whose assembly is significantly reduced in the absence of CpxR, due to insufficient expression of Cpx-regulated genes; *dsbA, degP*, and *cpxP* (Nevesinjac & Raivio, 2005; Vogt et al., 2010). Furthermore, it has been observed that T3SS assembly and the secretion of effector proteins through the *trans*-envelope organelle is likely regulated by the CpxR regulon (Carlsson, Liu, Edqvist, & Francis, 2007; MacRitchie, Acosta, & Raivio, 2012; Walker & Miller, 2009). Genes of the CpxR regulon differentially expressed in response to leaky pIV-E292K production include those involved in cell wall repair and biogenesis; protein folding; and biofilm and motility regulation (Spagnuolo, 2015). The CpxR regulon may not be pivotal mediating secretin-induced stress, (as seen with the more striking loss of cell viability with the loss of PspF and RcsB (Figure 14 & Table A2; Welch's T-Test; *P* value < 0.001)), as there is substantial overlap with other extracytoplasmic stress responses. This includes sigma-E which may respond to secretin-induced stress in the absence of the Cpx regulon. In its absence, negative regulation by CpxR of the sigma-E response does not occur (Miyadai, Tanaka-Masuda, Matsuyama, & Tokuda, 2004; Otto & Silhavy, 2002).

The exact nature of the pIV-dependent upregulation of the Cpx response is unclear. Transcription of *cpxP* occurs when CpxR is phosphorylated by CpxA. However, CpxP interacts with and inhibits the autokinase activity of CpxA unless it binds misfolded proteins in the periplasm before removal by DegP (Fleischer, Heermann, Jung, & Hunke, 2007; Raivio & Silhavy, 1997). It is therefore proposed that CpxP may interact with pIV-E292K subunits that are aggregated or misfolded allowing for activation of the Cpx response (Spagnuolo, 2015). This may potentially be due to an increased folding and assembly time for the leaky pIV variant (Spagnuolo, 2015). Genes upregulated by CpxR include *dsbA*, *degP*, *rotA, ppiA,* and *ppiD* which are all involved in protein folding (Duguay & Silhavy, 2004; Hunke *et al.*, 2011). It has been shown that DsbA has an important role in the correct assembly of T3SS secretin, YscC, in *Yersinia pestis* (Jackson & Plano, 1999).

Furthermore, a two-fold increase in DegP transcription (consistent with CpxR regulon expression) has been found to occur in the presence of leaky pIV-E292K (but not wild-type pIV) in *E. coli* K-12 (Spagnuolo, 2015). Alternatively, phosphorylation of CpxR may occur *via* the phosphate donor acetyl phosphate from the Pta-AckA pathway which is known to respond to changes in cell metabolism as may occur with a disruption in PMF because of pIV production. Genes of this pathway (*pta* and *ackA*) were upregulated in response to leaky pIV and wild-type pIV expression (Figure 8) (Fischer, Gräber, & Turina, 2000; Spagnuolo, 2015; Wolfe, Parikh, Lima, & Zemaitaitis, 2008).

4.1.3 Sox Response

The Sox response is upregulated in bacterial cells experiencing oxidative stress. The redox-sensing activator, SoxR, activates the transcriptional regulator, SoxS, upon the superoxide-dependent oxidation of its Fe-S containing centre (Figure 12). In the absence of an inducing signal, the Fe-S centre of SoxR is reduced by a membrane-embedded NADPH-dependent Sox reductase and the protein is inactivated (Blanchard *et al.*, 2007). Deletion of *soxR* in cells producing leaky pIV or wild-type pIV resulted in a decreased plating efficiency of ~35 – 40% (for both) (Figure 14 & Table A2; Welch's T-Test; *P* value < 0.001). In the absence of SoxS in *E.* coli K-12 producing leaky pIV or wild-type pIV, a reduction in plating efficiency of ~8 – 22% and ~35 – 40% occurred, respectively (Figure 14 & Table A2; Welch's T-Test; *P* value < 0.001). This is indicative of a requirment of SoxR and SoxS to mitigate secretin-induced stress. However, this was relatively minor in comparison with the ~99% reduction in plating efficiency observed for *ΔpspF* and *ΔrcsB* mutants. A requirement for SoxS (but not SoxR) for the survival of secretin-induced stress has been observed previously in cells expressing pIV and T3SS secretin, InvG (Khanum, 2015; Spagnuolo, 2015).

It is plausible that pIV-producing cells experience oxidative stress. Secretin-induced disruption of membrane integrity may result in elevated electron transport chain activity to maintain PMF, leading to elevated O^{2-} (superoxide) production (Turrens, 1997). RNA-Seq analysis of pIV-producing cells revealed an increase in SoxS induction reflecting an increase in superoxide (Figure 8) (Spagnuolo, 2015).

The SoxS regulon has been shown to upregulate genes involved in prevention of ROS (reactive oxygen species) damage and repair of ROS-damaged macromolecules, regeneration of NADPH, upregulation of ROS-removing enzymes (e.g. superoxide dismutase), and downregulation of proteins sensitive to ROS activity (Blanchard *et al.*, 2007; Chiang & Schellhorn, 2012). Despite this, transcriptional activation of genes that are solely upregulated by SoxS, have been shown to change (either up- or down-regulated) by less than a factor of two in pIV-producing *E. coli* K-12 (Spagnuolo, 2015). For example, in cells producing pIV-E292K but not wild-type pIV, the gene *sodA* (encodes a superoxide dismutase) was induced by less than a factor of two (Spagnuolo, 2015). Furthermore, the only SoxS-dependent transcript to be highly induced in leaky pIV-E292K producing cells; the *marRAB* operon (encodes oxidative stress genes), is also activated by CpxR-P (Spagnuolo, 2015). Regulatory redundancies exist where, for example, SoxS homologs MarA and Rob also regulate transcription of many genes within the SoxRS regulon (Miller & Sulavik, 1996). Therefore, any oxidative stress caused by pIV expression could be mediated in the absence of SoxS and/or SoxR, making them non-essential proteins for *E. coli* K-12 producing secretin.

4.1.4 Psp Response

Many secretins that lack cognate pilotins (which traffic secretin monomers to the OM), such as pIV, insert into the OM, but also the IM due to mistargeting. Such secretin mislocalisation has been shown to induce Psp response, which mitigates IM-associated stress (Darwin, 2005). In the presence of an inducer, PspF, the key transcriptional regulator, is released from PspA and upregulates gene expression within the Psp regulon (*pspA-E* and *G*) (Figure 9) (Darwin, 2005). Due to the striking reduction in plating efficiency observed in the *ΔpspF* mutant upon pIV production (Figure 14 & Table A2; Welch's T-Test; *P* value < 0.001), one or more effectors out of PspABCD or PspG is likely required for the survival of pIV-induced stress. The requirement of the Psp response in Gram-negative bacteria experiencing secretin-induced stress has been observed in multiple studies and is therefore not surprising (Jovanovic *et al.*, 2006; Lloyd *et al.*, 2004; Seo *et al.*, 2007). Furthermore, RNA-Seq analysis revealed a high induction of *pspA* and *pspG* in *E. coli* K-12 expressing pIV (Spagnuolo, 2015).

PspA and PspG are peripheral IM proteins which form highly organised complexes at the cell pole and lateral cell wall and have been proposed to interact with cellular components and maintain IM integrity (e.g., bind membrane lipids to 'plug' holes preventing proton leakage) (Darwin, 2013; Engl *et al.*, 2009). However, cells expressing naturally leaky secretins; EscC, InvG, and YscC, survive without PspA (Darwin & Miller, 2001; Horstman & Darwin, 2012; Khanum, 2015; Maxson & Darwin, 2006). Therefore this may not be the required effector. There is an expectation that pIV-E292K would behave similarly to channels that allow passage to molecules > 600 Da, though synthetic lethality analysis in the *ΔpspA* mutant has not been completed (Spagnuolo, 2015). Furthermore, a recent study used coimmunoprecipitation experiments to show that PspBC forms complexes with the mislocalised multimers of T3SS secretin, YscC, of *Y. enterocolitica*. This association extended to other secretins shown to induce the Psp response including the pIV secretin which also coimmunoprecipitated with PspBC (Srivastava, Moumene, Flores-Kim, & Darwin, 2017). Therefore it would be useful to complete synthetic lethality assays with deletions of other Psp genes.

Upon deletion of *pspF* in *E. coli* K-12 producing pIV-E292K, plating efficiency was reduced by ~99% (Figure 14 & Table A2; Welch's T-Test; *P* value < 0.001). In comparison, the ability of *E. coli* K-12 to form colonies decreased ~90% with wild-type pIV production (Figure 14 & Table A2; Welch's T-Test; *P* value < 0.001). Therefore, Psp is required for the survival of cells to mitigate secretin-induced stress, but more so for the survival of leaky or large-pore secretin production. This agrees with the observation that plating efficiency of *ΔpspF* cultures decreased 10^3-fold upon production of naturally leaky T3SS secretin, InvG (Khanum, 2015). Therefore, despite the level of Psp transcriptional activation being similar between leaky and gated pIV, the actual requirement of Psp response is dependent on the extent to which IM integrity is disrupted (Figure 14 & Table A2, (Spagnuolo, 2015)).

4.1.5 Rcs Response

As a highly mucoid phenotype is observed with leaky pIV-E292K production in the presence of RcsA and RcsB, it was expected that removal of these proteins from *E. coli* K-12 would have a striking effect on cell viability. However, loss of RcsA resulted in a reduction in cell viability of no more than 20% (relative to the vector control) when wild-type pIV or leaky pIV-E292K is produced (Figure 14 & Table A2; Welch's T-Test; *P* value < 0.01). By comparison, a ~99% and ~85% reduction in the ability of *ΔrcsB* mutant to form colonies upon induction of pIV-E292K or wild-type pIV expression, respectively, was observed (Figure 14 & Table A2; Welch's T-Test; *P* value < 0.001). As a transcriptional regulator, this suggests it is the RcsB-dependent branch of the Rcs regulon, which is controlled by the RcsB-homodimer (and not the RcsAB heterodimer), that is required for *E. coli* K-12 to mitigate pIV-induced stress. A very minor effect of *ΔrcsA* mutation on the viability of pIV-E292K expressing *E. coli* implies the mucoid phenotype is not necessary for the survival of *E. coli* producing pIV (Bury-Mone *et al.*, 2009; Marciano *et al.*, 1999; Spagnuolo *et al.*, 2010; Whitfield & Roberts, 1999). A recent study by Pando *et al.* (2017) showed that the Rcs-dependent mucoid capsule plays a role in maintaining the PMF in *Salmonella enterica* serovar *Typhimurium*. However, capsular polysaccharide synthesis has been previously shown to be induced by the RcsB-homodimer (Brill, Quinlan-Walshe, & Gottesman, 1988). They also propose that the regulation of PMF by the Rcs response is a compensatory role and is in addition to the PMF maintenance provided by the Psp response. This could explain the result in Figure 14 where PspF is required for all levels of secretin-induced stress whereas the lack of RcsB only results in a striking loss of cell viability with higher levels of secretin expression.

The number of genes regulated by the RcsB homodimer or by RcsB with other inducers is far greater than the number regulated by the RcsAB heterodimer (Majdalani & Gottesman, 2005). It is likely one or more of these target genes regulated by the RcsB homodimer (but not by the RcsAB heterodimer) that are required for *E. coli* to mitigate leaky pIV-induced stress.

RNA-Seq experiments identified several RcsB-homodimer-regulated genes where transcription is upregulated when leaky pIV-E292K and/or wild-type pIV is produced (Spagnuolo, 2015). There are two genes which respond to osmotic stress; *bdm* (encodes a motility modulator) and *osmB* (encodes a lipoprotein) that showed a 20- and 50-fold increase in transcription, respectively, in *E. coli* K-12 producing leaky pIV-E292K. By comparison, these genes were upregulated less than two-fold in cells producing wild-type pIV, relative to the vector control. Furthermore, transcription of *lolA* (OM lipoprotein translocation machinery component)*, rarA* (has roles in replication-associated recombination), *osmC* (osmotically inducible peroxiredoxin), and *ydeP* (acid resistance protein) increased by more than two-fold relative to the vector control in *E. coli* K-12 producing wild-type pIV or leaky pIV-E292K. It would appear then, that one or more genes involved in acid resistance, osmotic stress, and protein sorting and folding, enable *E. coli* K-12 to mitigate secretin-induced stress (Spagnuolo, 2015).

4.2 Conclusions and next steps

Previous studies have determined that it was the Psp regulon required for *E. coli* K-12 to survive secretin-induced stress, only. However, the data presented here also implicates the RcsB-homodimer-dependent branch of the Rcs regulon as necessary for survival, and to a lesser extent, CpxR. These three deletion mutants demonstrated the greatest reduction in cell viability (~99% for *ΔpspF* and *ΔrcsB* mutant and ~75% for *ΔcpxR* mutant) when leaky pIV-E292K production was induced (Figure 14 & Table A2). Attempts to confirm that any loss in viability was a result of secretin expression revealed the presence of revertants (cells that no longer expressed leaky pIV-E292K and are vancomycin resistant) in the K1508 strain containing *ΔrcsB* or *ΔpspF* mutations. This is in agreement with the intolerance of leaky pIV-E292K induced stress in the absence of RcsB and PspF. Indeed, as observed in TEM images, clear plasmolysis of the cell membrane was observed in many cells that were extracted from the 1 mM IPTG plate for the *ΔrcsB* mutant expressing pIV-E292K, in comparison with wild-type *E. coli* K-12.

This indicates that secretin expression occurred, though the stress was likely intolerable and a loss of pIV expression was selected for (e.g., through an acquired mutation). The observed plasmolysed cells in the colony were most likely dead (Figure 18C, bottom panels), whereas cells with a smooth OM were probably the surviving pIV-negative mutants (Figure 18D). Furthermore, expression of an open secretin channel (in comparison with the gated, wild-type pIV channel) induces Rcs-dependent capsular polysaccharide secretion. Leaky secretin, such as pIV-E292K, is open in physiological conditions and imposes greater stress on the cell as observed by capsular polysaccharide production (Figure 17), and a more global upregulation of stress responses genes indicative of increased IM, osmotic, and oxidative stress (Spagnuolo, 2015). As the role of RcsB in the survival of *E.coli* experiencing secretin-induced stress is a novel finding, it is necessary to confirm that it is directly, rather than indirectly, providing protection from pIV-induced stress. Restoring RcsB in *E. coli* cells producing pIV (and therefore inserting *rcsB* into pSB-RcsB) will provide more conclusive evidence that this transcriptional regulator is required (as observed by a significant increase in cell viability upon restoration of the missing gene).

An important next step is to complete epistatic analysis using the synthetic lethality assay to determine the importance of other genes within the Psp and Rcs regulons for the survival of secretin stress. Candidate genes for each pathway to be tested are; *pspA*, *pspB*, *pspC*, *pspD*, *pspE*, *pspF*, and *pspG* from Psp response, and; *rcsA*, *rcsB*, *rcsC*, *rcsD*, and *rcsF* from Rcs phosphorelay. Furthermore, as CpxR has been shown to be important for *E. coli* K-12 experiencing secretin-induced stress, it would be worthwhile to analyse the other positive regulator in the Cpx pathway, *cpxA*. It has been proposed by Jovanovic *et al.* (2006) that *pspG* and *pspA* are required for secretin-induced stress survival. Horstman and Darwin (2012) have also shown that the proteins PspB and PspC are critical to prevent secretin-induced toxicity in *Y. entercolitica*. Due to the apparent lack of importance of *rcsA*, it would be interesting to determine the effect on *E. coli* K-12 undergoing secretin-induced stress without genes involved in capsular polysaccharide production (and regulated in part by RcsA) as leaky pIV-E292K induced a mucoid phenotype.

In addition, it would be useful to extend this analysis to genes upregulated by the RcsB homodimer, particularly those known to be induced upon production of pIV such as *bdm* and *osmB* (Spagnuolo, 2015).

It would also be useful to implement a physiological approach to understand the nature of secretin-induced stress further. Though deletion of *soxR* and *soxS* resulted in a less striking reduction in cell viability in *E. coli* producing pIV, this is not evidence that pIV does not cause oxidative stress. RNA-Seq analysis by Spagnuolo (2015) demonstrated high induction of SoxS in pIV-producing cells, yet, genes upregulated by SoxS showed a change in expression of less than 2-fold. The only highly upregulated transcript, *marAB*, is not solely regulated by SoxS (Spagnuolo, 2015). Therefore, oxidative stress may still be induced by pIV but mediated by other proteins. The analysis should be undertaken in pIV-producing cells to determine the nature of oxidative stress and determine the amount of ROS produced, and the sensitivity of these cells to ROS.

It has also been suggested that pIV production disrupts PMF by allowing protons to leak back across the cell membrane (Darwin, 2013). A compromised PMF is in agreement with observations in this thesis that the cells are intolerant to co-producing Tet^R protein and pIV. Therefore physiological analysis should also be extended to include measurements of PMF in pIV-producing and non-producing *E. coli* cells.

Physiological assays can also be used for further investigation into the plasmolysis that was observed in the TEM images of *ΔrcsB* mutant expressing pIV-E292K. Such assays may be electrophysiology-based (Marciano *et al.*, 1999) or using fluorescent indicators (Muheim *et al.*, 2017) to determine membrane permeability. A functional membrane is able to maintain intra- and extracellular ions and solute concentrations, therefore subsequent treatments of plasmolysed cells with such solutes may be an indicator for the extent of cell membrane viability disruption (Blount, Iscla, & Li, 2008; Korber *et al.*, 1996).

Overall, this research shows evidence for the novel findings that RcsB and, to a lesser extent, CpxR, are required for the survival of *E. coli* experiencing secretin-induced stress. The data presented here also confirms the requirement for PspF in *E. coli* producing pIV secretin. These three proteins are potential drug targets that, when inhibited, may prevent management of membrane stress, thereby killing the pathogenic, secretin-producing bacteria.

5 References

Baba, T., Ara, T., Hasegawa, M., Takai, Y., Okumura, Y., Baba, M., Datsenko, K. A., Tomita, M., Wanner, B. L., & Mori, H. (2006). Construction of *Escherichia coli* K-12 in-Frame, Single-Gene Knockout Mutants: The Keio Collection. *Molecular Systems Biology, 2*(1).

Baneyx, F., & Georgiou, G. (1991). Construction and Characterization of *Escherichia coli* Strains Deficient in Multiple Secreted Proteases: Protease III Degrades High-Molecular-Weight Substrates *In Vivo*. *Journal of bacteriology, 173*(8), 2696-2703.

Baron, C. (2010). Antivirulence Drugs to Target Bacterial Secretion Systems. *Current opinion in microbiology, 13*(1), 100-105.

Battesti, A., & Bouveret, E. (2006). Acyl Carrier Protein/SpoT Interaction, the Switch Linking Spot-Dependent Stress Response to Fatty Acid Metabolism. *Molecular Microbiology, 62*(4), 1048-1063.

Beloin, C., Valle, J., Latour-Lambert, P., Faure, P., Kzreminski, M., Balestrino, D., Haagensen, J. A. J., Molin, S., Prensier, G., Arbeille, B., & Ghigo, J. M. (2004). Global Impact of Mature Biofilm Lifestyle on *Escherichia coli* K-12 Gene Expression. *Molecular Microbiology, 51*(3), 659-674.

Blanchard, J. L., Wholey, W. Y., Conlon, E. M., & Pomposiello, P. J. (2007). Rapid Changes in Gene Expression Dynamics in Response to Superoxide Reveal SoxRS-Dependent and Independent Transcriptional Networks. *PLoS ONE, 2*(11), e1186.

Blount, P., Iscla, I., & Li, Y. (2008). Mechanosensitive Channels and Sensing Osmotic Stimuli in Bacteria. In *Sensing with Ion Channels* (pp. 25-45): Springer.

Bolivar, F., Rodriguez, R. L., Greene, P. J., Betlach, M. C., Heyneker, H. L., Boyer, H. W., Crosa, J. H., & Falkow, S. (1977). Construction and Characterization of New Cloning Vehicles. II. A Multipurpose Cloning System. *Gene, 2*(2), 95-113.

Bonomo, R. A., Hooper, D. C., Kaye, K. S., Johnson, J. R., Clancy, C. J., Thaden, J. T., Stryjewski, M. E., & van Duin, D. (2017). Gram-Negative Bacterial Infections: Research Priorities, Accomplishments, and Future Directions of the Antibacterial Resistance Leadership Group. *Clinical Infectious Diseases, 64*(suppl_1), S30-S35.

Bougdour, A., & Gottesman, S. (2007). ppGpp Regulation of RpoS Degradation Via Anti-Adaptor Protein IraP. *Proceedings of the National Academy of Sciences, 104*(31), 12896-12901.

Boyd, E. S., Thomas, K. M., Dai, Y., Boyd, J. M., & Outten, F. W. (2014). Interplay between Oxygen and Fe–S Cluster Biogenesis: Insights from the Suf Pathway. *Biochemistry, 53*(37), 5834-5847.

Brill, J., Quinlan-Walshe, C., & Gottesman, S. (1988). Fine-Structure Mapping and Identification of Two Regulators of Capsule Synthesis in *Escherichia coli* K-12. *Journal of Bacteriology, 170*(6), 2599-2611.

Brissette, J. L., Russel, M., Weiner, L., & Model, P. (1990). Phage Shock Protein, a Stress Protein of *Escherichia coli*. *Proceedings of the National Academy of Sciences of the United States of America, 87*(3), 862-866.

Burghout, P., van Boxtel, R., Van Gelder, P., Ringler, P., Muller, S. A., Tommassen, J., & Koster, M. (2004). Structure and Electrophysiological Properties of the YscC Secretin from the Type III Secretion System of *Yersinia enterocolitica*. *Journal of Bacteriology, 186*(14), 4645-4654.

Bury-Mone, S., Nomane, Y., Reymond, N., Barbet, R., Jacquet, E., Imbeaud, S., Jacq, A., & Bouloc, P. (2009). Global Analysis of Extracytoplasmic Stress Signaling in *Escherichia coli*. *PLoS Genetics, 5*(9), 17.

Carlsson, K. E., Liu, J., Edqvist, P. J., & Francis, M. S. (2007). Extracytoplasmic-Stress-Responsive Pathways Modulate Type III Secretion in *Yersinia pseudotuberculosis*. *Infection & Immunity, 75*(8), 3913-3924.

Carra, J. H., & Schleif, R. F. (1993). Variation of Half-Site Organization and DNA Looping by AraC Protein. *The EMBO journal, 12*(1), 35-44.

Chami, M., Guilvout, I., Gregorini, M., Rémigy, H. W., Müller, S. A., Valerio, M., Engel, A., Pugsley, A. P., & Bayan, N. (2005). Structural Insights into the Secretin PulD and its Trypsin-Resistant Core. *Journal of Biological Chemistry, 280*(45), 37732-37741.

Cherepanov, P. P., & Wackernagel, W. (1995). Gene Disruption in *Escherichia coli*: TcR and KmR Cassettes with the Option of Flp-Catalyzed Excision of the Antibiotic-Resistance Determinant. *Gene, 158*(1), 9-14.

Chiang, S. M., & Schellhorn, H. E. (2012). Regulators of Oxidative Stress Response Genes in *Escherichia coli* and their Functional Conservation in Bacteria. *Archives of Biochemistry and Biophysics, 525*(2), 161-169.

Chng, S. S., Dutton, R. J., Denoncin, K., Vertommen, D., Collet, J. F., Kadokura, H., & Beckwith, J. (2012). Overexpression of the Rhodanese PspE, a Single Cysteine-Containing Protein, Restores Disulphide Bond Formation to an *Escherichia coli* Strain Lacking DsbA. *Molecular Microbiology, 85*(5), 996-1006.

Cook, W. R., MacAlister, T. J., & Rothfield, L. I. (1986). Compartmentalization of the Periplasmic Space at Division Sites in Gram-Negative Bacteria. *Journal of Bacteriology, 168*(3), 1430-1438.

Costa, T. R., Felisberto-Rodrigues, C., Meir, A., Prevost, M. S., Redzej, A., Trokter, M., & Waksman, G. (2015). Secretion Systems in Gram-Negative Bacteria: Structural and Mechanistic Insights. *Nature Reviews Microbiology, 13*(6), 343.

Daefler, S., Guilvout, I., Hardie, K. R., Pugsley, A. P., & Russel, M. (1997). The C-Terminal Domain of the Secretin PulD Contains the Binding Site for its Cognate Chaperone, PulS, and Confers PulS Dependence on pIV(F1) Function. *Molecular Microbiology, 24*(3), 465-475.

Daefler, S., & Russel, M. (1998). The *Salmonella typhimurium* InvH Protein is an Outer Membrane Lipoprotein Required for the Proper Localization of InvG. *Molecular Microbiology, 28*(6), 1367-1380.

Darwin, A. J. (2005). The Phage-Shock-Protein Response. *Molecular Microbiology, 57*(3), 621-628.

Darwin, A. J. (2013). Stress Relief During Host Infection: The Phage Shock Protein Response Supports Bacterial Virulence in Various Ways. *PLOS Pathogens, 9*(7), e1003388.

Darwin, A. J., & Miller, V. L. (2001). The Psp Locus of *Yersinia enterocolitica* is Required for Virulence and for Growth *In Vitro* When the Ysc Type III Secretion System is Produced. *Molecular Microbiology, 39*(2), 429-445.

DiGiuseppe, P. A., & Silhavy, T. J. (2003). Signal Detection and Target Gene Induction by the CpxRA Two-Component System. *Journal of Bacteriology, 185*(8), 2432-2440.

Duguay, A. R., & Silhavy, T. J. (2004). Quality Control in the Bacterial Periplasm. *Biochimica et Biophysica Acta (BBA)-Molecular Cell Research, 1694*(1-3), 121-134.

Durfee, T., Hansen, A.-M., Zhi, H., Blattner, F. R., & Jin, D. J. (2008). Transcription Profiling of the Stringent Response in *Escherichia coli*. *Journal of Bacteriology, 190*(3), 1084-1096.

Engl, C., Jovanovic, G., Lloyd, L. J., Murray, H., Spitaler, M., Ying, L., Errington, J., & Buck, M. (2009). *In Vivo* Localizations of Membrane Stress Controllers PspA and PspG in *Escherichia coli*. *Molecular Microbiology, 73*(3), 382-396.

Feng, J. n., Model, P., & Russel, M. (1999). A Trans-Envelope Protein Complex Needed for Filamentous Phage Assembly and Export. *Molecular Microbiology, 34*(4), 745-755.

Ferrieres, L., Aslam, S. N., Cooper, R. M., & Clarke, D. J. (2007). The yjbEFGH Locus in *Escherichia coli* K-12 is an Operon Encoding Proteins Involved in Exopolysaccharide Production. *Microbiology, 153*(4), 1070-1080.

Fischer, S., Gräber, P., & Turina, P. (2000). The Activity of the ATP Synthase from *Escherichia coli* Is Regulated by the Transmembrane Proton Motive Force. *Journal of Biological Chemistry, 275*(39), 30157-30162.

Fleischer, R., Heermann, R., Jung, K., & Hunke, S. (2007). Purification, Reconstitution, and Characterization of the CpxRAP Envelope Stress System of *Escherichia coli*. *Journal of Biological Chemistry, 282*(12), 8583-8593.

Flores-Kim, J., & Darwin, A. J. (2014). Regulation of Bacterial Virulence Gene Expression by Cell Envelope Stress Responses. *Virulence, 5*(8), 835-851.

Francez-Charlot, A., Laugel, B., Van Gemert, A., Dubarry, N., Wiorowski, F., Castanie-Cornet, M. P., Gutierrez, C., & Cam, K. (2003). RcsCDB His-Asp Phosphorelay System Negatively Regulates the FlhDC Operon in *Escherichia coli*. *Molecular Microbiology, 49*(3), 823-832.

Fung, D. C., & Berg, H. C. (1995). Powering the Flagellar Motor of *Escherichia coli* with an External Voltage Source. *Nature, 375*(6534), 809.

Gentry, D. R., & Cashel, M. (1996). Mutational Analysis of the *Escherichia coli* SpoT Gene Identifies Distinct but Overlapping Regions Involved in ppGpp Synthesis and Degradation. *Molecular Microbiology, 19*(6), 1373-1384.

Gibson, D. G., Young, L., Chuang, R.-Y., Venter, J. C., Hutchison III, C. A., & Smith, H. O. (2009). Enzymatic Assembly of DNA Molecules up to Several Hundred Kilobases. *Nature Methods, 6*(5), 343.

Gold, V. A. M., Salzer, R., Averhoff, B., & Kühlbrandt, W. (2015). Structure of a Type IV Pilus Machinery in the Open and Closed State. *eLife, 4*, e07380.

Gosink, K. K., & Häse, C. C. (2000). Requirements for Conversion of the Na^+-Driven Flagellar Motor of *Vibrio cholerae* to the H^+-Driven Motor of *Escherichia coli*. *Journal of Bacteriology, 182*(15), 4234-4240.

Guilvout, I., Chami, M., Engel, A., Pugsley, A. P., & Bayan, N. (2006). Bacterial Outer Membrane Secretin PulD Assembles and Inserts into the Inner Membrane in the Absence of its Pilotin. *EMBO Journal, 25*(22), 5241-5249.

Guzman, L.-M., Belin, D., Carson, M. J., & Beckwith, J. (1995). Tight Regulation, Modulation, and High-Level Expression by Vectors Containing the Arabinose pBAD Promoter. *Journal of Bacteriology, 177*(14), 4121-4130.

Hellweger, F. L. (2013). *Escherichia coli* Adapts to Tetracycline Resistance Plasmid (pBR322) by Mutating Endogenous Potassium Transport: *In Silico* Hypothesis Testing. *FEMS Microbiology Ecology, 83*(3), 622-631.

Hernandez, V. J., & Bremer, H. (1991). *Escherichia coli* ppGpp Synthetase II Activity Requires SpoT. *Journal of Biological Chemistry, 266*(9), 5991-5999.

Horne, S. M., Sayler, J., Scarberry, N., Schroeder, M., Lynnes, T., & Prüß, B. M. (2016). Spontaneous Mutations in the FlhD Operon Generate Motility Heterogeneity in *Escherichia coli* Biofilm. *BMC Microbiology, 16*(1), 262.

Horstman, N. K., & Darwin, A. J. (2012). Phage Shock Proteins B and C Prevent Lethal Cytoplasmic Membrane Permeability in *Yersinia enterocolitica*. *Molecular Microbiology, 85*(3), 445-460.

Hueck, C. J. (1998). Type III Protein Secretion Systems in Bacterial Pathogens of Animals and Plants. *Microbiology and Molecular Biology Reviews, 62*(2), 379-433.

Hunke, S., Keller, R., & Müller, V. S. (2011). Signal Integration by the Cpx-Envelope Stress System. *FEMS Microbiology Letters, 326*(1), 12-22.

Jackson, M. W., & Plano, G. V. (1999). DsbA Is Required for Stable Expression of Outer Membrane Protein YscC and for Efficient Yop Secretion in *Yersinia pestis. Journal of Bacteriology, 181*(16), 5126-5130.

Jacobsson, K., Rosander, A., Bjerketorp, J., & Frykberg, L. (2003). Shotgun Phage Display—Selection for Bacterial Receptins or Other Exported Proteins. *Biological Procedures Online, 5*(1), 123-135.

Johnson, T. L., Abendroth, J., Hol, W. G., & Sandkvist, M. (2006). Type II Secretion: From Structure to Function. *FEMS microbiology letters, 255*(2), 175-186.

Jones, S. E., Lloyd, L. J., Tan, K. K., & Buck, M. (2003). Secretion Defects That Activate the Phage Shock Response of *Escherichia coli*. *Journal of Bacteriology, 185*(22), 6707-6711.

Jovanovic, G., Lloyd, L. J., Stumpf, M. P. H., Mayhew, A. J., & Buck, M. (2006). Induction and Function of the Phage Shock Protein Extracytoplasmic Stress Response in *Escherichia coli*. *Journal of Biological Chemistry, 281*(30), 21147-21161.

Jovanovic, G., Weiner, L., & Model, P. (1996). Identification, Nucleotide Sequence, and Characterization of PspF, the Transcriptional Activator of the *Escherichia coli* Stress-Induced *Psp* Operon. *Journal of Bacteriology, 178*(7), 1936-1945.

Karaiskos, I., & Giamarellou, H. (2014). Multidrug-Resistant and Extensively Drug-Resistant Gram-Negative Pathogens: Current and Emerging Therapeutic Approaches. *Expert opinion on pharmacotherapy, 15*(10), 1351-1370.

Kehrenberg, C., Schwarz, S., Jacobsen, L., Hansen, L. H., & Vester, B. (2005). A New Mechanism for Chloramphenicol, Florfenicol, and Clindamycin Resistance: Methylation of 23s Ribosomal RNA at A2503. *Molecular Microbiology, 57*(4), 1064-1073.

Khanum, S. (2015). *Characterization of the Secretins, Large Outer Membrane Channels of Gram-Negative Bacteria: A Thesis Presented in Partial Fulfillment of the Requirements for the Degree of Doctor of Philosophy in Biochemistry at Massey University, Palmerston North, New Zealand.* Massey University.

Kitagawa, M., Ara, T., Arifuzzaman, M., Ioka-Nakamichi, T., Inamoto, E., Toyonaga, H., & Mori, H. (2005). Complete Set of ORF Clones of *Escherichia coli* ASKA Library (a Complete Set of *E. coli* K-12 ORF archive): Unique Resources for Biological Research. *DNA Research, 12*(5), 291-299.

Koraimann, G. (2003). Lytic Transglycosylases in Macromolecular Transport Systems of Gram-Negative Bacteria. *Cellular and Molecular Life Sciences CMLS, 60*(11), 2371-2388.

Korber, D., Choi, A., Wolfaardt, G., & Caldwell, D. (1996). Bacterial Plasmolysis as a Physical Indicator of Viability. *Applied and Environmental Microbiology, 62*(11), 3939-3947.

Korotkov, K. V., Gonen, T., & Hol, W. G. J. (2011). Secretins: Dynamic Channels for Protein Transport Across Membranes. *Trends in Biochemical Sciences, 36*(8), 433-443.

Korotkov, K. V., Pardon, E., Steyaert, J., & Hol, W. G. (2009). Crystal Structure of the N-Terminal Domain of the Secretin GspD from ETEC Determined with the Assistance of a Nanobody. *Structure, 17*(2), 255-265.

Krin, E., Danchin, A., & Soutourina, O. (2010). RcsB Plays a Central Role in H-Ns-Dependent Regulation of Motility and Acid Stress Resistance in *Escherichia coli. Research in microbiology, 161*(5), 363-371.

Kulp, A., & Kuehn, M. J. (2010). Biological Functions and Biogenesis of Secreted Bacterial Outer Membrane Vesicles. *Annual Review of Microbiology, 64*, 163-184.

Laubacher, M. E., & Ades, S. E. (2008). The Rcs Phosphorelay is a Cell Envelope Stress Response Activated by Peptidoglycan Stress and Contributes to Intrinsic Antibiotic Resistance. *Journal of Bacteriology, 190*(6), 2065-2074.

Lessl, M., Balzer, D., Lurz, R., Waters, V., Guiney, D., & Lanka, E. (1992). Dissection of IncP Conjugative Plasmid Transfer: Definition of the Transfer Region Tra2 by Mobilization of the Tra1 Region *In Trans*. *Journal of Bacteriology, 174*(8), 2493-2500.

Levy, S. (2002). Active Efflux, a Common Mechanism for Biocide and Antibiotic Resistance. *Journal of Applied Microbiology, 92*(s1).

Li, L., Kromann, S., Olsen, J. E., Svenningsen, S. W., & Olsen, R. H. (2017). Insight into Synergetic Mechanisms of Tetracycline and the Selective Serotonin Reuptake Inhibitor, Sertraline, in a Tetracycline-Resistant Strain of *Escherichia coli*. *The Journal of Antibiotics, 70*(9), 944.

Linderoth, N. A., Model, P., & Russel, M. (1996). Essential Role of a Sodium Dodecyl Sulfate-Resistant Protein IV Multimer in Assembly-Export of Filamentous Phage. *Journal of Bacteriology, 178*(7), 1962-1970.

Linderoth, N. A., Simon, M. N., & Russel, M. (1997). The Filamentous Phage pIV Multimer Visualized by Scanning Transmission Electron Microscopy. *Science, 278*(5343), 1635-1638.

Lloyd, L. J., Jones, S. E., Jovanovic, G., Gyaneshwar, P., Rolfe, M. D., Thompson, A., Hinton, J. C., & Buck, M. (2004). Identification of a New Member of the Phage Shock Protein Response in *Escherichia coli*, the Phage Phock Protein G (PspG). *Journal of Biological Chemistry, 279*(53), 55707-55714.

Lobell, R. B., & Schleif, R. F. (1990). DNA Looping and Unlooping by AraC Protein. *Science, 250*(4980), 528-532.

MacRitchie, D. M., Acosta, N., & Raivio, T. L. (2012). DegP Is Involved in Cpx-Mediated Post-transcriptional Regulation of the Type III Secretion Apparatus in Enteropathogenic *Escherichia coli*. *Infection & Immunity, 80*(5), 1766-1772.
Majdalani, N., & Gottesman, S. (2005). The Rcs Phosphorelay: A Complex Signal Transduction System. *Annual Review of Microbiology, 59*, 379-405.
Marciano, D. K., Russel, M., & Simon, S. M. (1999). An Aqueous Channel for Filamentous Phage Export. *Science, 284*(5419), 1516-1519.
Marciano, D. K., Russel, M., & Simon, S. M. (2001). Assembling Filamentous Phage Occlude pIV Channels. *Proceedings of the National Academy of Sciences of the United States of America, 98*(16), 9359-9364.
Markovitz, A. (1964). Regulatory Mechanisms for Synthesis of Capsular Polysaccharide in Mucoid Mutants of *Escherichia coli* K12. *Proceedings of the National Academy of Sciences, 51*(2), 239-246.
Marvin, D., Symmons, M., & Straus, S. (2014). Structure and Assembly of Filamentous Bacteriophages. *Progress in biophysics and molecular biology, 114*(2), 80-122.
Maxson, M. E., & Darwin, A. J. (2006). PspB and PspC of *Yersinia enterocolitica* are Dual Function Proteins: Regulators and Effectors of the Phage-Shock-Protein Response. *Molecular Microbiology, 59*(5), 1610-1623.
Miller, P. F., & Sulavik, M. C. (1996). Overlaps and Parallels in the Regulation of Intrinsic Multiple-Antibiotic Resistance in *Escherichia coli*. *Molecular Microbiology, 21*(3), 441-448.
Miyada, C. G., Stoltzfus, L., & Wilcox, G. (1984). Regulation of the *araC* Gene of *Escherichia coli*: Catabolite Repression, Autoregulation, and Effect on araBAD Expression. *Proceedings of the National Academy of Sciences, 81*(13), 4120-4124.
Miyadai, H., Tanaka-Masuda, K., Matsuyama, S.-i., & Tokuda, H. (2004). Effects of Lipoprotein Overproduction on the Induction of DegP (HtrA) Involved in Quality Control in the *Escherichia coli* Periplasm. *Journal of Biological Chemistry, 279*(38), 39807-39813.
Muheim, C., Götzke, H., Eriksson, A. U., Lindberg, S., Lauritsen, I., Nørholm, M. H. H., & Daley, D. O. (2017). Increasing the Permeability of *Escherichia coli* Using MAC13243. *Scientific Reports, 7*(1), 17629.
Nans, A., Kudryashev, M., Saibil, H. R., & Hayward, R. D. (2015). Structure of a Bacterial Type III Secretion System in Contact with a Host Membrane *In Situ*. *Nature Communications, 6*, 101-114.
Natale, P., Brüser, T., & Driessen, A. J. (2008). Sec-and Tat-Mediated Protein Secretion Across the Bacterial Cytoplasmic Membrane—Distinct Translocases and Mechanisms. *Biochimica et Biophysica Acta (BBA)-Biomembranes, 1778*(9), 1735-1756.
Nevesinjac, A. Z., & Raivio, T. L. (2005). The Cpx Envelope Stress Response Affects Expression of the Type IV Bundle-Forming Pili of Enteropathogenic *Escherichia coli. Journal of Bacteriology, 187*(2), 672-686.
Nikaido, H. (1996). Multidrug Efflux Pumps of Gram-Negative Bacteria. *Journal of Bacteriology, 178*(20), 5853.
Opalka, N., Beckmann, R., Boisset, N., Simon, M. N., Russel, M., & Darst, S. A. (2003). Structure of the Filamentous Phage pIV Multimer by Cryo-Electron Microscopy. *Journal of Molecular Biology, 325*(3), 461-470.

Otto, K., & Silhavy, T. J. (2002). Surface Sensing and Adhesion of *Escherichia coli* Controlled by the Cpx-Signaling Pathway. *Proceedings of the National Academy of Sciences, 99*(4), 2287-2292.

Pando, J. M., Karlinsey, J. E., Lara, J. C., Libby, S. J., & Fang, F. C. (2017). The Rcs-Regulated Colanic Acid Capsule Maintains Membrane Potential in *Salmonella Enterica Serovar Typhimurium*. *mBio, 8*(3), e00808-00817.

Pannen, D., Fabisch, M., Gausling, L., & Schnetz, K. (2016). Interaction of the RcsB Response Regulator with Auxiliary Transcription Regulators in *Escherichia coli*. *Journal of Biological Chemistry, 291*(5), 2357-2370.

Pelicic, V. (2008). Type IV Pili: E Pluribus Unum? *Molecular Microbiology, 68*(4), 827-837.

Price, N. L., & Raivio, T. L. (2009). Characterization of the Cpx Regulon in *Escherichia coli* Strain MC4100. *Journal of Bacteriology, 191*(6), 1798-1815.

Raivio, T. L., Popkin, D. L., & Silhavy, T. J. (1999). The Cpx Envelope Stress Response is Controlled by Amplification and Feedback Inhibition. *Journal of Bacteriology, 181*(17), 5263-5272.

Raivio, T. L., & Silhavy, T. J. (1997). Transduction of Envelope Stress in *Escherichia coli* by the Cpx Two-Component System. *Journal of Bacteriology, 179*(24), 7724-7733.

Rakonjac, J. (2012). Filamentous Bacteriophages: Biology and Applications. *eLS*.

Rehm, F. (2016). *Assessing the Requirement of Stress Responses for Surviving Secretin PulD from a Type II Secretion System.* (Bachelor's of Science with Honours Honour's thesis), Massey University Manawatu, New Zealand

Reichow, S. L., Korotkov, K. V., Hol, W. G., & Gonen, T. (2010). Structure of the Cholera Toxin Secretion Channel in its Closed State. *Nature Structural and Molecular Biology, 17*(10), 1226.

Russel, M. (1998). Macromolecular Assembly and Secretion across the Bacterial Cell Envelope: Type II Protein Secretion Systems. *Journal of Molecular Biology, 279*(3), 485-499.

Russel, M., & Kazmierczak, B. (1993). Analysis of the Structure and Subcellular Location of Filamentous Phage-pIV. *Journal of Bacteriology, 175*(13), 3998-4007.

Russel, M., Linderoth, N. A., & Sali, A. (1997). Filamentous Phage Assembly: Variation on a Protein Export Theme. *Gene, 192*(1), 23-32.

Sambrook, J., Fritsch, E. F., & Maniatis, T. (1989). *Molecular Cloning: A Laboratory Manual* (2nd ed. Vol. 1-3). Cold Spring Harbor, NY: Cold Spring Harbor Laboratory Press.

Schauder, S., & Bassler, B. L. (2001). The Languages of Bacteria. *Genes & Development, 15*(12), 1468-1480.

Seo, J., Savitzky, D. C., Ford, E., & Darwin, A. J. (2007). Global Analysis of Tolerance to Secretin-Induced Stress in *Yersinia enterocolitica* Suggests That the Phage-Shock-Protein System May Be a Remarkably Self-Contained Stress Response. *Molecular Microbiology, 65*(3), 714-727.

Silhavy, T. J., Kahne, D., & Walker, S. (2010). The Bacterial Cell Envelope. *Cold Spring Harbor Perspectives in Biology, 2*(5), a000414.

Skaar, E. P. (2010). The Battle for Iron between Bacterial Pathogens and Their Vertebrate Hosts. *PLOS Pathogens, 6*(8), e1000949.

Spagnuolo, J. (2015). *Extracytoplasmic Stress Responses Induced by a Model Secretin: A Dissertation Presented in Partial Fulfilment of the Requirements for the Degree of Doctor of Philosophy in Biochemistry at Massey University, Manawatū, New Zealand.* Massey University.

Spagnuolo, J., Opalka, N., Wen, W. X., Gagic, D., Chabaud, E., Bellini, D., Bennett, M., Norris, G. E., Darst, S. A., Russel, M., & Rakonjac, J. (2010). Identification of the Gate Regions in the Primary Structure of the Secretin pIV. *Molecular Microbiology, 76*(1), 133-150.

Spira, B., Hu, X., & Ferenci, T. (2008). Strain Variation in ppGpp Concentration and RpoS Levels in Laboratory Strains of *Escherichia coli* K-12. *Microbiology, 154*(9), 2887-2895.

Srijaruskul, K., Charoenlap, N., Namchaiw, P., Chattrakarn, S., Giengkam, S., Mongkolsuk, S., & Vattanaviboon, P. (2015). Regulation by SoxR of *mfsA*, Which Encodes a Major Facilitator Protein Involved in Paraquat Resistance in *Stenotrophomonas maltophilia*. *PLOS ONE, 10*(4), e0123699.

Srivastava, D., Moumene, A., Flores-Kim, J., & Darwin, A. J. (2017). Psp Stress Response Proteins Form a Complex with Mislocalized Secretins in the *Yersinia enterocolitica* Cytoplasmic Membrane. *mBio, 8*(5), e01088-01017.

Thanassi, D. G., & Hultgren, S. J. (2000). Multiple Pathways Allow Protein Secretion Across the Bacterial Outer Membrane. *Current Opinion in Cell Biology, 12*(4), 420-430.

Tolia, N. H., & Joshua-Tor, L. (2006). Strategies for Protein Co-expression in *Escherichia coli*. *Nature Methods, 3*(1), 55-64.

Tosi, T., Estrozi, Leandro F., Job, V., Guilvout, I., Pugsley, Anthony P., Schoehn, G., & Dessen, A. (2014). Structural Similarity of Secretins from Type II and Type III Secretion Systems. *Structure, 22*(9), 1348-1355.

Traxler, M. F., Summers, S. M., Nguyen, H. T., Zacharia, V. M., Hightower, G. A., Smith, J. T., & Conway, T. (2008). The Global, ppGpp-Mediated Stringent Response to Amino Acid Starvation in *Escherichia coli*. *Molecular Microbiology, 68*(5), 1128-1148.

Tsai, C.-L., Burkinshaw, B. J., Strynadka, N. C., & Tainer, J. A. (2015). The *Salmonella* Type III Secretion System Virulence Effector Forms a New Hexameric Chaperone Assembly for Export of Effector/Chaperone Complexes. *Journal of Bacteriology, 197*(4), 672-675.

Tseng, T.-T., Tyler, B. M., & Setubal, J. C. (2009). Protein Secretion Systems in Bacterial-Host Associations, and Their Description in the Gene Ontology. *BMC Microbiology, 9*(1), S2.

Turrens, J. F. (1997). Superoxide Production by the Mitochondrial Respiratory Chain. *Bioscience Reports, 17*(1), 3-8.

Viarre, V., Cascales, E., Ball, G., Michel, G. P. F., Filloux, A., & Voulhoux, R. (2009). HxcQ Liposecretin is Self-Piloted to the Outer Membrane by its N-Terminal Lipid Anchor. *Journal of Biological Chemistry, 284*(49), 33815-33823.

Vinella, D., Albrecht, C., Cashel, M., & D'Ari, R. (2005). Iron Limitation Induces SpoT-Dependent Accumulation of ppGpp in *Escherichia coli*. *Molecular Microbiology, 56*(4), 958-970.

Vogt, S. L., Nevesinjac, A. Z., Humphries, R. M., Donnenberg, M. S., Armstrong, G. D., & Raivio, T. L. (2010). The Cpx Envelope Stress Response Both Facilitates and

Inhibits Elaboration of the Enteropathogenic *Escherichia coli* Bundle-Forming Pilus. *Molecular Microbiology, 76*(5), 1095-1110.

Walker, K. A., & Miller, V. L. (2009). Synchronous Gene Expression of the *Yersinia enterocolitica* Ysa Type III Secretion System and its Effectors. *Journal of Bacteriology, 191*(6), 1816-1826.

Waterhouse, A., Bertoni, M., Bienert, S., Studer, G., Tauriello, G., Gumienny, R., Heer, F. T., de Beer, T. A. P., Rempfer, C., & Bordoli, L. (2018). Swiss-Model: Homology Modelling of Protein Structures and Complexes. *Nucleic Acids Research*.

Wehland, M., & Bernhard, F. (2000). The RcsAB Box Characterization of a New Operator Essential for the Regulation of Exopolysaccharide Biosynthesis in Enteric Bacteria. *Journal of Biological Chemistry, 275*(10), 7013-7020.

Wellington, E. M., Boxall, A. B., Cross, P., Feil, E. J., Gaze, W. H., Hawkey, P. M., Johnson-Rollings, A. S., Jones, D. L., Lee, N. M., & Otten, W. (2013). The Role of the Natural Environment in the Emergence of Antibiotic Resistance in Gram-Negative Bacteria. *The Lancet infectious diseases, 13*(2), 155-165.

Whitfield, C., & Roberts, I. S. (1999). Structure, Assembly, and Regulation of Expression of Capsules in *Escherichia coli*. *Molecular Microbiology, 31*(5), 1307-1319.

Wolfe, A. J., Parikh, N., Lima, B. P., & Zemaitaitis, B. (2008). Signal Integration by the Two-Component Signal Transduction Response Regulator CpxR. *Journal of Bacteriology, 190*(7), 2314-2322.

Worrall, L., Hong, C., Vuckovic, M., Deng, W., Bergeron, J., Majewski, D., Huang, R., Spreter, T., Finlay, B., & Yu, Z. (2016). Near-Atomic-Resolution Cryo-Em Analysis of the *Salmonella* T3S Injectisome Basal Body. *Nature, 540*(7634), 597.

Worthington, R. J., Blackledge, M. S., & Melander, C. (2013). Small-Molecule Inhibition of Bacterial Two-Component Systems to Combat Antibiotic Resistance and Virulence. *Future Medicinal Chemistry, 5*(11), 1265-1284.

Yamaguchi, S., Reid, D. A., Rothenberg, E., & Darwin, A. J. (2013). Changes in Psp Protein Binding Partners, Localization, and Behaviour Upon Activation of the *Yersinia enterocolitica* Phage Shock Protein Response. *Molecular Microbiology, 87*(3), 656-671.

Yan, Z., Yin, M., Xu, D., Zhu, Y., & Li, X. (2017). Structural Insights into the Secretin Translocation Channel in the Type II Secretion System. *Nature Structural and Molecular Biology, 24*(2), 177.

Yong-Seok, K., Joong-Soo, H., & Jai-Kyung, K. (1987). Chloramphenicol Acetyltransferase from Chloramphenicol-Resistant Clinical Isolates (*E. coli* 71b, *S. aureus*). *Experimental and Molecular Medicine, 19*(2), 119-130.

Zgurskaya, H. I., López, C. A., & Gnanakaran, S. (2015). Permeability Barrier of Gram-Negative Cell Envelopes and Approaches to Bypass It. *ACS Infectious Diseases, 1*(11), 512-522.

Zheng, M., Doan, B., Schneider, T. D., & Storz, G. (1999). OxyR and SoxRS Regulation of Fur. *Journal of Bacteriology, 181*(15), 4639-4643.

Zhou, X., Keller, R., Volkmer, R., Krauss, N., Scheerer, P., & Hunke, S. (2011). Structural Basis for Two-Component System Inhibition and Pilus Sensing by the Auxiliary CpxP Protein. *Journal of Biological Chemistry, 286*(11), 9805-9814.

Zowawi, H. M., Harris, P. N., Roberts, M. J., Tambyah, P. A., Schembri, M. A., Pezzani, M. D., Williamson, D. A., & Paterson, D. L. (2015). The Emerging Threat of Multidrug-Resistant Gram-Negative Bacteria in Urology. *Nature Reviews Urology, 12*(10), 570.

6 Appendix 1: Synthetic lethality results: BW25113 wild-type *E. coli* background

Table A1: Synthetic lethality results: BW25113 wild-type *E. coli* background

[IPTG] (mM)	Strain	Plasmid	Ratio[a]	ci. positive[b]	ci. negative[b]	P-value[c]
0	BW25113	pPMR132	74.29719	74.5558	74.03944476	0.001729371
0.1	BW25113	pPMR132	76.867816	77.1423	76.59423092	0.005616474
1	BW25113	pPMR132	70.317002	70.5750	70.05986065	0.001173
0	BW25113	pPMR132-E292K	70.01339	70.26133	69.76628	0.001264
0.1	BW25113	pPMR132-E292K	0.824713	0.84642	0.803428	0.000775
1	BW25113	pPMR132-E292K	0.018876	0.0224	0.015782	0.000486
0	*ΔcpxR*	pPMR132	43.15961	43.22184	43.09746	0.000169
0.1	*ΔcpxR*	pPMR132	33.73494	33.78961	33.68035	0.002216
1	*ΔcpxR*	pPMR132	6.438632	6.46169	6.415638	0.001786
0	*ΔcpxR*	pPMR132-E292K	57.98046	58.05622	57.90479	0.071684
0.1	*ΔcpxR*	pPMR132-E292K	0.005146	0.005764	0.004579	0.001919
1	*ΔcpxR*	pPMR132-E292K	0.005775	0.006483	0.005126	0.001748
0	*ΔpspF*	pPMR132	21.41901	21.78817	21.05512	3.17E-05
0.1	*ΔpspF*	pPMR132	21.36054	21.73214	20.9943	0.00016
1	*ΔpspF*	pPMR132	14.73397	15.03487	14.438	2.06E-05
0	*ΔpspF*	pPMR132-E292K	32.66399	33.13994	32.19402	7.42E-05
0.1	*ΔpspF*	pPMR132-E292K	0.168707	0.201181	0.140301	0.000136
1	*ΔpspF*	pPMR132-E292K	0.193724	0.228375	0.163146	0.00034

Table A1: Synthetic lethality results: BW25113 wild-type *E. coli* background (continued)

[IPTG] (mM)	Strain	Plasmid	Ratio[a]	ci. positive[b]	ci. negative[b]	P-value[c]
0	*ΔrcsB*	pPMR132	86.7031	86.80961	86.59672	0.051132
0.1	*ΔrcsB*	pPMR132	50.70671	50.77879	50.63473	0.009248
1	*ΔrcsB*	pPMR132	19.12568	19.16566	19.08578	0.000266
0	*ΔrcsB*	pPMR132-E292K	115.847	115.9794	115.7148	0.682816
0.1	*ΔrcsB*	pPMR132-E292K	0.009912	0.010767	0.009108	0.003431
1	*ΔrcsB*	pPMR132-E292K	0.007104	0.007845	0.006416	0.001531
0	*ΔsoxS*	pPMR132	82.44514	82.54038	82.35001	0.032395
0.1	*ΔsoxS*	pPMR132	58.55379	58.63317	58.47452	0.025383
1	*ΔsoxS*	pPMR132	40.6308	40.69467	40.56701	0.00051
0	*ΔsoxS*	pPMR132-E292K	84.95298	85.05031	84.85575	0.04221
0.1	*ΔsoxS*	pPMR132-E292K	4.409171	4.426868	4.391529	0.005873
1	*ΔsoxS*	pPMR132-E292K	0.001985	0.002399	0.001627	0.000692

Dataset corresponds to Figure 13.

[a] Calculated by determining the colony forming units per mL (CFU/mL) derived from the colony counts of three technical replicates and expressing it as a ratio relative to the vector control (isogenic deletion mutant or wild-type (CFU/mL) : vector control (CFU/mL)).

[b] 95% confidence intervals derived from exact Poisson test.

[c] Welch's one-tailed T-test was used to determine whether colony counts were significantly lower than that of the vector controls. Significance is determined by a P-value of less than 0.05.

7 Appendix 2: Synthetic lethality with K1508 wild-type background

Table A2: Synthetic lethality with K1508 wild-type background

[IPTG] (mM)	Strain	Plasmid	Ratio[a]	ci. positive[b]	ci. negative[b]	P-value[c]
0	K1508	pPMR132	62.13184	67.61351	57.07045	$6.55x10^{-10}$
0.1	K1508	pPMR132	58.52795	63.81765	53.65006	$9.31x10^{-9}$
1	K1508	pPMR132	59.32337	64.96776	54.14037	$1.74x10^{-9}$
0	K1508	pPMR132-E292K	80.57504	87.14671	74.48651	$3.06x10^{-6}$
0.1	K1508	pPMR132-E292K	76.50389	82.86817	70.61325	$3.46x10^{-10}$
1	K1508	pPMR132-E292K	51.29819	56.42224	46.60486	$1.15x10^{-9}$
0	*ΔcpxR*	pPMR132	71.30359	73.36524	69.29753	$5.95x10^{-6}$
0.1	*ΔcpxR*	pPMR132	66.54867	68.52449	64.62706	$8.44x10^{-8}$
1	*ΔcpxR*	pPMR132	61.77285	63.69051	59.90964	$3.42x10^{-8}$
0	*ΔcpxR*	pPMR132-E292K	61.67979	63.54359	59.86752	$3.57x10^{-7}$
0.1	*ΔcpxR*	pPMR132-E292K	59.82301	61.65885	58.03851	$1.77x10^{-9}$
1	*ΔcpxR*	pPMR132-E292K	24.57987	25.64696	23.55072	$3.85x10^{-9}$
0	*ΔpspF*	pPMR132	10.98326	11.04057	10.9262	$4.99x10^{-9}$
0.1	*ΔpspF*	pPMR132	9.944212	9.998486	9.890173	$4.77x10^{-11}$
1	*ΔpspF*	pPMR132	9.93353	9.989357	9.877953	$1.20x10^{-8}$
0	*ΔpspF*	pPMR132-E292K	0.35007	0.359908	0.340436	$2.76x10^{-9}$
0.1	*ΔpspF*	pPMR132-E292K	0.267782	0.276401	0.259368	$3.37x10^{-11}$
1	*ΔpspF*	pPMR132-E292K	0.035155	0.03846	0.032067	$5.43x10^{-9}$
0	*ΔrcsA*	pPMR132	93.02147	95.35734	90.74232	0.012567
0.1	*ΔrcsA*	pPMR132	89.55224	91.91563	87.24881	0.000591
1	*ΔrcsA*	pPMR132	87.53363	89.95247	85.17879	0.002957
0	*ΔrcsA*	pPMR132-E292K	92.71472	95.0449	90.44115	0.087015
0.1	*ΔrcsA*	pPMR132-E292K	89.46932	91.8311	87.16746	0.000193
1	*ΔrcsA*	pPMR132-E292K	80.3139	82.58638	78.1023	$2.49x10^{-6}$

Table A2: Synthetic lethality with K1508 wild-type background (continued)

[IPTG] (mM)	Strain	Plasmid	Ratio[a]	ci. positive[b]	ci. negative[b]	P-value[c]
0	*ΔrcsB*	pPMR132	45.51989	45.63046	45.40955	8.35×10^{-15}
0.1	*ΔrcsB*	pPMR132	41.57303	41.67828	41.46802	8.65×10^{-10}
1	*ΔrcsB*	pPMR132	14.2585	14.31539	14.20179	4.87×10^{-11}
0	*ΔrcsB*	pPMR132-E292K	27.64734	27.72807	27.56681	1.51×10^{-16}
0.1	*ΔrcsB*	pPMR132-E292K	19.78505	19.85186	19.71843	4.78×10^{-10}
1	*ΔrcsB*	pPMR132-E292K	0.07173	0.0756	0.068011	2.64×10^{-11}
0	*ΔsoxR*	pPMR132	62.49167	67.84872	57.53486	1.78×10^{-10}
0.1	*ΔsoxR*	pPMR132	65.30758	71.03887	60.01613	2.25×10^{-8}
1	*ΔsoxR*	pPMR132	60	65.55333	54.88984	2.44×10^{-11}
0	*ΔsoxR*	pPMR132-E292K	62.15856	67.49613	57.22015	1.77×10^{-6}
0.1	*ΔsoxR*	pPMR132-E292K	64.23462	69.90112	59.00422	4.96×10^{-9}
1	*ΔsoxR*	pPMR132-E292K	60.67669	66.27234	55.52669	4.44×10^{-13}
0	*ΔsoxS*	pPMR132	65.45894	71.56835	59.84584	1.27×10^{-6}
0.1	*ΔsoxS*	pPMR132	65.7767	71.92216	60.13125	1.50×10^{-6}
1	*ΔsoxS*	pPMR132	59.43709	65.24251	54.11786	7.63×10^{-8}
0	*ΔsoxS*	pPMR132-E292K	92.35105	100.1499	85.1539	0.085429
0.1	*ΔsoxS*	pPMR132-E292K	86.8932	94.37279	79.99677	0.002139
1	*ΔsoxS*	pPMR132-E292K	78.31126	85.33769	71.84706	0.000119

Dataset corresponds to Figure 14.

[a] Calculated by determining the colony forming units per mL (CFU/mL) derived from the colony counts of three technical and biological replicates and expressing it as a ratio relative to the vector control (isogenic deletion mutant or wild-type (CFU/mL) : vector control (CFU/mL)).

[b] 95% confidence intervals derived from exact Poisson test.

[c] Welch's one-tailed T-test was used to determine whether colony counts were significantly lower than that of the vector controls. Significance is determined by a P-value of less than 0.05.

8 Appendix 3: Data for synthetic lethality assay: Expressing pIV from a plasmid expressing a tetracycline resistance marker

Table A3: Dataset for synthetic lethality assay: Expressing pIV from a plasmid expressing a tetracycline resistance marker

[IPTG] (mM)	Strain	Plasmid	Ratio[a]	ci. positive[b]	ci. negative[b]	P-value[c]
0	K1508	pPMR132t	83.97976	84.29687	83.66382	0.053709
0.1	K1508	pPMR132t	15.38596	15.49577	15.2768	0.009865
1	K1508	pPMR132t	0.370858	0.388147	0.354155	7.22×10^{-5}
0	K1508	pPMR132t-E292K	9.241147	9.322389	9.160468	0.002005
0.1	K1508	pPMR132t-E292K	8.614035	8.693828	8.534823	0.008646
1	K1508	pPMR132t-E292K	0.1998	0.212585	0.187602	7.20×10^{-5}
0	*ΔcpxR*	pPMR132t	63.23251	63.42646	63.03913	0.00966
0.1	*ΔcpxR*	pPMR132t	66.1157	66.32487	65.90716	0.01028
1	*ΔcpxR*	pPMR132t	41.28828	41.44244	41.13463	0.001217
0	*ΔcpxR*	pPMR132t-E292K	7.155009	7.207975	7.10235	0.000795
0.1	*ΔcpxR*	pPMR132t-E292K	3.966942	4.007612	3.926592	0.00144
1	*ΔcpxR*	pPMR132t-E292K	0.056494	0.061492	0.051807	0.001019
0	*ΔpspF*	pPMR132t	38.73762	38.77339	38.70189	1.65×10^{-5}
0.1	*ΔpspF*	pPMR132t	34.64187	34.67702	34.60676	0.005046
1	*ΔpspF*	pPMR132t	5.123796	5.13574	5.111874	0.004932
0	*ΔpspF*	pPMR132t-E292K	52.90842	52.95229	52.86457	0.000457
0.1	*ΔpspF*	pPMR132t-E292K	56.26722	56.31547	56.219	0.014949
1	*ΔpspF*	pPMR132t-E292K	0.008487	0.008974	0.00802	0.004592
0	*ΔrcsA*	pPMR132t	45.87983	46.21342	45.54842	0.00189
0.1	*ΔrcsA*	pPMR132t	40.34632	40.65454	40.0402	0.000139
1	*ΔrcsA*	pPMR132t	32.85088	33.12332	32.5804	0.003119
0	*ΔrcsA*	pPMR132t-E292K	13.2618	13.42017	13.10495	0.002297
0.1	*ΔrcsA*	pPMR132t-E292K	5.91342	6.016396	5.811823	0.000575
1	*ΔrcsA*	pPMR132t-E292K	0.14386	0.160315	0.1287	0.001641

Table A3: Dataset for synthetic lethality assay: Expressing pIV from a plasmid expressing tetracycline resistance marker (continued)

[IPTG] (mM)	Strain	Plasmid	Ratio[a]	ci. positive[b]	ci. negative[b]	P-value[c]
0	*ΔrcsB*	pPMR132t	21.42857	21.44315	21.414	$3.66x10^{-5}$
0.1	*ΔrcsB*	pPMR132t	19.63968	19.65385	19.62551	0.000956
1	*ΔrcsB*	pPMR132t	0.09657	0.097573	0.095575	0.002779
0	*ΔrcsB*	pPMR132t-E292K	3.050595	3.055666	3.045531	$1.45x10^{-9}$
0.1	*ΔrcsB*	pPMR132t-E292K	0.393683	0.395525	0.391848	0.00107
1	*ΔrcsB*	pPMR132t-E292K	0.002899	0.003077	0.002729	0.002774
0	*ΔsoxR*	pPMR132t	45.30806	46.41846	44.22179	0.000277
0.1	*ΔsoxR*	pPMR132t	32.3301	33.23743	31.44446	0.00142
1	*ΔsoxR*	pPMR132t	5.318627	5.653859	4.999006	0.00013
0	*ΔsoxR*	pPMR132t-E292K	26.25592	27.04575	25.4859	$7.96x10^{-6}$
0.1	*ΔsoxR*	pPMR132t-E292K	4.587379	4.896748	4.293305	0.001169
1	*ΔsoxR*	pPMR132t-E292K	2.338235	2.560589	2.130855	0.00015
0	*ΔsoxS*	pPMR132t	1.936208	1.94034	1.932084	0.006017
0.1	*ΔsoxS*	pPMR132t	0.530451	0.532954	0.527956	0.00071
1	*ΔsoxS*	pPMR132t	0.035767	0.036422	0.03512	0.001172
0	*ΔsoxS*	pPMR132t-E292K	12.51123	12.52226	12.50021	0.007499
0.1	*ΔsoxS*	pPMR132t-E292K	2.880633	2.886527	2.874749	0.000742
1	*ΔsoxS*	pPMR132t-E292K	0.006104	0.006379	0.005839	0.001171

Dataset corresponds to Figure 19.

[a] Calculated by determining the colony forming units per mL (CFU/mL) derived from the colony counts of three technical replicates and expressing it as a ratio relative to the vector control (isogenic deletion mutant or wild-type (CFU/mL) : vector control (CFU/mL)).

[b] 95% confidence intervals derived from exact Poisson test.

[c] Welch's one-tailed T-test was used to determine whether colony counts were significantly lower than that of the vector controls. Significance is determined by a P-value of less than 0.05.